Accessory mineral chemistry of high Ba-Sr granites from northern Scotland: constraints on petrogenesis and records of whole rock signature

E. Bruand[1], C. Storey[1], M. Fowler[1]

[1]School of Earth and Environmental Sciences, University of Portsmouth, Portsmouth PO1 3QL, UK

* Corresponding author. Address: School of Earth and Environmental Sciences, Portsmouth University, Burnaby building, Burnaby Road, Portsmouth PO1 3QL, United-Kingdom

E-mail address: emilie.bruand@port.ac.uk

ABSTRACT

The Rogart and Strontian high Ba-Sr plutons (Northern Highlands, Scotland) comprise a range of lithologies from felsic to ultramafic rocks (so-called appinites). The latter rocks are mantle-derived and their differentiation to produce the felsic components is the result of fractional crystallisation and variable assimilation of the surrounding Moine metasediments. New results presented here demonstrate that accessory phase chemistry can give further insight into petrogenesis and highlight the petrological potential of apatite and titanite. Furthermore, in some cases, whole-rock trace element concentrations can be calculated by the use of accessory mineral chemistry.

Three of the main accessory phases (titanite, apatite and zircon), bearing most of the rare earth elements (REE) in the high Ba-Sr plutons, are studied here. Results on apatite and titanite show that careful imaging and in-situ trace element analyses give constraints on the petrogenetic history of the host rock. In both plutons, apatite and titanite record in-situ crystallisation and fractionation. In Strontian, apatite and titanite from the granitoids both record a mixing event with mafic magma in their rim compositions. Apatite and titanite chemistries are sensitive to the nature of their host rocks (felsic versus appinitic) and some elements (Sr, V) closely reflect whole rock chemistry and the degree of fractionation. Thus, trace elements in accessory phases can give direct access to the nature and the crystallisation history of plutonic rocks. This petrologic tool will allow further constraints in provenance studies using accessory phases, and since high Ba-Sr plutons have recently been equated with Archaean sanukitoids, might also be important in constraining the temporal distribution of this important magma type.

KEY WORDS: accessory phases; apatite; high Ba-Sr granites; petrogenesis; titanite

INTRODUCTION

Strontian and Rogart plutons are typical high Ba-Sr granites in that they have high Ba-Sr contents, are extremely rich in light rare earth elements (LREE), have relatively low Nb, Ta, and heavy rare earth elements (HREE). They have been discussed in the literature for their high modal abundance of accessory phases (mainly titanite, apatite with lesser zircon and monazite; e.g. Paterson *et al.*, 1989; Paterson & Stephens, 1992). Their whole rock chemistry and isotope systematics (O, Nd and Sr) argue for a mantle-derived source associated with host metasediment assimilation (Fowler *et al.*, 2008). Although the whole rock chemistry (trace elements, radiogenic and stable isotopes) of Rogart and Strontian plutons is well constrained (Fowler *et al.*, 2001; Fowler *et al.*, 2008), studies of accessory phases elsewhere have proven that some can give information on petrogenesis (e.g. Sha & Chappell, 1999; Hoskin *et al.*, 2000; Tiepolo *et al.*, 2002). The incorporation of trace elements and more particularly rare earth elements (REE) into their structures make them ideal minerals for this purpose. More specifically, previous studies concentrating on titanite and apatite have suggested that they might be sensitive to mixing processes, fO_2, fluid circulation or *PT* conditions (e.g. Tepper & Kuehner, 1999; Piccoli *et al.*, 2000; Belousova *et al.*, 2002a; Smith *et al.*, 2009; McLeod *et al.*, 2011). Recent work also shows promise in linking apatite compositions to their whole rocks (Chu *et al.*, 2000; Belousova *et al.*, 2002, Jennings *et al.*, 2010). On the other hand, altough zircon is a well-know accessory phase with many geological applications, its utility as a petrogenetic tracer is still not fully understood (e.g. Hoskin *et al.*, 2000; Hoskin & Schaltegger, 2003; Gagnevin et al., 2010). While most studies focus on describing one of the accessory phase contained within a suite of rocks (e.g. Sha & Chappell, 1999; Tepper & Kuehner, 1999; Piccoli *et al.*, 2000; Belousova *et al.*, 2002a; McLeod *et al.*, 2011), the comparison of the different accessory phases within a suite of samples has been rarely done (Hoskin *et al.*, 2000). As they all bear REE, systematic

comparative studies are essential to understand their behaviour in different conditions. In this contribution, we propose the study of apatite, titanite and zircon in a suite of different rocks from the High Ba-Sr granites to develop new petrographic tool to understand the behaviour of these phases in a range of felsic to mafic samples.

Such recent advances in mineral trace element chemistry may also be exploited for sedimentary provenance studies and in order to constrain crustal evolution. Similarities of high Ba-Sr granites with sanukitoid chemistry have led previous workers to describe them as "Phanerozoic sanukitoids" (Fowler & Rollinson, 2012). Sanukitoids are interpreted as being the product of a metasomatized mantle wedge and have been reported as occurring during a short time span (~2.7-2.5 Ga; Martin *et al.*, 2009). They have been interpreted by various workers (e.g. Martin *et al.*, 2009) as the result of the evolution from a shallow to a steep subduction style in this time interval and therefore might mark the onset of modern plate tectonics. Given this potentially pivotal role, it is important to constrain their temporal distribution. Assuming that accessory minerals record the elemental characteristics of their host magmas, it should be possible to recognise different igneous protoliths in detrital heavy mineral assemblages. For example, if the high Ba-Sr (sanukitoid) "fingerprint" is shown to be robust, then it can be sought in representative sediments of different ages, to monitor sanukitoid abundance with time.

This paper presents a detailed petrographic study and systematic laser ablation ICP-MS analysis of trace elements of apatite, titanite and zircon, with two main aims; to pursue constraint of the petrogenesis of high Ba-Sr granites, and to test the assumption that their characteristic chemistry is recorded by the abundant accessory minerals that they contain.

GEOLOGICAL SETTING AND SAMPLES

Late Caledonian high Ba-Sr plutons

The late Caledonian orogeny in Scotland is marked by voluminous and well-known granite magmatism, resulting from collision between Laurentia, Baltica and Avalonia that followed closure of Iapetus during the Silurian (Soper *et al.*, 1992; Atherton & Ghani, 2002). The plutons have a broadly calc-alkaline composition and are widespread within the Scottish Highlands north of the Iapetus Suture (Soper, 1986; Fig. 1). Three suites may usefully be distinguished (after Stephens & Halliday, 1984): the Argyll suite (now modified to the Argyll and Northern Highlands suite – Stephenson *et al.*, 1999), the Cairngorm suite and the South of Scotland suite. Most plutons of the latter have recently been subsumed into the Trans-Suture suite (Brown *et al.*, 2008). High Ba-Sr granites (Tarney & Jones, 1994) characterise the Argyll and Northern Highlands suite and are the particular focus of this contribution. Their origin has been ascribed to slab break off (Atherton & Ghani, 2002; Fowler *et al.*, 2008).

In the Northern Highlands, the Caledonian foreland is separated from Moine Supergroup metasediments, into which the high Ba-Sr plutons have been emplaced, by the Moine Thrust. In the south, the Great Glen Fault defines the boundary between the Northern Highland Terrane and the Grampian Terrane. The Midland Valley and Southern Uplands define the southern part of the Scottish Highlands between the Grampian Highlands and the Iapetus suture.

The late Caledonian high Ba-Sr suite intruding the Northern Highland terrane can be divided petrographically into two groups: (1) a western area dominated by syenitic plutons and (2) a central-eastern area dominated by granitic plutons (e.g. Fowler *et al.*, 2008 and references therein). We present results obtained from individual mineral grains (titanite, apatite, zircon) from the Rogart and Strontian plutons, which are both granite-dominated igneous complexes from the central-eastern area (Fig. 1).

Rogart and Strontian igneous complexes

The Rogart and Strontian igneous complexes have a broadly concentric geometry and are mainly made up of biotite-hornblende granodiorite. Emplacement of the Strontian complex caused contact metamorphism from cordierite-K feldspar to sillimanite-K feldspar assemblages (Soper, 1963; Tyler & Ashworth, 1983) while no contact metamorphism is observed around the Rogart pluton. Strontian has a biotite granodiorite central facies surrounded by hornblende-biotite granodiorite, which grades from porphyritic to non-porphyritic at its margin (Sabine, 1963). The hornblende-biotite granodiorite has been dated at 425 ± 3Ma (U-Pb on zircon) and 423 ± 3Ma (U-Pb on titanite; Rogers & Dunning, 1991). The Rogart igneous complex is made up of an inner granodiorite and an outer tonalite, which are cross cut by a later granite. It is coeval with Strontian and has been dated around 420 Ma (K-Ar on biotite; Brown *et al.*, 1968) and 425 ± 1.5 Ma (U-Pb on zircon; Kocks *et al.*, 2013). Mafic magma bodies (from centimetres to hundreds of metres scale) called appinites were first described in Appin (Scotland) by Bailey & Maufe (1916) and are present in the main facies of both the Strontian and Rogart plutonic bodies. Appinites are mantle derived rocks with shoshonitic affinities (Fowler, 1988; Fowler *et al.*, 2008), and are widely believed to be the plutonic equivalents of calc-alkaline lamprophyres (Rock, 1984; Murphy, 2013). Their high Mg, Ni, Cr and V contents indicate the contribution of the mantle during their genesis. In these rocks, hornblende is the dominant mafic mineral and occurs mainly as large prismatic crystals contain in a groundmass constituted by hornblende-feldspar+/-quartz. Local mingling and mixing relationships can be observed between the main plutonic facies and the appinitic bodies, especially at Strontian. The Strontian pluton was derived from a depleted mantle source and Rogart from enriched mantle, as discussed in detail by Fowler *et al.* (2008). Both plutons evolved by fractional crystallisation and variable assimilation of the surrounding Moine metasediments.

In this contribution, seven samples in total have been studied: two hb-bi granodiorites (SR1, SR3) and one appinite (SR2) from Strontian, and two tonalites (RT1, R2), one granite (RHG1) and one appinite (RA1) from Rogart. All samples from both plutons contain abundant accessory minerals such as titanite, apatite and zircon and are exceptional in that respect (Table 1). The hb-bi granodiorite samples from Strontian are chemically similar with SiO_2 ranging from 62.81% to 63.83% (Fowler *et al.*, 2008) and an Aluminium Saturation Index (ASI, calculated as molecular: $Al_2O_3/(Na_2O+K_2O+CaO)$) ranging from 0.87 to 0.90. Overall their trace element contents are likewise similar and are described in detail within Fowler *et al.* (2008). Granitoid compositions from Rogart vary extensively (Fowler *et al.*, 2001). In Rogart, tonalites vary in SiO_2 between 62.98% and 71.20%, Fe_2O_3 between 2.78% and 4.71% and their ASI are 0.81 (RT1) and 0.91 (R2). The granitic sample (RHG1) has a somewhat comparable chemistry in major elements to R2 with an ASI of 0.92 but with slightly higher K_2O and CaO contents (Fowler *et al.*, 2001). Trace element content varies significantly between the Rogart samples (e.g. Sr ranges from 693 ppm (RHG-1) to 1333 ppm (RT1); see Fowler *et al.* (2001) for analyses). In the tonalitic samples, RT1 has higher contents of Cr, Ni and Nb compared to R2, which can be linked to less fractionation following Fowler *et al.* (2001).

Appinites in the central-eastern Northern Highlands carry the high Ba-Sr elemental signature, but are commonly even more enriched in LILEs (e.g. Sr, Ba), HFSEs (e.g. Nb, Th) and transition metals (e.g. Cr, Ni, V) than associated granodiorites and granites (Fowler *et al.*, 2008). These characteristics can be observed in the two appinitic samples studied in this work (SR2 and RA1). However, some compositional differences do exist between them. In terms of major elements, the Strontian appinite is richer in Fe_2O_3 but has a higher ASI (0.59, c.f. Rogart ASI = 0.49). That from Rogart is enriched in Sr, Ba and LREE compared to Strontian but has lower HREE, Zr, Cr and Ni.

ANALYTICAL METHODS

Image acquisition

The samples were crushed (jaw-crusher, ball mill or Selfrag™), sieved (<355 μm, 355-500 μm and 500-1000 μm fractions) and passed over a Wilfley table. A diamagnetic separator was then used to obtain fractions of different heavy minerals based on their diamagnetic properties. Titanite, apatite and zircon were handpicked, mounted in epoxy resin discs and polished for in-situ chemical analysis. Titanite and apatite have also been analysed within thick sections (c.150μm). Back-scattered electron (BSE) images of titanites were taken with a scanning electron microscope (SEM) JEOL JSM-6100 at the University of Portsmouth (accelerating voltage = 20 kV). Cathodoluminescence (CL) images of apatites and zircons were taken with a KeDev Centaurus cathodoluminescence detector housed within a JEOL 6060LV SEM also at the University of Portsmouth (accelerating voltage = 15 kV).

Electron probe microanalysis (EPMA)

A Cameca SX-100 microprobe at Bristol University was used for determination of major elements in titanite and zircon using TAP, LPET, PET and LLIF crystals. PC0, TAP, LPET and LLIF crystals were used for apatite. An electron beam of 1 μm was used for titanite and 10 μm for apatite, both with 20 kV accelerating voltage and, 40nA and 10 nA beam currents respectively. An electron beam of 5 μm was used for zircon with an accelerating voltage of 17 kV and a beam current of 100 nA. Several trace elements in these minerals were also analysed for comparison with laser ablation ICP-MS (LA-ICPMS) data. The Durango apatite standard (Marks *et al.*, 2012) and the 91500 zircon standard (Wiedenbeck *et al.*, 2004) were analysed during sessions to monitor data quality.

200 **Laser ablation-inductively coupled plasma mass spectrometry (LA-ICPMS)**

201 Trace element contents of titanite, apatite and zircon were analysed by LA-ICPMS at the
202 University of Portsmouth using an Agilent 7500cs (quadrupole) ICPMS and a New-Wave
203 UP213 (λ=213 nm) solid state Nd:YAG laser. Each analysis consisted of ca. 30 s background
204 acquisition and 60 s sample acquisition. The diameter of the laser beam was 30 µm for
205 titanite and apatite and either 30 µm or 40 µm for zircon (with a 10 Hz repetition rate, an
206 output energy of 0.01-0.1 mJ/Pulse, and a fluence kept ~ 4J/cm^2). Each analytical run had
207 either 9 or 16 spot analyses with at least two external standard analyses at the beginning and
208 end of each run (either NIST 610 or NIST 612). NIST 610 standard (Pearce *et al.*, 1997) was
209 analysed with a laser beam diameter of 55 µm before and after titanite and apatite unknown
210 runs. In addition, Durango apatite (reference value used: Marks *et al.*, 2012) was also
211 analysed with a laser beam diameter of 30 µm at the beginning of each apatite run. NIST 612
212 standard (Pearce *et al.*, 1997) was analysed before and after zircon unknown runs with a
213 laser beam diameter of 55 µm. 91500 standard was analysed (Wiedenbeck *et al.*, 2004) with a
214 diameter of 40 µm at the beginning of each zircon run. Details of standard analyses and their
215 comparison with literature data can be found in the Supplementary Data Electronic Electronic
216 appendix 1. Internal references used for normalisation of LA-ICPMS data were ^{43}Ca for
217 apatite and titanite, and ^{29}Si for zircon and were obtained by EPMA.

218

219 **PETROGRAPHY**

220 Hb-bi granodiorite samples from Strontian (SR1-SR3) mainly comprise hornblende, feldspar
221 and biotite. Both samples contain titanite, apatite, zircon (Table 1) +/- allanite. The two
222 tonalite samples from Rogart (R2 and RT1) are made up of biotite, feldspar, hornblende and
223 muscovite. Accessory phases present in these samples are titanite, apatite, zircon and +/-
224 allanite. The granite sample in Rogart (RHG-1) is mainly made up of partly sericitized

feldspar and biotite which is often replaced by chlorite and calcite. This sample is therefore more affected by alteration than the others presented in this study. Titanite, apatite and zircon are present.

Appinitic samples in both locations (SR2 and RA1) are mainly made up of hornblende, biotite, feldspar and +/- calcite. Sample RA1 contains pyroxene, fractured and often partially replaced by calcite, in contrast to SR2. Paterson *et al.* (1989) have mentioned the exceptional amount of titanite in these rocks (see table 1). Appinitic samples contain also a large amount of apatite, together with minor zircon and allanite.

Titanite, apatite and zircon occurring in every sample are the focus of this study and their characteristics within the different samples selected are presented in the following section. Accessory allanite has been occasionally observed in Rogart (R2 and RT1 samples) and less so in Strontian. Allanite is not a ubiquitous mineral across the range of samples analysed and was therefore not analysed in this study.

Titanite

Bi-hb granodiorite

Samples SR1and SR3 Titanites are euhedral and large (up to ~ 1cm in length; Fig. 2). Using back-scattered electron (BSE) images at least three zones grading from a bright core toward a dark rim are identified in titanite crystals (Fig. 2 a-b). Occasionally, a thin (~ 10-40 µm) and darker external rim is present (Fig. 2a). The bright core often shows fir-tree zoning but also some oscillatory zoning, both of which are characteristic of titanite crystals (e.g. Paterson & Stephens, 1992; Watson & Lyang, 1995; Hayden *et al.*, 2008; McLeod *et al.*, 2011, Fig. 2 a-b). Locally, rare dissolution-reprecipitation textures have been identified. Apatite, oxides and zircon have been found as inclusions within titanite cores and rims.

Granite

Sample RHG-1 Two generations of titanite can be identified on the basis of size and petrographic relationship with the rock-forming minerals. Large titanites (>500 µm in length) are euhedral, often replaced by oxides and/or calcite and are also found as inclusions in feldspar. Smaller titanites (<500 µm in length) are subhedral, locally replaced with chlorite and always present as inclusions in biotite, aligned parallel to the basal cleavage. The chemical zoning pattern within this sample is more complicated than from the Strontian granodiorites. Cores usually display fir tree zoning, surrounded by several successive bright to dark zones (10-50 µm width, Fig. 2c) which seem to develop following dissolution-reprecipitation episodes (Fig. 2c-e). Such titanites locally contain many oxides and some apatite inclusions.

Tonalite

Samples R2 and RT1 Titanites are large (up to 1.5 mm in length) and euhedral. In RT1, titanite is often altered and replaced by calcite. Titanite zoning is comparable to RHG-1 with dissolution-reprecipitation textures observed. The results of several dissolution-reprecipitation events lead to complicated zoning made of up to 6 different zones around the core (e.g. Fig. 2e). Although oxides are abundant as inclusions within titanite, apatite inclusions are rarer.

Appinite

Samples SR2 and RA1 In appinitic samples, titanite has distinctive features. Titanite is anhedral and larger than from the granitoids (up to several cm; Fig. 2f-g). In SR2, titanites are interstitial between the main minerals (amphibole, biotite and feldspar) which suggests that they have grown late in the crystallisation sequence. Titanites from RA1 are anhedral-

subhedral and in contrast to SR2 do not show obvious interstitial texture. In both samples, they can be texturally in contact with apatite crystals but rarely contain inclusions. They always have sector and often oscillatory zoning (Fig. 2 f-g). However, in contrast to the granitoids, they do not contain any systematic core to rim zoning. The sectored and brighter zones can appear either at the edge or in the core. Rarely, a thin and external dark rim is present.

Apatite

Bi-hb granodiorite

Samples SR1 and SR3 In both samples, apatite is found mainly as inclusions within biotite and amphibole and more rarely within feldspar. Apatite is also common as inclusions within titanite and zircon. Apatite grains are either big and subhedral (up to 500 µm in length) or small and euhedral (<300 µm). In CL, they are zoned and made up of an oscillatory zoned core enclosed by an homogeneous rim (<50 µm; Fig. 3 a-b). Some crystals are entirely homogeneous in CL.

Granite and Tonalites

Samples RHG-1, RT1 and R2 Apatites are mainly present within biotite and green amphibole. As for the Strontian granodiorite, apatite inclusions have been found within titanite and zircon. CL reveals oscillatory zoning in most of crystal which is sometimes absent at the rim (Fig. 3 c-e).

Appinite

Sample SR2 In this sample, two apatite types can be identified: one of which is homogeneous in CL and the other, which has an homogeneous, partly dissolved core and a bright rim (Fig.

3f). These can be linked to different textural locations, the former within feldspar and the latter as inclusions in amphiboles or in late titanite. As feldspar is usually an early crystallising phase compared with amphibole, it is likely that apatite within feldspar crystallised early and apatite rims present within titanite crystallised later.

Sample RA1 Apatites in the Rogart appinite are large (up to 1 cm in length; Fig. 3g) and have a significant modal abundance (Table 1). Indeed, the amount of apatite is much higher than titanite. This is not the case in SR2 in which the proportion of both phases is roughly the same. Apatite can be found as inclusions within amphibole and feldspar or in contact with titanite. In CL images, apatite textures are similar to the second type of apatite found within SR2 with a dark core showing dissolution features surrounded by a brighter rim (Fig. 3g).

Zircon

Bi-hb granodiorite

Samples SR1 and SR3 In these samples, zircons have been identified within the three main phases (biotite, green amphibole and feldspar) and can be up to 500 µm in length. They are abundant and have a typical igneous oscillatory zoning in CL (Fig 4 a-b). Inherited cores are rare.

Granite and Tonalites

Samples RHG-1, RT1 and R2 Zircons in these samples have the same characteristics as the Strontian granodiorite described above. The only different feature is that a darker rim (<30 µm) has been occasionally observed (Fig. 4 e).

Appinites

Sample SR2 Within SR2 a few zircons have been identified, of which two types could be distinguished. One shows clear igneous oscillatory features (Fig. 4f) and the second shows sector zoning.

Sample RA1 Within this sample zircons have not been observed in thin section and only a couple of tiny crystals could be extracted. Unfortunately, these zircons are extensively cracked and altered (Fig. 4g) and therefore could not be analysed.

RESULTS

LA-ICPMS in-situ chemical data obtained from titanite, apatite and zircon crystals from the different Strontian and Rogart samples are described in the following section, concentrating on rare earth elements (REE) because of their central role in the petrogenetic discussion, with other trace elements discussed as appropriate.

Titanite Chemistry

Rare earth elements

Strontian Chondrite-normalized REE data have been plotted in figure 5 and show that titanites from the granodiorite samples are similar but can be divided into three groups (Fig. 5a). The first group (Group 1) has high REE content and a significant negative Eu anomaly ($(Eu/Eu^*)_N$ = 0.56-0.85; Table 2 and Electronic Supplementary Material, Electronic appendix 2). These analyses have been made within the broad core of the crystals and the fir-tree zones. The second group (Group 2) has lower REE content (especially LREE) and a Eu anomaly which is slightly negative ($(Eu/Eu^*)_N$ = 0.75-0.93). This group of analyses are exclusively from the rims of the crystals. The third group (group 3) has the lowest REE contents and a positive Eu anomaly ($(Eu/Eu^*)_N$ = 1.06-1.59). This last group is rare and could

only be analysed when a darker external rim was present and was wider than the laser spot size (30 μm, Fig. 2a).

Appinitic titanite REE-patterns are somewhat different with a general pattern showing a slightly positive Eu anomaly (Fig. 5c), but two groups can be distinguished. Group 1 represents analyses made on bright to dark sector zones. Group 2 represents analyses made on rare external dark rims. Group 1 is LREE enriched with a slightly negative to positive Eu anomaly ($(Eu/Eu^*)_N$ = 0.89-1.50). Different parts of the sector zones have REE patterns that overlap within a limited range of compositions (Fig. 5c), the brightest zones usually contain higher REE and the darkest the lowest REE (Table 2; Supplementary data, Electronic appendix 2). The external dark rims have lower LREE contents than group 1 and are characterized mainly by a negative Eu anomaly ($((Eu/Eu^*)_N$ = 0.80-1.51).

Rogart Chondrite-normalized REE patterns of the Rogart granite and tonalites have core patterns (Group 1) with a convex-upward LREE shape and a negative Eu anomaly similar to titanite in the Strontian granodiorite. Rim compositions of Rogart granite/tonalite (Group 2) have lower LREE than Group 1 (Fig. 5b) and have a similar or slightly less pronounced negative Eu anomaly. Rim compositions of the granite sample (RHG-1) vary more than R2/RT1 rims with a lower LREE content and no Eu anomaly (Table 2; Supplementary data, Electronic appendix 2). This could be linked to the two generations of titanite found within the RHG-1 thin-section of which one grew late. Bright dissolution-reprecipitation zones in R2 crystals (Group 3) have a convex-upward LREE-pattern and a slightly negative to absent Eu anomaly.

Chondrite-normalized REE patterns for the Rogart appinite are more enriched in LREE than the Strontian appinite and have no Eu anomaly (Fig. 5c). Titanites from this sample are also characterised by a convex-upward shape in the LREE. The different sector

zones observed within titanite crystals all have similar concentrations and patterns.

Other trace elements

Strontian Previous studies on titanite zoning in the Strontian pluton (Paterson *et al.*, 1989, Paterson & Stephens, 1992) suggested that sector zoning is out of equilibrium with the magma. On the other hand, modelling and recent experimental studies (Watson & Liang, 1995; Hayden *et al.*, 2008) have shown that although the most enriched sector zones do seem to be out of equilibrium (e.g. fir-tree features - FT), other parts of titanite zones are not and therefore titanite can be used as a petrogenetic tool (e.g. Hayden *et al.*, 2008; McLeod *et al.*, 2011). These studies have also shown that brightest part of the sector zones preferentially incorporate a substantial amount of certain elements (such as Zr and some REE) on a set of growth surfaces. Such "enriched" sector zones have been interpreted as representing an area or face of growth entrapment (Watson & Liang, 1995). Watson & Liang (1995) have shown that there is a "critical ratio of growth rate to lattice diffusivity" above which sector zoning is developing leading to the abnormal enrichment of REE and some traces (e.g. Nb and Zr). This was confirmed in a later study (Hayden *et al.*, 2008) in which experiments with titanite crystallisation have shown that the Zr content of these bright sector zones resulted in an overestimation of the temperature of crystallisation of the titanite (see discussion in Hayden *et al.*, 2008). Results from FT and bright sector zones in titanites in our study similarly have a substantially higher Zr content (Table 2; Supplementary data, electronic appendix 2). Although analyses of FT/brightest sector zones always correspond to the highest REE contents (Table 2; Supplementary Data, electronic appendix 2), their chondrite-normalized REE-patterns are not clearly distinguishable from the other parts of the crystals. Similar to Zr content, FT zone Nb contents are much higher (ranging from 2000 ppm to 3500 ppm) than the non-FT zoned cores of the granodiorite (between 1000 and 1700 ppm). The brightest

400 sector zones of the appinite sample reveal the same systematics, with Nb being much higher
401 than in the other sector zones (Table 2; Supplementary Data, electronic appendix 2).
402 Following results of experimental and modelling studies (Watson & Liang, 1995; Hayden *et*
403 *al.*, 2008), these anomalously high Nb and Zr contents in the FT/sector zones are interpreted
404 as being out of equilibrium with the magma composition and will not be considered further
405 here.

406 Discarding FT/brightest sector zone data, two trends are apparent within the Strontian
407 granitoids analyses on a Nb vs Gd plot (Fig. 6a), corresponding to core and rim compositions.
408 Core compositions have a constant Nb content although Gd generally decreases outwards.
409 Rim analyses correspond to an abrupt decrease in Nb and Gd contents, comparable and
410 parallel to that defined by the appinite titanite compositions.

411 On a $(Eu/Eu^*)_N$ versus $(La/Sm)_N$ diagram (Fig. 7a), two trends (cores and rims) can
412 again be identified within the granitoid samples. Core compositions mostly plot between 1
413 and ~5 ($(La/Sm)_N$) with a couple of core analyses and all the rims plotting above 5; $(La/Sm)_N$
414 increases and the negative Eu anomaly reduces towards the rim. One analysis representing
415 the dark external rim and a couple of analyses of the rim within SR1 have positive Eu
416 anomalies and plot in the same area as the appinite trend. The $(La/Sm)_N$ ratio within Strontian
417 appinite has a positive correlation with $(Eu/Eu^*)_N$.

418 Hayden *et al.* (2008) have shown that Zr content of titanite is temperature dependent.
419 Considering that the different plutons cooled at similar pressures during titanite
420 crystallisation (13-14 km depth following Tyler & Ashworth, 1983), Figure 7b can be
421 interpreted in terms of temperature versus HREE content (Y being a proxy for HREE). Once
422 again, two groups can be distinguished following core-rim compositions. Core compositions
423 vary from high Y content (> 3000 ppm) toward lower Y content (~1000 ppm, external part of
424 the core) with comparable Zr content (500-700ppm). Rim values of Y plot below 1000 ppm

but have Zr content decreasing more rapidly (ranging from 600 to ~400 ppm). Rims from SR1 have much lower Zr contents (~200 ppm). Titanites from Strontian appinite have a similar range of Y concentration (from ~1000 to ~500 ppm; Fig. 7b) to titanite rims from the granitoids. The Zr content of titanite from the appinite decreases from ~650 ppm to 100 ppm in their dark external rims. Thus, following the Zr-in-titanite thermometer (Hayden *et al.*, 2008 who estimate the uncertainty at ± 20 °C), titanite in the Strontian granitoids began to crystallise at ~ 772 °C and finished at ~ 709 °C from maximum Zr contents in the core toward minimum Zr contents in the rim (Table 2; Supplementary Data, electronic appendix 2). Using maximum and minimum values within appinite, titanites crystallised between ~772°C and ~682°C. These values are maximum estimates assuming activities of TiO_2 and SiO_2 in our calculations were unity as quartz is present and the amount of titanite in the samples are more likely to lead to high $aTiO_2$. For example, using a lower activity of aTiO2= 0.5 (suggested as the lower limit for typical crustal rock, e.g. Hayden & Watson, 2007; Ferry & Watson, 2007) in the calculations would decrease the temperature results by about 50 °C.

Rogart As for the titanite from Strontian, analyses from Rogart (Table 2; Supplementary Data, electronic appendix 2) show a wide scatter between FT and sector zone analyses, consistent with disequilibrium conditions. Removing these FT and bright sector zones, the data show a single Nb vs Gd trend within the granite and tonalite samples (Fig. 6b). Although Gd content decreases from the core towards the rim (from ~1100 ppm to 200 ppm), Nb contents are mostly between 1000 and 1400 ppm with analyses from areas interpreted as having undergone reprecipitation being higher (up to 2030 ppm). Except for one data point plotting at extremely high Nb and Gd contents, the appinitic titanites analysed define a trend with Gd and Nb content positively correlated.

Rogart granite and tonalite analyses are also plotted on the $(Eu/Eu^*)_N$ versus

$(La/Sm)_N$ diagram (Fig. 7a). Core values plot within the core trend of Strontian analyses. However, the rim compositions are different with $(La/Sm)_N$ ratio values ranging from 1 to 3 and a Eu anomaly tending toward 1. The spread of titanite values in Rogart is more restricted than in Strontian (Fig. 7a). Similarly, the appinite values plot in a narrow range between 1 and 2 in $(La/Sm)_N$ ratio and around 1 for $(Eu/Eu^*)_N$. Although $(Eu/Eu^*)_N$ values are comparable to those for the Strontian appinite, the $(La/Sm)_N$ ratio is much lower in Rogart.

Zr and Y values are plotted in Figure 7b. In contrast to Strontian granitoid titanites, those in Rogart define a single trend with Zr and Y contents decreasing from cores (Y= 3240 ppm) toward rims (Y= 924 ppm). Zr content ranges from ~654 ppm in the core toward 303 ppm within the rim corresponding to temperatures between ~771°C and ~728°C. The titanites from the appinites apparently crystallised between ~759°C and ~731°C.

Apatite Chemistry

Strontian Chondrite-normalized patterns of apatites from granodiorite samples (Samples SR1 and SR3) are parallel and define two groups (Fig. 8a). One group (Group 1) has higher REE content and a negative Eu anomaly ($(Eu/Eu^*)_N$ = 0.47-0.93) and a second group has lower REE content and only a slightly negative Eu anomaly ($(Eu/Eu^*)_N$ = 0.78-0.94). These two groups correspond respectively to analyses made in the oscillatory zoned cores and the rims of the apatite crystals (Fig.3 a-b). Both groups have enriched LREE relative to MREE. The $(La/Sm)_N$ ratio, representing the slope of the LREE, has been plotted against Gd, representing the MREE concentrations, to observe the behaviour of the two apatite groups. Figure 9a confirms that two apatite compositions following core and rim compositions can be distinguished within the granodiorite. As for titanite (Fig. 5a), apatite records a distinct change in REE composition during its growth. Moreover, the Ce versus Y diagram also highlights a compositional gap in apatite between cores and rims (Fig 9c). Minimum Ce

concentrations for core compositions are ~2300 ppm and maximum Ce values for rim compositions are ~1500 ppm. Interestingly, no other trace elements other than REE have shown systematic variations between core and rim compositions.

The appinite sample (SR2) has apatite REE-patterns evolving continuously from high and flat LREE-MREE content with a strong negative Eu anomaly toward higher LREE/MREE and slightly negative to absent Eu anomaly (Fig. 8c). The lower REE contents correspond to apatite rims when they occur as inclusions in amphibole and titanite or simply in contact with them. Apatites in appinites display a general increase in $(La/Sm)_N$ and decrease in Gd content toward the bright rims of the crystals (when this rim has been identified - see petrography description Fig. 3f,h, Fig. 9a). Figure 9a highlights the decrease of MREE in apatite rims being in contact with late phases such as titanite.

Rogart Apatite chondrite-normalized REE patterns from the granite and the two tonalites are presented in figure 8b. In contrast to Strontian apatites, REE-patterns of cores and rims within apatite crystals overlap. Therefore, core and rim patterns of the different samples have been merged for easier inter-sample comparison. R2 REE-patterns are tightly clustered with a flat LREE-pattern and a slight negative Eu anomaly. RT1 is similar but also has more enriched LREE compare to MREE. RHG-1 patterns are more clustered and have in general the lowest pattern of these three samples. However, RHG-1 patterns show exactly the same characteristics (flat LREE-pattern and slight negative Eu anomaly) as the other two samples. Core compositions of the RHG-1 apatite tend to have the highest total REE (Table 3; Supplementary Data, electronic appendix 3). For all three samples, despite overlap, there is a trend to lower total REE concentration from cores towards rims (Table 3; Supplementary Data, electronic appendix 3). Apatite compositions in Rogart tonalites/granite do not show abrupt changes in composition. They are characterised by large variations in Gd and small

variations in $(La/Sm)_N$ (Fig. 9b).

Apatite chondrite-normalized patterns from the Rogart appinite are different from the Strontian appinite, with a flat LREE-pattern and a slightly negative to absent Eu anomaly (Fig. 8c). Analyses either from the core or rim plot in a tightly clustered area and do not show significant differences. The flat LREE and the Eu anomaly of apatite REE-patterns in the Rogart appinite have similar characteristics to the titanite from the same location (Fig. 5c). Apatite $(La/Sm)_N$ values are around 2 as for the other more evolved samples (Fig. 9b). Appinite apatites have a Gd content ranging from ~ 200 ppm to ~ 80 ppm. Appinite and tonalites/granite cannot be distinguished based on their apatite composition in this diagram and have a rather constant $(La/Sm)_N$ ratio. There is a positive correlation between Ce and Y within each Rogart sample with a general continuous decrease of these elements from cores toward rims (Fig. 9c).

Zircon

REE chondrite-normalized patterns of zircon within Strontian granodiorite (SR1 and SR3) are homogeneous and have typical igneous zircon REE-patterns (e.g. Hoskin & Schaltegger, 2003) with large positive Ce anomalies, negative Eu anomalies and strong HREE enrichment (Fig. 10a). No systematic core to rim composition groups have been observed, in contrast to apatite and titanite (Fig. 5a; 8a). Appinitic zircon compositions have similar REE-patterns although the REE content is systematically higher. This is opposite to the Belousova *et al.* (2002b) compilation of zircon data, which infers an increase of REE content within zircon from ultramafic toward granitoid compositions. Generally Th/U ratio is <0.5 for igneous zircons (Hoskin & Schaltegger, 2003) and although Th/U zircons from our granitoids are consistent with this, the appinitic sample has slightly higher Th/U values (Th/U = ~0.5-1.6, Table 4 and Supplementary Data, electronic appendix 4).

525 Rogart tonalites/granite zircons have comparable REE patterns and concentrations to
526 Strontian (Fig. 10b). Other trace elements analysed within these zircons do not show any
527 variation between core and rim zones (Table 4; Supplementary Data, electronic appendix 4).
528
529 **DISCUSSION**
530 **Petrogenetic records during apatite and titanite crystallisation**
531 Mineral chemical data from the Rogart and Strontian plutons allow constraint of
532 crystallisation history, generally in terms of *in situ* crystal fractionation and mixing processes
533 during crystallisation of the magmas.
534
535 *Saturation of accessory phases*
536 Zircon saturation temperature estimates within granitoids have been studied for several
537 decades (e.g. Larsen, 1973; Watson, 1979; Watson & Harrison, 1983; Barrie, 1995 and
538 reference therein; Miller *et al.*, 2003; Harrison *et al.*, 2007; Fu *et al.*, 2008) and have
539 promoted significant understanding of zircon behaviour in plutons. However, similar data
540 have not been intensively constrained for apatite and titanite since the work of Harrison &
541 Watson (1984) and Green & Pearson (1986). Hoskin *et al.* (2000), in a detailed paper about a
542 cogenetic suite of plutonic rocks (Boggy Plain pluton, Australia), described the behaviour of
543 titanite, apatite and zircon trace element chemistry and used an integrated approach to
544 identify accessory mineral saturation during differentiation. Despite the value of such work,
545 there is a lack of data for other pluton chemistries and geological settings. Several studies
546 (including Hoskin *et al.*, 2000) have shown that zircon usually saturates in felsic melts
547 ($SiO_2 \geq 65\%$) but not in those that are less evolved. In the Boggy Plain suite, Hoskin *et al.*
548 (2000) estimated that apatite probably saturates throughout the range of compositions (Aplite
549 to diorite) while titanite was interpreted as never saturating within the suite. Titanites in these

550 samples were anhedral (except for the most evolved samples) and their abundance was
551 limited.

552 In contrast with Boggy Plain, all granitoids studied herein are extremely rich in
553 accessory phases (titanite, apatite, zircon; > 3% modal proportion). These are euhedral and
554 present as inclusions within all of the rock-forming minerals, all of which strongly suggests
555 that saturation has been reached. Zircons are large, abundant and contain apatite inclusions.
556 Apatites are large, euhedral in every sample and have been found as inclusions in the other
557 accessory phases (titanite and zircon). Therefore, textural relationships suggest that the three
558 accessory phases grew simultaneously and that apatite might have started to crystallise
559 slightly earlier. But the homogeneous composition of apatite core in these samples does not
560 confirm this last statement. In the appinites, apatite is commonly found as inclusions within
561 all the rock-forming minerals, occasionally within titanite but was not found within zircon.
562 Therefore, either apatite could have saturated and stopped crystallising before zircon
563 crystallisation or the low abundance of zircon may obscure the relationship between these
564 mineral. In SR2, titanites are abundant, anhedral and interstitial, and are therefore interpreted
565 to have crystallised late, possibly in melt pools as described by Hoskin *et al.* (2000). In
566 contrast, titanites in RA1 are anhedral-subhedral but not interstitial and therefore might have
567 saturated and started to crystallise slightly earlier. Zircons are tiny, extremely rare and free of
568 apatite inclusions, and therefore interpreted as not crystallising early in these ultramafic
569 samples. REE-patterns (Fig. 10) support the suggestion that such zircons seem to have
570 crystallised from REE-enriched melt pockets.

571

572 *The granitoids: in-situ crystal fractionation and a late mixing event?*

573 In the Strontian granitoids, both apatite and titanite exhibit two chemical groups which
574 presumably relate to the same petrogenetic events. The first group (crystal cores) has higher

REE content and more significant negative Eu anomaly. The second group (crystal rims) has a lower REE content with slightly negative to absent Eu anomaly.

Cores of titanite and apatite in Strontian record a systematic outward decrease in trace elements (Fig. 6a, 7a-b, 9a, c, 11). For example, figure 7b shows a correlation between Zr and Y content, the latter of which can be used as a proxy for HREE which are compatible in titanite. The progressive decrease of Y is consistent with in-situ crystal fractionation, as titanite and other accessory minerals progressively deplete the remaining melt in trace elements. The same systematics are observed in apatite cores (Fig. 9a-c) suggesting that cores of titanite and apatite grew during the same interval.

However, progressive in-situ crystal fractionation cannot explain the sudden compositional change observed in titanite and apatite rims in Strontian (Fig. 6a, 7a-b, 9c-d, 11). There are several possible causes, such as a change in oxygen fugacity, fluid circulation/hydrothermal alteration or magma composition (e.g. Piccoli *et al.*, 2000; Prowatke & Klemme, 2005, 2006; Smith *et al.*, 2009; McLeod *et al.*, 2011). A change in oxygen fugacity during titanite growth implies different characteristics exposed in the following. Reduction of magma conditions will lead to the dissolution of part of titanite crystals resulting in the stabilisation of ilmenite within titanite and the regrowth of titanite with a lower REE content. (e.g. Piccoli *et al.*, 2000; McLeod *et al.*, 2011). Although presence of titanite-magnetite-quartz in a felsic magma indicate relatively high fO_2, decreasing fO_2 in this magma has been shown to induce crystallisation of ilmenite (Wones, 1989). Moreover, under reduced conditions, lower activity of ferric iron induces the need to charge balance REE in titanite structure which can partly explain the lower REE uptake. Except for the change in REE content, the other features that characterize a change in fO_2 are not observed in the Strontian titanite. Moreover, Belousova *et al.* (2002a) have shown that La/Sm, Ce/Th and Y/ΣREE of apatite compositions are dependent upon oxygen fugacity of the magma. La/Sm

and Ce/Th increase with fO_2 although Y/ΣREE will tend to decrease. None of these ratios between apatite cores and rims show systematic differences in the samples discussed here (Table 2; Supplementary Data, electronic appendix 2). It is therefore unlikely that abrupt REE changes between cores and rims of apatite/titanite can be explained by a simple change of fO_2. Hydrothermal alteration of titanites is characterized by patchy zoning and anhedral crystals with trace element contents depending on the nature and chemistry of the fluids (e.g. Piccoli *et al.*, 2000; Horie *et al.*, 2008; Smith *et al.*, 2009; McLeod *et al.*, 2011). Titanites from the Strontian granitoids are euhedral and have typical magmatic zoning and do not reveal obvious hydrothermal alteration between cores and rims (Fig. 2 a-b). Finally, Prowatke & Klemme (2005) have shown that $D_{titanite/melt}$ for REE and some other trace elements (Ta, Nb) is strongly influenced by melt composition (Fig. 11a). They have shown that $D_{titanite/melt}$ increases significantly for these elements from mafic to felsic magma compositions. For instance Gd $D_{titanite/melt}$ varies from about 1 in mafic compositions to 370 in their most felsic compositions. Our results show major systematic changes for the same elements (REE, Ta, Nb) between cores and rims with the rim values plotting within the field for appinites (Table 2; Supplementary Data, electronic appendix 2; Fig. 5a, 6a-b). Another example is illustrated in figure 11b by using Nb/Ta ratio in titanite. On this figure, Nb/Ta ratios in Strontian titanites increase significantly towards the appinite and in the rims of the granitoids. This phenomenon can be best explained looking at the $D_{titanite/melt}$ for Nb and Ta for titanite (Fig. 11a). Indeed, D_{Nb}/D_{Ta} felsic<< D_{Nb}/D_{Ta} mafic which is mimiced by the Ta/Nb ratio in titanite. Similarly, Prowatke & Klemme (2006) have shown that $D_{apatite/melt}$ increases from mafic toward felsic melt composition for REE. Again, our apatites reveal changes of REE composition between cores and rims and no systematic changes for the other trace elements were observed. It therefore seems likely that titanite and apatite rims from Strontian granitoids record a mixing event with a more mafic magma characterized in these minerals

by: (i) an abrupt decrease in REE in the rim of both minerals, (ii) an abrupt decrease in Nb, Ta in titanite rims and (iii) rim compositions comparable with appinite apatite/titanite compositions (Fig. 12b). This conclusion, at the micrometer scale, is consistent with numerous macro-scale mixing and mingling features between the granitoids and mafic magmas observed at the locality from which the samples were taken, including abundant microgranular mafic enclaves and a disrupted synplutonic microdiorite dyke.

In Rogart, titanite and apatite trace element contents decrease generally from core towards rim (Fig. 7a-b, 8b, 9b, c). On the other hand, unlike Strontian there is no abrupt change in their chemistry at the rim, and the overall trends are consistent with progressive in-situ crystallisation of minerals that crystallised simultaneously (Fig. 12b). Petrographic description and some analyses have highlighted dissolution-reprecipitation BEI-bright zones (Fig. 2e). When these zones were big enough to be analysed, they were shown to be enriched in certain elements (e.g. HREE+Y and Nb, Figs. 6b, 7b; Table 2; Supplementary Data, electronic appendix 2). These brighter zones are always succeeded by a zone which plots within the general core to rim trend of Rogart titanite compositions (Figs. 2e (e.g. a14), 6b, 7b). Thus, these dissolution-reprecipitation episodes are thought to be a consequence of several magma pulses of the same magma, which is consistent with recent interpretation of the construction of the pluton (Kocks *et al.*, 2013).

The appinites: in-situ crystal fractionation?

The petrogenetic interpretation of the appinite titanite and apatite compositions are somewhat different since titanite is a late phase in sample SR2 (interstitial growth) and is anhedral/euhedral in sample RA1 (Fig. 2 f-g). In Rogart, titanite and apatite REE-patterns are similar (flat LREE with an absent or slightly positive Eu anomaly; Figs. 5c, 8c). This would imply that $D_{apatite/melt}$ and $D_{titanite/melt}$ for the different REE are comparable for a given magma

composition and that the minerals crystallised at a similar time, consistent with the data of Prowatke & Klemme (2005, 2006) on mafic magma composition. In contrast, appinitic titanites and apatites from Strontian have rather different REE-patterns and apatite cores and rims have distinctive REE contents (Supplementary Data, electronic appendices 2-3; Fig. 9a, c). It is also observed that apatite with BEI-bright rims is systematically present as inclusions in late phases such as interstitial titanite or amphibole (Fig. 3f), suggesting that apatite rim growth is synchronous with titanite. Changes in REE content between core and rim in apatite may therefore be related to late growth of titanite (Fig. 12a). Progressive depletion of the melt in LREE-MREE as a result of early apatite saturation may explain the difference in titanite REE-patterns between appinites from Rogart and Strontian (Fig. 5c).

Summary of apatite-titanite crystallisation history

Following the different results and observations made above, it is possible to reconstruct the different stages of growth of apatite and titanite and link them to pluton petrogenesis (Fig. 12a-b). For this purpose, the average (Sr/Sm) ratio is used in figure 12c because it allows discrimination of the nature of the magma from which the mineral has crystallised. Average Sr composition in cores or rims of the two minerals is homogeneous and correlates with the Sr whole rock content (see following section). Sm is used as it has been shown by experiments studies (Prowatke & Klemme, 2005, 2006) that titanite and apatite distribution coefficients vary significantly between mafic and felsic magma compositions. Bearing those points in mind, the following crystallisation sequence for granitoids is interpreted:

(i) In the granitoids, inclusion of apatites within titanite and zircon demonstrate that apatite is an early phase in the crystallisation sequence. The presence of apatite within titanite zones implies that apatite crystallised slightly earlier than or simultaneously with titanite. Most of the time, apatite inclusions do not appear

within the FT zones which crystallised first in titanite. Moreover, both apatite and titanite show a homogeneous core with an abrupt change of REE composition at their rims. Finally, if titanite had crystallised later than apatite, a shift in apatite REE pattern due to the new intake of LREE-MREE by titanite might be expected (see Sr2 sample in Fig. 8c). This is not observed in the samples (Fig. 8). All these observations strongly suggest that these minerals have crystallised simultaneously. In figure 12c, Strontian and Rogart titanite/apatite core compositions plot in the same area.

(ii) Subsequently, rims of both minerals within the different granitoids crystallised (Fig. 12b-c). The abrupt chemistry change of rim compositions of Strontian samples plot close to the mafic samples in Sr/Sm space, revealing the mixing event between the granitoid and a mafic magma. On the other hand, Rogart granitoid rim data plot close to their previous mineral core compositions. Due to *in situ* crystal fractionation, the Sr/Sm ratio for both mineral increased slightly but still cluster in a tight area (Fig. 12c).

For appinite, (Sr/Sm) ratio for each mineral is characteristically higher than for the granitoid and plot in an area where $(Sr/Sm)_{Apatite}$>10 and $(Sr/Sm)_{Titanite}$>0.20. RA1 apatite and titanite grew simultaneously and have core and rim composition plotting in a tight area. On the other hand, apatite cores in SR2 have crystallised first indicated by the increase of $(La/Sm)_N$ of apatite toward the rim and the interstitial habit of titanite crystal (Fig. 12a). Therefore, $(Sr/Sm)_{Titanite}$ for SR2 plots at a higher value in figure 12c.

Thus, the $(Sr/Sm)_{Apatite}$ versus $(Sr/Sm)_{Titanite}$ of a given sample can be used to track *in situ* crystallisation and to discriminate the nature of the magma from which the accessory minerals crystallised (felsic or mafic). In this example, it identifies a mixing event in

699 Strontian granitoids, but further work on different samples and magma composition needs to
700 be done to assess if this kind of diagram can be used more widely as a discrimination tool. In
701 this case, this diagram is only of use when associated with a detailed petrographic study. This
702 contribution has shown that detailed study of accessory minerals highlights petrogenetic
703 processes not visible with whole rock data only. On the other hand, whole rock chemistry and
704 isotope systems (O, Nd, Sr) argue for petrogenetic aspects that could not be observed in
705 apatite, titanite or zircon trace elements chemistry, for example metasediment assimilation
706 (Fowler et al., 2008). This is consistent with the bulk of such contamination occurring before
707 crystallisation of the accessory phases, i.e. *en route* to the site of emplacement.

708

709 **Accessory mineral records of whole rock composition**

710 *Sr-V in Apatite and Titanite*

711 $V_{apatite}$, $Sr_{titanite}$ and $Sr_{apatite}$ have significant potential to reflect the content of these elements in
712 the whole rock and therefore have potential applications for provenance studies. Previous
713 studies have suggested a link between apatite composition and that of the whole rock (e.g.
714 Hoskin *et al.*, 2000; Belousova *et al.*, 2001, 2002a; Chu *et al.*, 2009; Jennings *et al.*, 2011;
715 Miles *et al.*, 2013). From these studies, several correlations have been highlighted, such as Sr
716 in apatite ($Sr_{apatite}$) reflecting the degree of fractionation of the host granite. Chu *et al.* (2009)
717 have also used Sr, MnO and F content in apatite to infer different settings of pluton genesis.
718 In the Scottish samples studied here, differences between Sr content of cores and rims of the
719 apatite grains are minor (Fig. 13a, Table 3; Supplementary Data, electronic appendix 3),
720 which is consistent with work by Tepper & Kuehner (1999) suggesting that elements
721 occupying the Ca site (Mn, Fe, Sr) in apatite have been redistributed between zones by
722 intracrystalline diffusion. $Sr_{apatite}$ data versus Sr_{WR} define two separate groups corresponding
723 with ultramafic and granitoid compositions (Fig. 13a). Literature values for granitoid samples

have also been plotted (Hoskin *et al.*, 2000; Belousova *et al.*, 2002a; Chu *et al.*, 2009; Jennings *et al.*, 2011), which correspond well with the new data. "Gabbros" from the same suite of complex intrusive body studied by Jennings *et al.* (2011) also plot in the same region as the appinites (Jennings & Marschall, personal communication). The data distribution in Fig 13a therefore suggests that magma composition may have some influence on Sr partition coefficients, in contrast with the conclusions of Klemme & Prowatke (2005). Similarly, V content is quite homogeneous in apatite crystals ($V_{apatite}$). Figure 13b shows the relationship with $V_{WR.}$ There is an increase of $V_{apatite}$ from felsic toward ultramafic samples, again discriminating the two main compositions.

Although such apatite and whole rock compositional correspondence has been investigated in recent years, the similar use of titanite has not. Figure 13c-d shows that Sr in titanite ($Sr_{titanite}$) correlates with $Sr_{apatite}$ and therefore with Sr_{WR}. There is a good correlation between the Sr content of both minerals and there is a consistent factor of about 10 between them (Fig. 13d). Sparse available data from the literature (Hoskin *et al.*, 2000) plot on the same trend.

Figures 14a-b demonstrates that Sr_{WR} and V_{WR} reflect the degree of fractionation of the samples, although Sr values are rather more scattered (Fig. 14a, b). Reported SiO_{2WR}-$Sr_{apatite}$ values of the felsic samples are consistent with literature data (Hoskin *et al.*, 2000; Belousova *et al.*, 2002a ; Chu *et al.*, 2009; Jennings *et al.*, 2011) although in general our samples have higher $Sr_{apatite}$ for similar SiO_2 values (Fig. 14c). This can be explained by the characteristic high Ba-Sr content of the samples (Fowler *et al.*, 2001, 2008). Comparable ultramafic compositions (Jennings & Marschall, personal data) and our appinitic samples (Fig. 14c) define a second trend (see above, Fig. 13a). Similarly, $Sr_{titanite}$ (Fig. 14c,d), and $V_{apatite}$ show similar trends. In summary, $Sr_{apatite}$, $Sr_{titanite}$, $V_{apatite}$ seem also to reflect the degree of fractionation of Strontian and Rogart samples.

749

750 *Apatite and Titanite: recovery of whole rock REE content*

751 Application of distribution coefficients to early crystallising apatite and titanite should allow
752 recovery of the original melt composition. Zircon is not tested because previous workers have
753 shown that back-calculation for this mineral was difficult either due to substitution with
754 xenotime (e.g Hoskin *et al.*, 2000) or because of the lack of experimental data for our felsic
755 range of composition. Strontian samples have been affected by a mixing event (see discussion
756 above) and therefore cannot be used to calculate original whole rock values. We therefore test
757 the back-calculation on Rogart titanite and apatite which have fairly homogeneous
758 compositions. In a first stage, calculations for felsic samples were done with available K_D
759 from experimental works for both minerals (e.g. Prowatke & Klemme, 2005, 2006; Tiepolo
760 *et al.*, 2002), giving results that appear to be completely inconsistent (especially for titanite)
761 with the whole rock data (Appendix 5). Compositions used during these experiments are
762 dissimilar from the composition of our samples. Therefore, apatite and titanite K_D were
763 chosen from natural samples (mineral/glass; Luhr *et al.*, 1984) with a bulk composition that is
764 more appropriate. Results calculated with apatite and titanite core compositions from RHG-1
765 and RT1 samples show pleasing comparability with whole-rock chondrite-normalized REE
766 patterns (Fig. 15 a-b, Fowler *et al.*, 2001; Table 4 and Supplementary Data, electronic
767 appendix 4). Calculations with sample R2 give similar pattern shape but systematically lower
768 REE content from the whole rock data (Fig. 15c). Apatite gives more reliable results than
769 titanite but HREE calculations for both minerals plot far above the whole rock data. This
770 cannot be explained by later saturation of zircon in which HREE are extremely compatible
771 because apatite crystals have been found as inclusions parallel to zircon growth zoning
772 inferring that they grew at the same time. R2 apatites systematically plot lower in La/Sm, and
773 higher in Y/(ΣREE) than the other samples (Table 4; Supplementary Data, electronic

appendix 4) which could suggest a different fO_2 for this sample (Belousova *et al.*, 2002a), although there is a lack of experimental data to confirm this. Further, in plutonic igneous rocks such as these, it is entirely possible that the whole rock itself does not represent a melt composition. Each sample is a combination of evolving melt and entrained crystals, such that for sample R2 admixture of a low heavy-REE mineral (e.g. feldspar) would effectively reduce whole-rock heavy REE content. The observed mismatch might therefore be related to different fO_2 conditions, to dissimilarity with the apatite compositions of Luhr *et al.* (1984) or to a difference of composition between the whole rock composition and the evolving magma as recorded in the accessory phases.

For the Rogart appinite, K_D for basic rocks are taken from Prowatke & Klemme (2006) (Table 4; Supplementary Data, electronic appendix 4). Calculations using apatite, which crystallised early in RA1 (Fig. 15d), have LREE concentrations consistent with whole rock data. Those done with titanite, which is a late crystallising phase, do not reflect the whole rock data (Fig. 15d). The lack of experimental data for HREE distribution coefficients does not allow for comparison with HREE.

What about zircons?

Zircon is undoubtedly one of the most widely used mineral to date rocks (e.g. Compston *et al.*, 1984; Feng *et al.*, 1993; Kosler & Sylvester, 2003 and references therein), is extremely valuable for provenance studies (e.g. Fedo, 2000), to track magma source (using O and Hf isotopes, e.g. Hawkesworth & Kemp, 2006; Dhuime *et al.*, 2012) and to potentially estimate oxygen fugacity (e.g. Ballard *et al.*, 2002; Trail *et al.*, 2011; Burnham & Berry, 2012). Nevertheless, previous authors (Heaman *et al.*, 1990; Belousova *et al.*, 2002b) have tried to discriminate source rock type using trace elements in zircons but the systematics remain unclear (see Hoskin & Schaltegger, 2003). The use of trace elements in single grain of zircon

to record petrogenetic processes has been described as unsuccessful (e.g. Hoskin *et al.*, 2000), but a recent study by Gagnevin *et al.* (2010) interpreted that U-Th-Y variations in zircon could reflect a magma mixing event. No significant elemental differences have been found within the zircon analytical data produced for this study. The only noticeable difference is the higher REE content of the appinite sample compared to the granitoids, which is suggested to be the consequence of late crystallisation from REE-enriched melt pockets. Therefore, zircon seems not to be the best candidate to track petrogenetic processes.

CONCLUSION

Careful imaging and chemical characterisation of single grain accessory phases (apatite and titanite) is a powerful petrogenetic tool. With the new results presented here, several conclusions can be made:

1- Apatite and titanite trace element data allow constraint of a part of the petrogenetic history of the plutons. In-situ crystal fractionation is evident during the crystallisation of both the Strontian and Rogart plutons, and a late mixing event with mafic magma can be identified in Strontian, the latter of which was not evident in whole-rock data.
2- Other petrogenetic events, such as metasediment assimilation recorded in whole-rock isotope systematics, are not visible in the mineral chemical data presented here (trace elements). This may be a matter of timing, with in-situ crystallisation of the accessory minerals post-dating assimilation that occurred during magma transport.
3- Many elements within apatite and titanite (e.g. Sr, V, REE) closely reflect whole rock chemistry and the degree of fractionation of the samples.
4- All accessory phases studied here can be dated by U-Pb and therefore, the association of U-Pb dating and trace elements analysis could add important constraints on the source interpretations of provenance studies (e.g. McAteer *et al.*, 2010). Although

TTG were the main plutonic rocks generated during the Archean, an important change around 2.7 Ga led to the genesis of the sanukitoids. This event is often interpreted as the result of the change from shallow to steep subduction and would represent the onset of modern plate tectonic. Ultimately, this study on accessory mineral within sanukitoid-like rocks has implications for the recognition of the sanukitoid signature through time. Further work on sanukitoid accessory phases is now needed to confirm that these also reflect their original magma compositions. If successful, this will be helpful in defining the temporal distribution of sanukitoids from the detrital record.

5- Elemental variations within zircon crystals are not petrogenetically informative.

ACKNOWLEDGMENTS

We are particularly grateful to M. Tiepolo, D. Chew and M. Ducea for the reviews provided and their helpful comments. We are grateful to Stuart Kearns for the help provided with the microprobe analyses, Christine Hugh and Tony Butcher for assistance during the SEM and Cathodoluminescence work and Geoff Long for amazing technical support. We wish to thank the Selfrag company (Kerzers, Switzerland) for the use of the Selfrag machine during the preparation of the samples. This work was supported by the Natural Environment Research Council [Grant number NE/I025573/1]. This is a contribution to International Geoscience Programme (IGCP) 599.

SUPPLEMENTARY DATA

Supplementary data for this paper are available of Journal of Petrology online.

REFERENCES

Atherton, M. P. & Ghani, A. A. (2002). Slab breakoff: a model for Caledonian, Late Granite syn-collisional magmatism in the orthotectonic (metamorphic) zone of Scotland and Donegal, Ireland. *Lithos* **62**, 65-85.

Bailey, E. B. & Maufe, H. B. (1916). The geology of Ben Nevis and Glen Coe and the surrounding country. *1st edn. Memoir of the Geological Survey of Great Britain*, Sheet 53 (Scotland).

Ballard, J. R., Palin, J. M. & Campbell, I. H. (2002). Relative oxidation states of magmas inferred from Ce(IV)/Ce(III) in zircon: application to porphyry copper deposits of northern Chile. *Contributions to Mineralogy and Petrology* **144**, 347-364.

Barrie, C. T. (1995). Zircon Thermometry of High-Temperature Rhyolites near Volcanic-Associated Massive Sulfide Deposits, Abitibi Subprovince, Canada. *Geology* **23**, 169-172.

Belousova, E. A., Griffin, W. L., O'Reilly, S. Y. & Fisher, N. I. (2002a). Apatite as an indicator mineral for mineral exploration: trace-element compositions and their relationship to host rock type. *Journal of Geochemical Exploration* **76**, 45-69.

Belousova, E. A., Griffin, W. L., O'Reilly, S. Y. & Fisher, N. I. (2002b). Igneous zircon: trace element composition as an indicator of source rock type. *Contributions to Mineralogy and Petrology* **143**, 602-622.

Belousova, E. A., Walters, S., Griffin, W. L. & O'Reilly, S. Y. (2001). Trace-element signatures of apatites in granitoids from the Mt Isa Inlier, northwestern Queensland. *Australian Journal of Earth Sciences* **48**, 603-619.

Burnham, A. D. & Berry, A. J. (2012). An experimental study of trace element partitioning between zircon and melt as a function of oxygen fugacity. *Geochimica Et Cosmochimica Acta* **95**, 196-212.

Brown, P. E., Miller, J. A. & Grasty, R. L. (1968). Isotopic ages of Late Caledonian granitic intrusions in the British Isles. *Proceedings of the Yorkshire Geological Society* **36**, 51-276.

Brown, P.E., Ryan, P.D., Soper, N.J. & Woodcock, N.H. (2008). The Newer granite problem revisited: a transtensional origin for the early Devonian Trans-suture suite. *Geological Magazine* **145**, 235-256.

Chu, M. F., Wang, K. L., Griffin, W. L., Chung, S. L., O'Reilly, S. Y., Pearson, N. J. & Iizuka, Y. (2009). Apatite Composition: Tracing Petrogenetic Processes in Transhimalayan Granitoids. *Journal of Petrology* **50**, 1829-1855.

Compston, W., Williams, I. S. & Meyer, C. (1984). U-Pb geochronology of zircons from lunar breccia 73217 using a sensitive high massresolution ion microprobe. *Journal of Geophysical Research-Solid Earth and Planets* **89**, B252-B534.

Dhuime, B., Hawkesworth, C. J., Cawood, P. A. & Storey, C. D. (2012). A Change in the Geodynamics of Continental Growth 3 Billion Years Ago. *Science* **335**, 1334-1336.

Fedo, C. M. (2000). Setting and origin for problematic rocks from the > 3.7 Ga Isua Greenstone Belt, southern west Greenland: Earth's oldest coarse elastic sediments. *Precambrian Research* **101**, 69-78.

Feng, R., Machado, N. & Ludden, J. (1993). Lead geochronology of zircon by laserprobe-inductively coupled plasma-mass spectrometry (LP-ICPMS). *Geochimica Et Cosmochimica Acta* **57**, 3479-3486.

890 Ferry, J. M. & Watson, E. B. (2007). New thermodynamic models and revised calibrations
891 for the Ti-in-zircon and Zr-in-rutile thermometers. *Contributions to Mineralogy and*
892 *Petrology* **154**, 429-437.

893 Fowler, M. B. (1988). Ach'uaine hybrid appinite pipes: evidence for mantle-derived
894 shoshonitic parent magmas in Caledonian granite gneiss. *Geology* **16**, 1026-1030.

895 Fowler, M. & Rollinson, H. (2012). Phanerozoic sanukitoids from Caledonian Scotland:
896 Implications for Archean subduction. *Geology* **40**, 1079-1082.

897 Fowler, M. B., Henney, P. J., Darbyshire, D. P. F. & Greenwood, P. B. (2001). Petrogenesis
898 of high Ba-Sr granites: the Rogart pluton, Sutherland. *Journal of the Geological Society* **158**,
899 521-534.

900 Fowler, M. B., Kocks, H., Darbyshire, D. P. F. & Greenwood, P. B. (2008). Petrogenesis of
901 high Ba-Sr plutons from the Northern Highlands Terrane of the British Caledonian Province.
902 *Lithos* **105**, 129-148.

903 Fu, B., Page, F. Z., Cavosie, A. J., Fournelle, J., Kita, N. T., Lackey, J. S., Wilde, S. A. &
904 Valley, J. W. (2008). Ti-in-zircon thermometry: applications and limitations. *Contributions to*
905 *Mineralogy and Petrology* **156**, 197-215.

906 Gagnevin, D., Daly, J. S. & Kronz, A. (2010). Zircon texture and chemical composition as a
907 guide to magmatic processes and mixing in a granitic environment and coeval volcanic
908 system. *Contributions to Mineralogy and Petrology* **159**, 579-596.

909 Green, T. H. & Pearson, N. J. (1986). Ti-Rich Accessory Phase Saturation in Hydrous Mafic-
910 Felsic Compositions at High P,T. *Chemical Geology* **54**, 185-201.

911 Harrison, T. M. & Watson, E. B. (1984). The Behavior of Apatite during Crustal Anatexis -
912 Equilibrium and Kinetic Considerations. *Geochimica Et Cosmochimica Acta* **48**, 1467-1477.

913 Harrison, T. M., Watson, E. B. & Aikman, A. B. (2007). Temperature spectra of zircon
914 crystallization in plutonic rocks. *Geology* **35**, 635-638.

915 Hawkesworth, C. J. & Kemp, A. I. S. (2006). Using hafnium and oxygen isotopes in zircons
916 to unravel the record of crustal evolution. *Chemical Geology* **226**, 144-162.

917 Hayden, L. A. & Watson, E. B. (2007). Rutile saturation in hydrous siliceous melts and its
918 bearing on Ti-thermometry of quartz and zircon. *Earth and Planetary Science Letters* **258**,
919 561-568.

920 Hayden, L. A., Watson, E. B. & Wark, D. A. (2008). A thermobarometer for sphene
921 (titanite). *Contributions to Mineralogy and Petrology* **155**, 529-540.

922 Heaman, L. M., Bowins, R. & Crocket, J. (1990). The Chemical-Composition of Igneous
923 Zircon Suites - Implications for Geochemical Tracer Studies. *Geochimica Et Cosmochimica*
924 *Acta* **54**, 1597-1607.

925 Horie, K., Hidaka, H. & Gauthier-Lafaye, F. (2008). Elemental distribution in apatite, titanite
926 and zircon during hydrothermal alteration: Durability of immobilization mineral phases for
927 actinides. *Physics and Chemistry of the Earth* **33**, 962-968.

928 Hoskin, P. W. O., Kinny, P. D., Wyborn, D. & Chappell, B. W. (2000). Identifying accessory
929 mineral saturation during differentiation in granitoid magmas: an integrated approach.
930 *Journal of Petrology* **41**, 1365-1396.

931 Hoskin, P. W. O. & Schaltegger, U. (2003). The composition of zircon and igneous and
932 metamorphic petrogenesis. In: Hanchar, J. M. & Hoskin, P. W. O. (eds.) *Zircon*. Washington:
933 Mineralogical Soc America, 27-62.

934 Jennings, E. S., Marschall, H. R., Hawkesworth, C. J. & Storey, C. D. (2011).
935 Characterization of magma from inclusions in zircon: Apatite and biotite work well, feldspar
936 less so. *Geology* **39**, 863-866.

937 Kocks, H., Strachan, R.A., Evans, J.A. & Fowler, M.B. (2013). Contrasting magma
938 emlacement mechanism within Rogart igneous complex, NW Scotland, record the switch
939 from regional contraction to strike-slip during Caledonian orogeny. *Geological Magazine*,
940 **Accepted**.

941 Kosler, J. & Sylvester, P. J. (2003). Present trends and the future of zircon in geochronology:
942 Laser ablation ICPMS. *Zircon* **53**, 243-275.

943 Larsen, L. H. (1973). Measurement of Solubility of Zircon (Zrsio4) in Synthetic Granitic
944 Melts. *Transactions-American Geophysical Union* **54**, 479-&.

945 Luhr, J. F., Carmichael, I. S. E. & Varekamp, J. C. (1984). the 1982 eruptions of el-chichon
946 volcano, chiapas, mexico - mineralogy and petrology of the anhydrite-bearing pumices.
947 *Journal of Volcanology and Geothermal Research* **23**, 69-108.

948 Marks, M. A. W., Wenzel, T., Whitehouse, M. J., Loose, M., Zack, T., Barth, M., Worgard,
949 L., Krasz, V., Eby, G. N., Stosnach, H. & Markl, G. (2012). The volatile inventory (F, Cl, Br,
950 S, C) of magmatic apatite: An integrated analytical approach. *Chemical Geology* **291**, 241-
951 255.

952 Martin, H., Moyen, J.-F. Rapp, & R. (2009). The sanukitoid series: Magmatism at the
953 Archaean-Proterozoic transition. *Royal Society of Edinburgh Transactions* **100**, 15–33.

954 McAteer, C. A., Daly, J. S., Flowerdew, M. J., Connelly, J. N., Housh, T. B. & Whitehouse,
955 M. J. (2010). Detrital zircon, detrital titanite and igneous clast U-Pb geochronology and
956 basement-cover relationships of the Colonsay Group, SW Scotland: Laurentian provenance
957 and correlation with the Neoproterozoic Dalradian Supergroup. *Precambrian Research* **181**,
958 21-42.

959 McDonough, W. F. & Sun, S. S. (1995). The Composition of the Earth. *Chemical Geology*
960 **120**, 223-253.

961 McLeod, G. W., Dempster, T. J. & Faithfull, J. W. (2011). Deciphering Magma-Mixing
962 Processes Using Zoned Titanite from the Ross of Mull Granite, Scotland. *Journal of*
963 *Petrology* **52**, 55-82.

964 Miles, A. J., Graham, C. M., Hawkesworth, C. J., Gillespie, M. R. & Hinton, R. W. (2013).
965 Evidence for distinct stages of magma history recorded by the compositions of accessory
966 apatite and zircon. *Contributions to Mineralogy and Petrology* **166**, 1-19.

967 Miller, C. F., McDowell, S. M. & Mapes, R. W. (2003). Hot and cold granites? Implications
968 of zircon saturation temperatures and preservation of inheritance. *Geology* **31**, 529-532.

969 Murphy, J. B. (2013). Appinite suites: A record of the role of water in the genesis, transpport,
970 emplacement and crystallization of magma. *Earth-Science Reviews* **119**, 35-59.

971 Paterson, B. A. & Stephens, W. E. (1992). Kinetically Induced Compositional Zoning in
972 Titanite - Implications for Accessory-Phase Melt Partitioning of Trace-Elements.
973 *Contributions to Mineralogy and Petrology* **109**, 373-385.

974 Paterson, B. A., Stephens, W. E. & Herd, D. A. (1989). Zoning in Granitoid Accessory
975 Minerals as Revealed by Backscattered Electron Imagery. *Mineralogical Magazine* **53**, 55-
976 61.

977 Pearce, N. J. G., Perkins, W. T., Westgate, J. A., Gorton, M. P., Jackson, S. E., Neal, C. R. &
978 Chenery, S. P. (1997). A compilation of new and published major and trace element data for
979 NIST SRM 610 and NIST SRM 612 glass reference materials. *Geostandards Newsletter-the*
980 *Journal of Geostandards and Geoanalysis* **21**, 115-144.

981 Piccoli, P., Candela, P. & Rivers, M. (2000). Interpreting magmatic processes from accessory
982 phases: titanite - a small-scale recorder of large-scale processes. *Transactions of the Royal*
983 *Society of Edinburgh-Earth Sciences* **91**, 257-267.

984 Prowatke, S. & Klemme, S. (2005). Effect of melt composition on the partitioning of trace
985 elements between titanite and silicate melt. *Geochimica Et Cosmochimica Acta* **69**, 695-709.

986 Prowatke, S. & Klemme, S. (2006). Trace element partitioning between apatite and silicate
987 melts. *Geochimica Et Cosmochimica Acta* **70**, 4513-4527.

988 Rock, N.M.S. (1984). Nature and origin of cal-alkaline lamprophyre: minettes, vogesites,
989 kersantites and spessartites. *Transactions of the Royal Society of Edinburgh, Earth Sciences*
990 **74**, 193-227.

991 Rogers, G. & Dunning, G. R. (1991). Geochronology of Appinitic and Related Granitic
992 Magmatism in the W-Highlands of Scotland - Constraints on the Timing of Transcurrent
993 Fault Movement. *Journal of the Geological Society* **148**, 17-27.

994 Sabine, P. A. (1963). The Strontian granite complex, Argyllshire. *Bulletin of the Geological*
995 *Survey* **20**, 6-42.

996 Sha, L. K. & Chappell, B. W. (1999). Apatite chemical composition, determined by electron
997 microprobe and laser-ablation inductively coupled plasma mass spectrometry, as a probe into
998 granite petrogenesis. *Geochimica Et Cosmochimica Acta* **63**, 3861-3881.

999 Smith, M. P., Storey, C. D., Jeffries, T. E. & Ryan, C. (2009). In Situ U-Pb and Trace
1000 Element Analysis of Accessory Minerals in the Kiruna District, Norrbotten, Sweden: New
1001 Constraints on the Timing and Origin of Mineralization. *Journal of Petrology* **50**, 2063-2094.

1002 Soper, N. J. (1963). The structure of the Rogart igneous complex, Sutherland, Scotland.
1003 *Quarterly Journal of the Geological Society* **119**, 445-478.

1004 Soper, N. J. (1986). The newer granite problem - a geotectonic view. *Geological Magazine*
1005 **123**, 227-236.

1006 Soper, N. J., England, R. W., Snyder, D. B. & Ryan, P. D. (1992). The Iapetus Suture Zone in
1007 England, Scotland and Eastern Ireland - a Reconciliation of Geological and Deep Seismic
1008 Data. *Journal of the Geological Society* **149**, 697-700.

1009 Stephens, W.E. & Halliday, A.N. (1984). Geochemical contrasts between late Caledonian
1010 granitoid pluton and morthern, central and southern Scotland. *Transactions of the Royal*
1011 *Society of Edinburgh*, Earth Sciences **75**, 259-273.

1012 Stephenson, D., Bevins, R. E., Millward, D., Highton, A. J., Parsons, I., Stone, P. &
1013 Wadsworth, W. J. (1999). Caledonian igneous rocks of Great Britain. *Geological*
1014 *Conservation Review Series* **17**, 648.

1015 Tarney, J. & Jones, C. E. (1994). Trace-Element Geochemistry of Orogenic Igneous Rocks
1016 and Crustal Growth-Models. *Journal of the Geological Society* **151**, 855-868.

1017 Tepper, J. H. & Kuehner, S. M. (1999). Complex zoning in apatite from the Idaho batholith:
1018 A record of magma mixing and intracrystalline trace element diffusion. *American*
1019 *Mineralogist* **84**, 581-595.

1020 Tiepolo, M., Oberti, R. & Vannucci, R. (2002). Trace-element incorporation in titanite:
1021 constraints from experimentally determined solid/liquid partition coefficients. *Chemical*
1022 *Geology* **191**, 105-119.

1023 Tyler, I. M. & Ashworth, J. R. (1983). The Metamorphic Environment of the Foyers Granitic
1024 Complex. *Scottish Journal of Geology* **19**, 271-285.

1025 Trail, D., Watson, E. B. & Tailby, N. D. (2011). The oxidation state of Hadean magmas and
1026 implications for early Earth's atmosphere. *Nature* **480**, 79-U238.

1027 Watson, E. B. (1979). Zircon Saturation in Felsic Liquids - Experimental Results and
1028 Applications to Trace-Element Geochemistry. *Contributions to Mineralogy and Petrology*
1029 **70**, 407-419.

1030 Watson, E. B. & Harrison, T. M. (1983). Zircon Saturation Revisited - Temperature and
1031 Composition Effects in a Variety of Crustal Magma Types. *Earth and Planetary Science*
1032 *Letters* **64**, 295-304.

1033 Watson, E. B. & Liang, Y. (1995). A simple model for sector zoning in slowly grown
1034 crystals: Implications for growth rate and lattice diffusion, with emphasis on accessory
1035 minerals in crustal rocks. *American Mineralogist* **80**, 1179-1187.

1036 Wiedenbeck, M., Hanchar, J. M., Peck, W. H., Sylvester, P., Valley, J., Whitehouse, M.,
1037 Kronz, A., Morishita, Y., Nasdala, L., Fiebig, J., Franchi, I., Girard, J. P., Greenwood, R. C.,
1038 Hinton, R., Kita, N., Mason, P. R. D., Norman, M., Ogasawara, M., Piccoli, R., Rhede, D.,

Satoh, H., Schulz-Dobrick, B., Skar, O., Spicuzza, M. J., Terada, K., Tindle, A., Togashi, S., Vennemann, T., Xie, Q. & Zheng, Y. F. (2004). Further characterisation of the 91500 zircon crystal. *Geostandards and Geoanalytical Research* **28**, 9-39.

Figure Captions

Figure 1: Map from the Northern Highland region (Scotland) modified after Fowler *et al.* (2008) showing samples localities and ages from Roger & Dunning (1991) and Brown *et al.* (1968).

Figure 2: Back-scattered images of titanite crystals in Strontian locality (a-b, f) and Rogart locality (c-e, g). (a-b) Titanites show core rim zoning from fir-tree bright core toward dark rim. (c-e) Titanites show different zones with multiple dissolution-reprecipitaion features. (f-g) Appinitic titanites from Strontian and Rogart respectively show typical sector zoning.

Figure 3: Cathodoluminescence images of apatites crystals for granitoids (a-e) and appinites (f-g) samples from (a-b, f) Strontian locality and (c-e, g) Rogart locality. (a-b) Apatites from Strontian granitoids are made up of oscillatory cores and unoscillatory rims. (c-e) Apatites from Rogart granitoids are characterised by an oscillatory zoning. (f-g) Apatites from appinitic samples are characterised by a main dark zone (type 1) which can be dissolved at its rim and reprecipitate a bright rim (type 2).

Figure 4: Cathodoluminescence images of zircons in Strontian locality (granitoids: a-b; appinite: f) and in Rogart locality (granitoids: c-e; appinite: g). (a-f) Zircons are characterized by a typical igneous oscillatory zoning. (g) Typical altered and cracked Rogart appinite

zircon.

Figure 5: Chondrite-Normalized REE patterns (using McDonough & Sun (1995) chondrite values) for titanites in (a) Strontian granodiorites (SR1-SR3), (b) Rogart granite (RHG-1) and Tonalites (RT1-R2) and (c) Rogart and Strontian appinites (RA1-SR2). See Table 2 and Supplementary Electronic Material, appendix 2.

Figure 6: Nb content (ppm) versus Gd (ppm) content diagrams for titanite from (a) Strontian and Rogart (b) localities. Analyses reported in this figure are without the FT/bright sector zones analyses (See Table 2; Supplementary data, electronic appendix 2). Reprecipitation analyses are indicated by smaller symbols.

Figure 7: (a) Eu/Eu* versus $(La/Sm)_N$ diagram showing Strontian and Rogart granitoids titanites compositions and appinites titanites compositions. Cores and rims compositions of the different crystals are also reported. (b) Zr content (ppm) versus Y content (ppm) diagram for Rogart and Strontian titanites.

Figure 8: Chondrite-Normalized REE patterns for apatites in (a) Strontian granodiorites (SR1-SR3), (b) Rogart granite (RHG-1) and Tonalites (RT1-R2) and (c) Rogart and Strontian appinites (RA1-SR2). See Table 3 and Supplementary Data, electronic appendix 3.

Figure 9: (a-b) $(La/Sm)_N$ versus Gd (ppm) content diagrams for apatites from (a) Strontian and (b) Rogart localities. (c) Ce content (ppm) versus Y (ppm) content diagram for apatites from Strontian and Rogartlocalities. Analyses of cores and rims for granitoids and appinitic samples are reported in these figures.

Figure 10: Chondrite-Normalized REE patterns for zircons in (a) Strontian granodiorites (SR1-SR3) and appinite (SR2), (b) Rogart granite (RHG-1) and Tonalites (RT1-R2) and (c) Rogart and Strontian appinites (RA1-SR2). See Table 4 and Supplementary Data, electronic appendix 4.

Figure 11: (a) Selected mineral/ melt partition coefficient for apatite and titanite for felsic and mafic compositions (From Prowatke & Klemme, 2005, 2006). (b) Nb/Ta ratio versus Y (ppm) content diagram for titanites from Strontian and Rogart localities showing the record of mixing event in titanite rims of Strontian granitoids (grey field).

Figure 12: (a-b) Summary of the crystallisation history of titanite and apatite in felsic and mafic samples from Rogart and Strontian. (c) Diagram discriminating the host rock nature (felsic from mafic) using Sr/Sm ratio in apatite and titanite from a given samples. Each sample point represents the average composition for core and rim (Supplementary data, appendices 2-3).

Figure 13: Plots for trace elements content in apatite (a-b) and titanite (c) versus whole rock data (Fowler *et al.*, 2001, 2008). Average compositions for cores and rims have been plotted for each sample (See Electronic Supplementary data, Appendices 2-3). (a) Average apatites values from Hoskin *et al.* (2000, cross symbols), Belousova *et al.* (2002a, empty circles); Chu *et al.* (2009, plus symbols); Jennings *et al.* (2010) and Jenning & Marschall (personal communication; empty triangles) have been reported. (c-d) Available values from Hoskin *et al.* (2000, cross symbols) have been reported. (d) Sr_{Ap} versus Sr_{Tit} correlating in Rogart and Strontian samples.

Figure 14: (a-b) Plots of selected whole rock trace elements content versus SiO_2 in the whole rock for the different samples studied in this contribution. Data available in Fowler *et al.* (2001, 2008). (c,e) Plots of Sr (ppm) and V (ppm) contents in apatite versus SiO_{2WR}. (d) Plots of Sr (ppm) contents in titanite versus SiO_{2WR}. Compositions of these elements within apatites and titanites are evolving with SiO_{2WR} content and seems to reflect the degree of fractionation of the samples.(c) Literature values have been reported. See figure 13 for references.

Figure 15: Chondrite-Normalized REE patterns modelled by back-calculating whole rock data using titanites and apatites average cores compositions in Rogart samples (Electronic Supplementary Material, Appendices 2-3). Calculations have been performed using $D_{apatite/melt}$ and $D_{titanite/melt}$ from Luhr *et al.* (1984) for granitoids (a-c) and from Prowatke & Klemme (2005, 2006) for appinite (d). Supplementary Data, electronic appendix 5. XRF whole rock data are from Fowler *et al.* (2001) of the same samples.

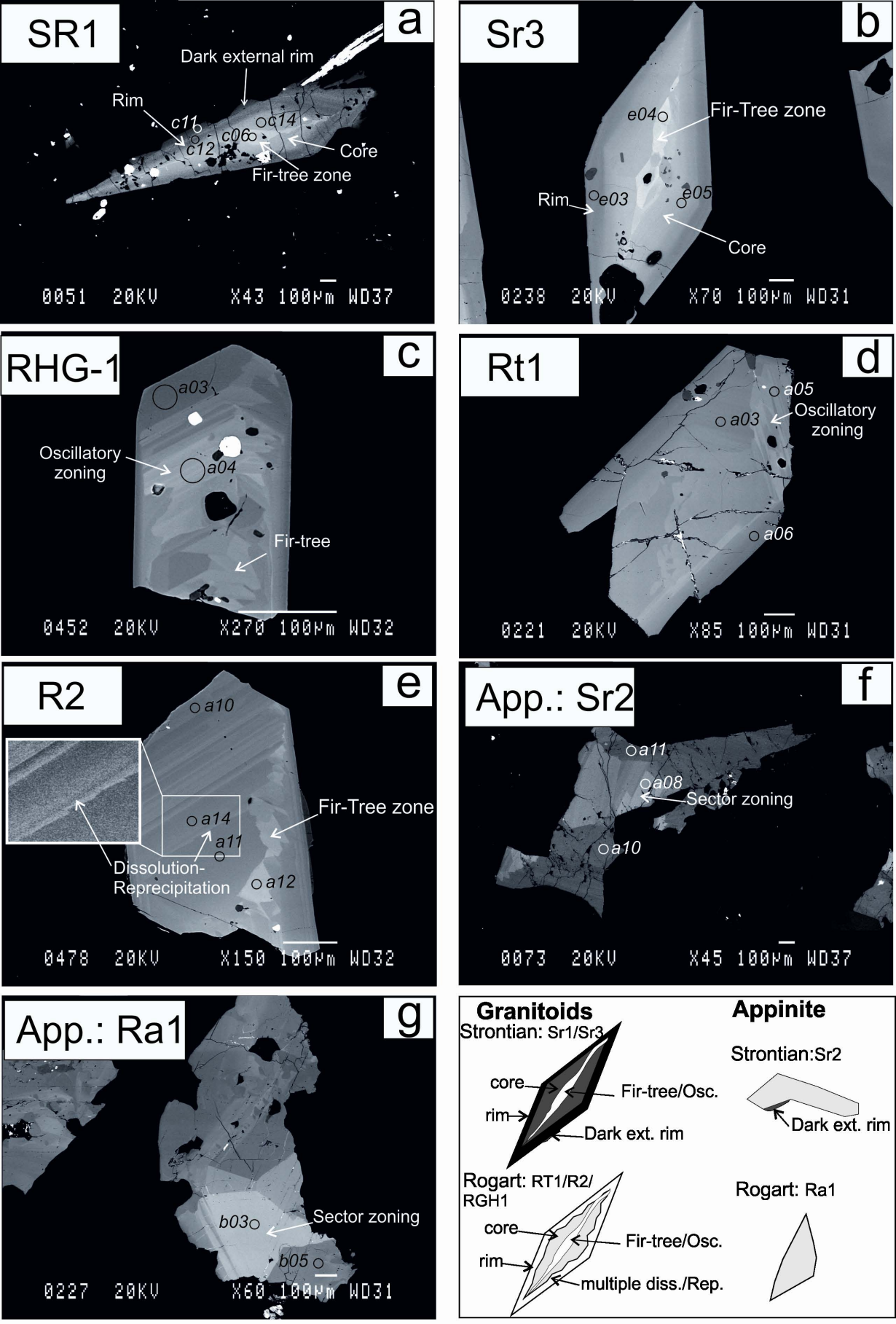

Fig. 2, Bruand et al. (2013)

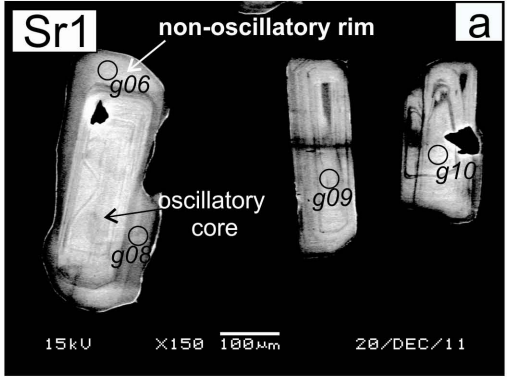

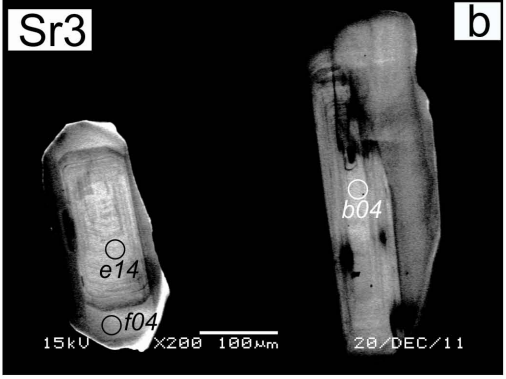

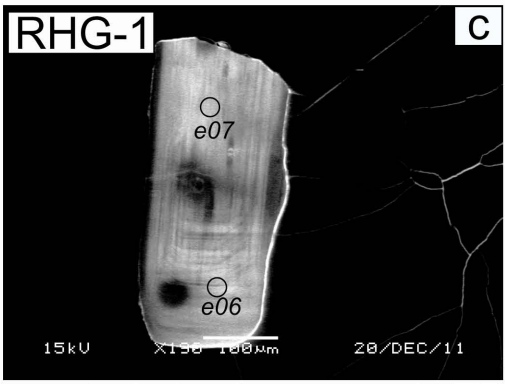

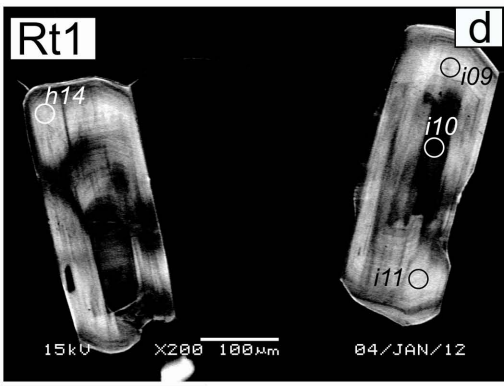

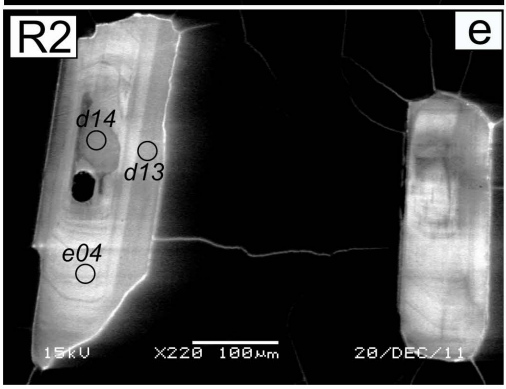

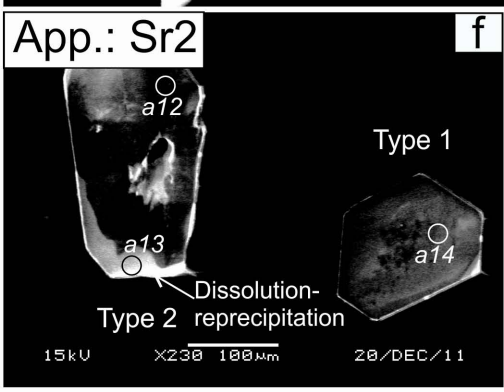

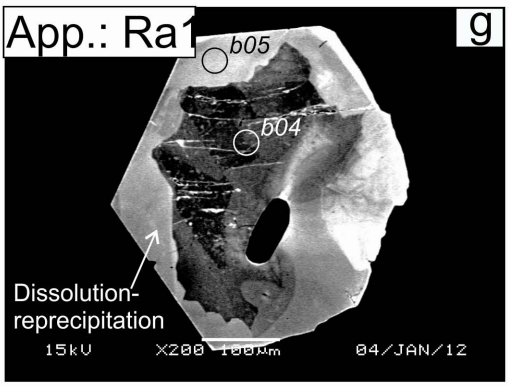

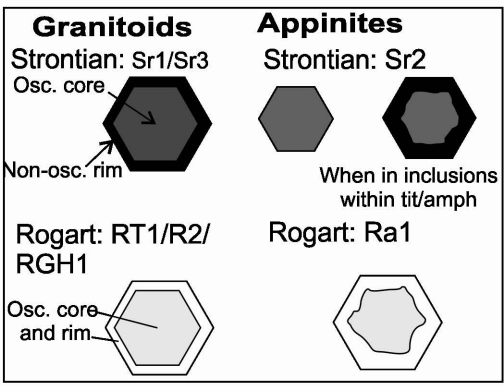

Fig.3, Bruand et al. (2013)

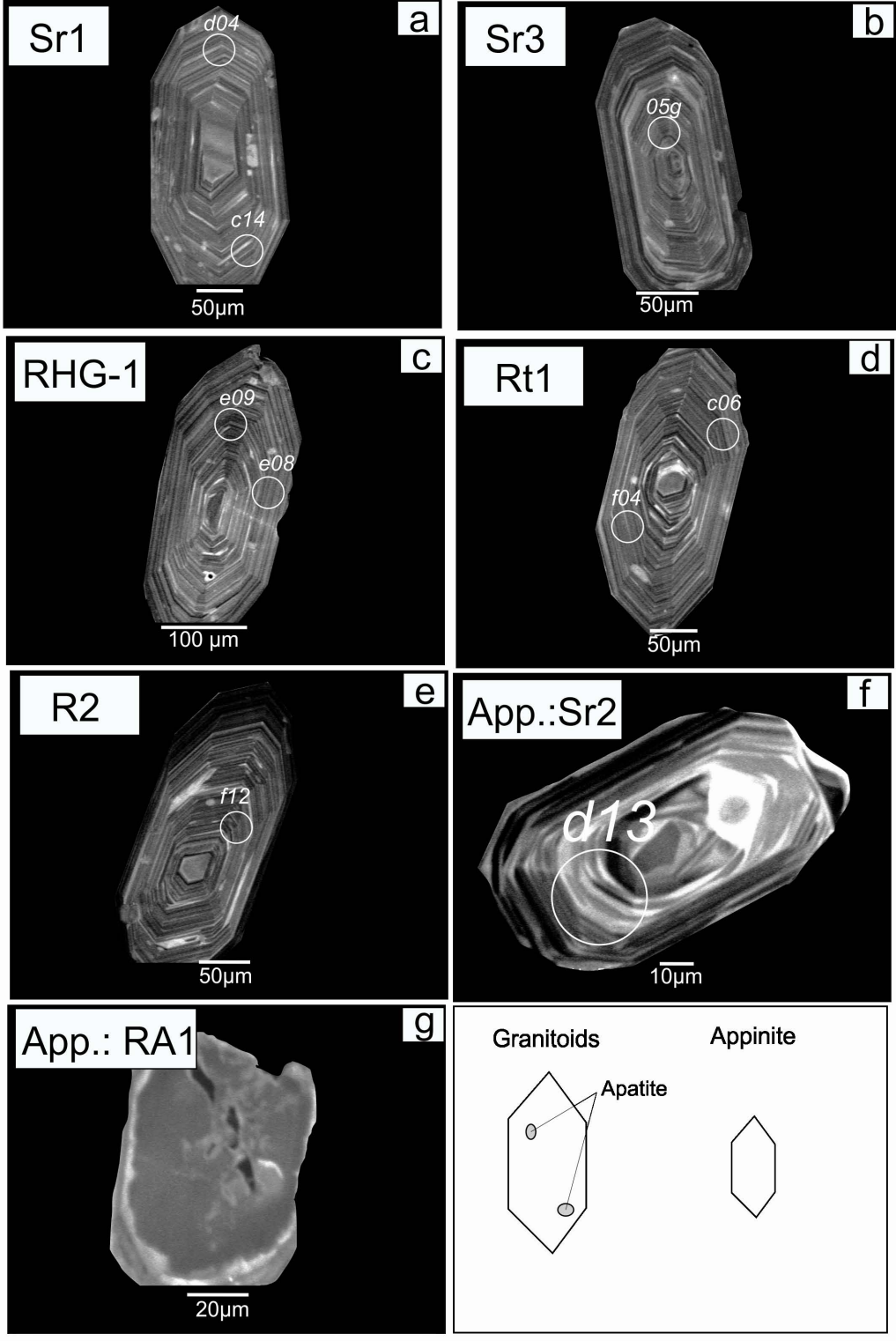

Fig. 4, Bruand et al. (2013)

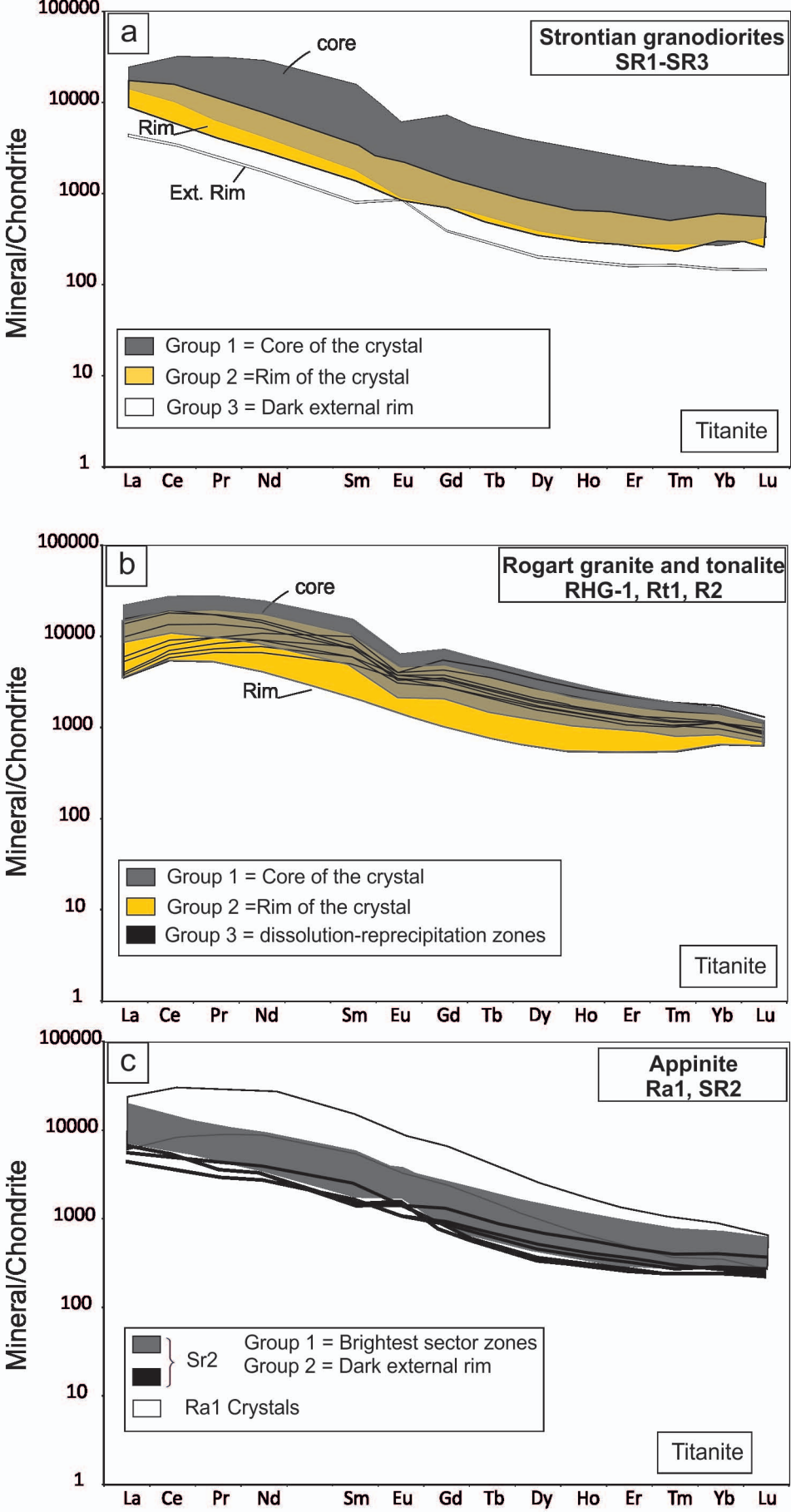

Fig. 5, Bruand et al. (2013)

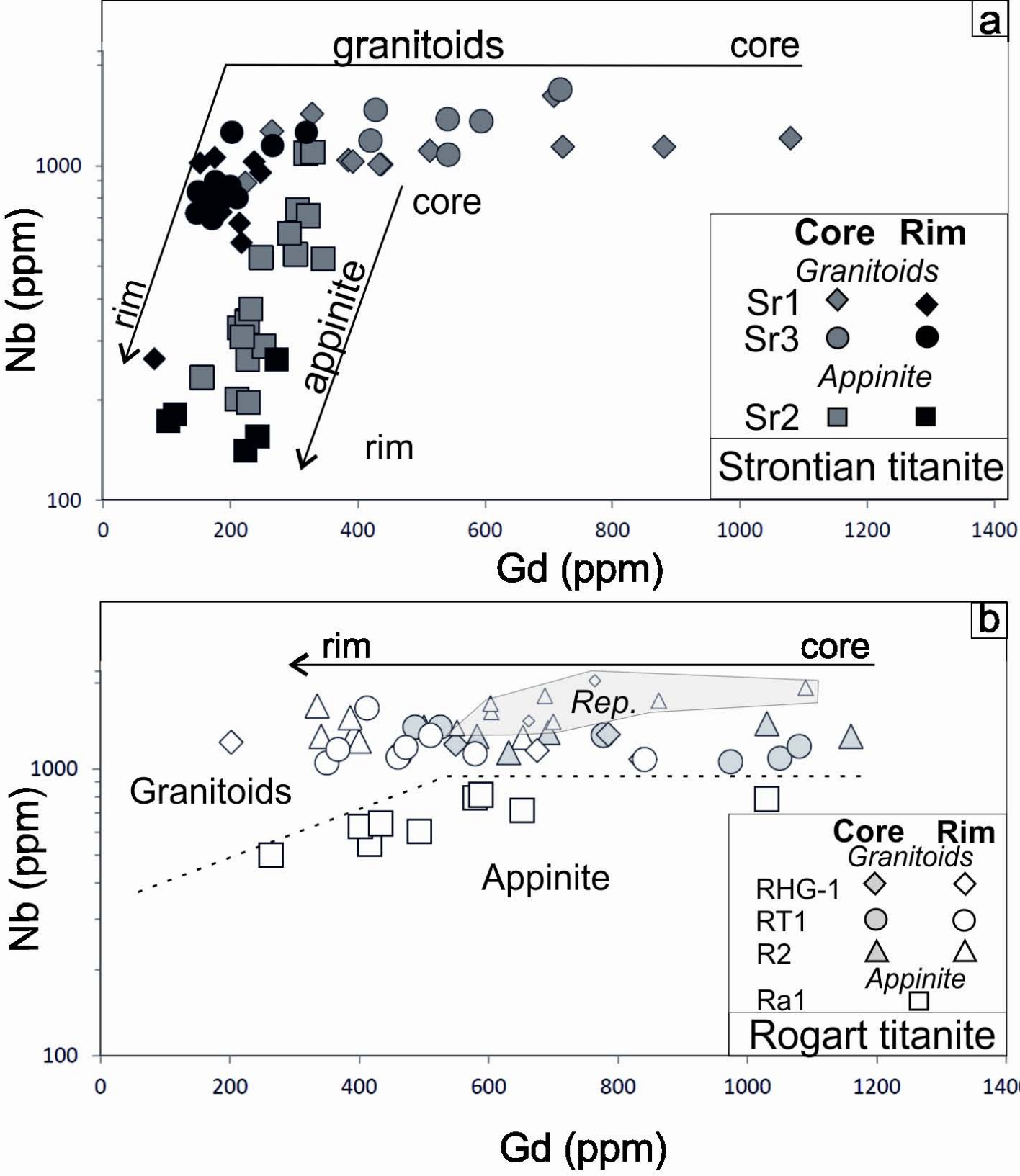

Figure 6, Bruand et al. (2013)

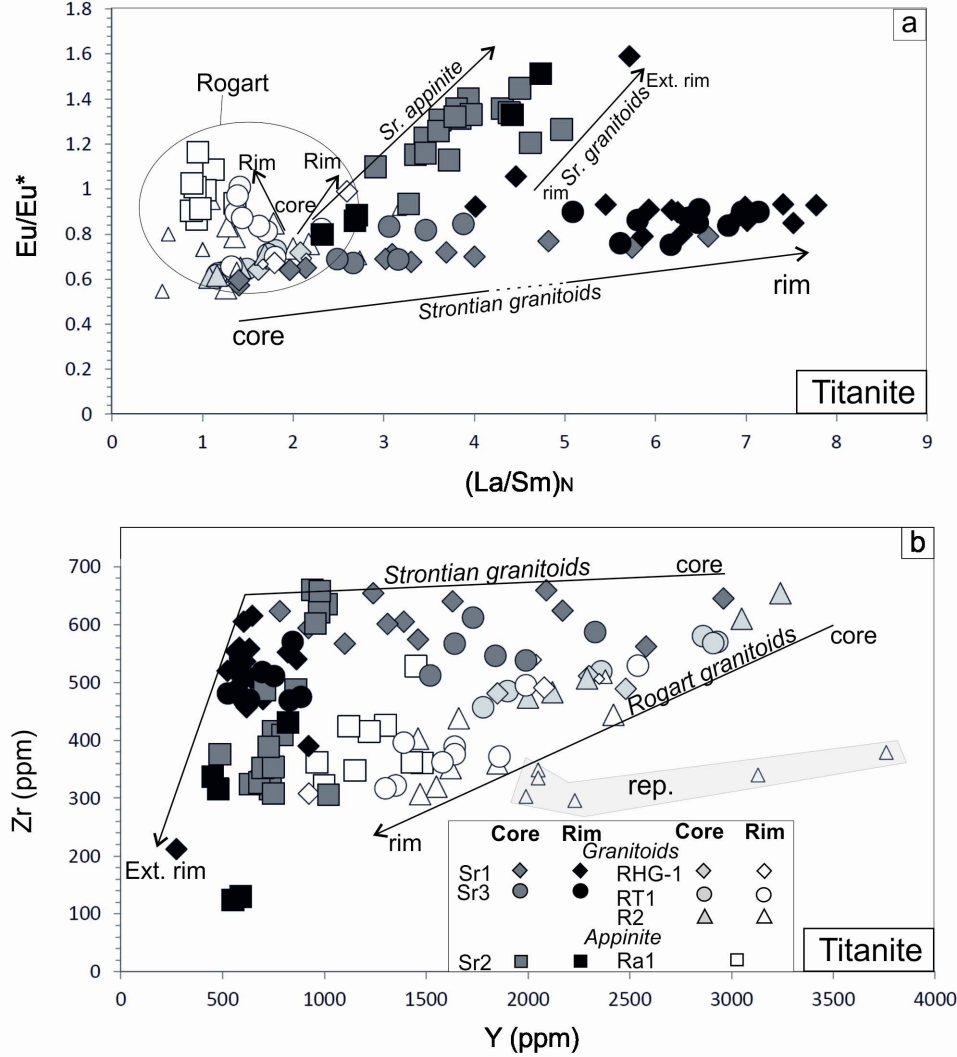

Figure 7, Bruand et al. (2013)

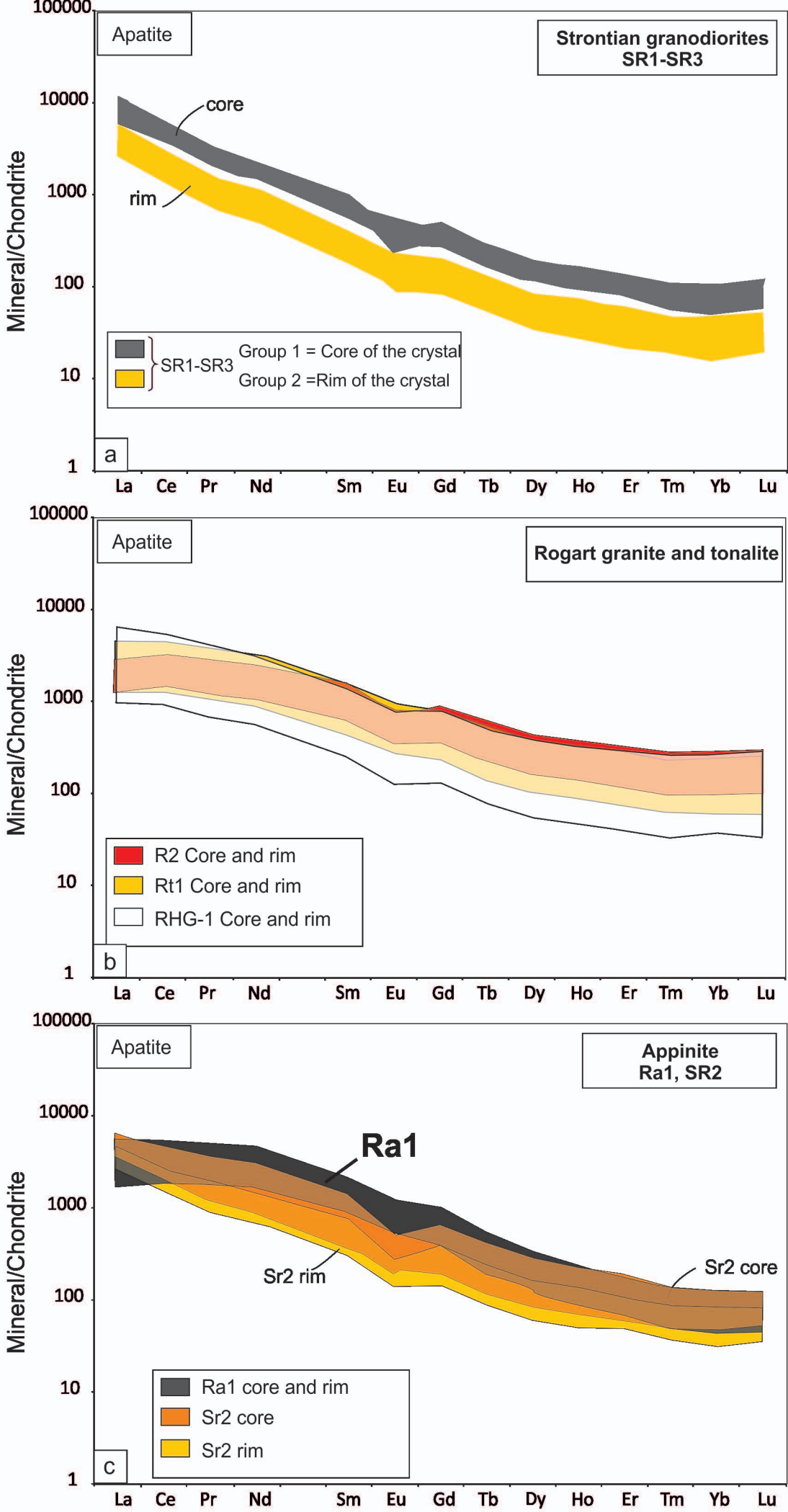

Figure 8, Bruand et al. (2013)

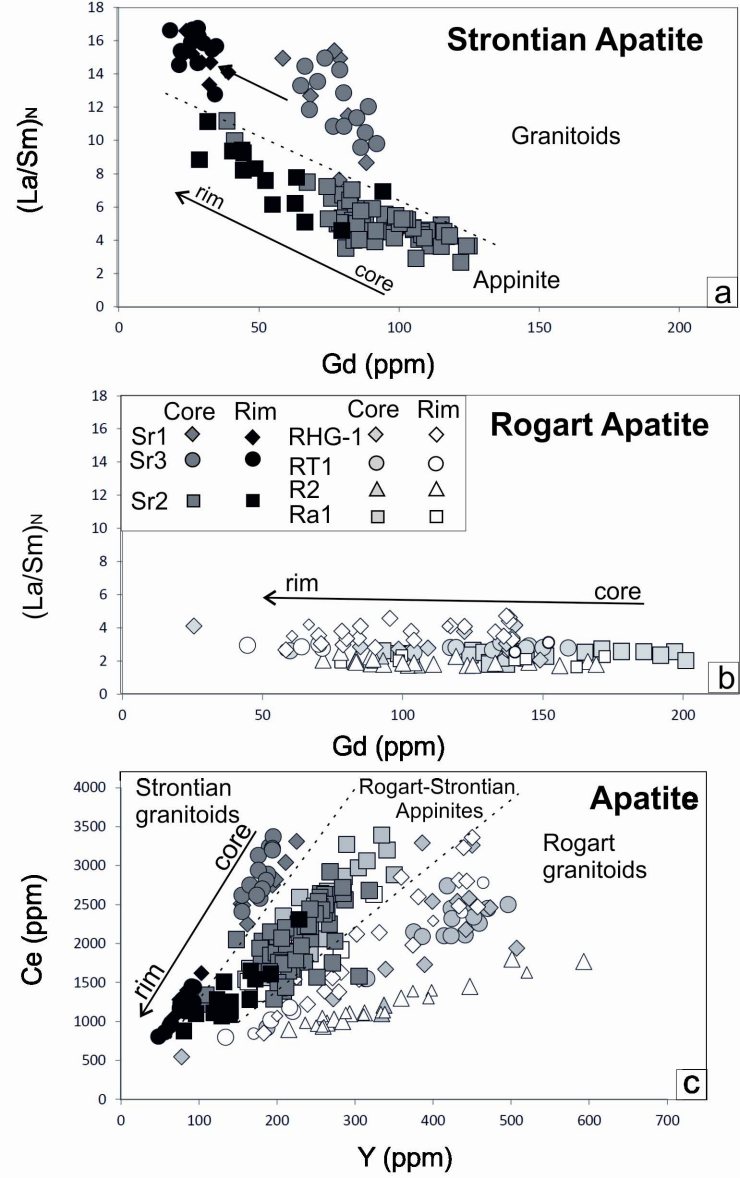

Figure 9, Bruand et al. (2013)

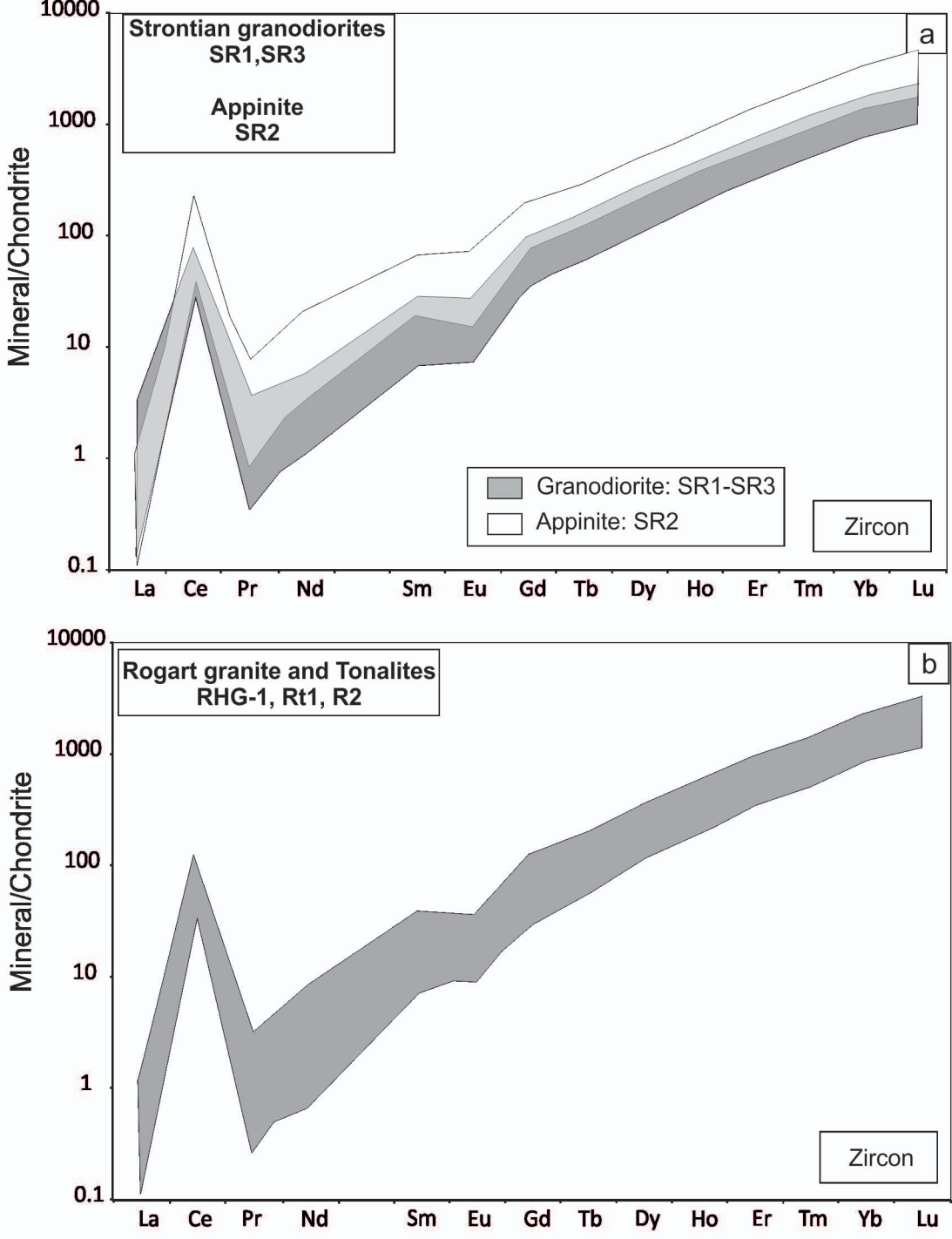

Fig. 10, Bruand et al. (2013)

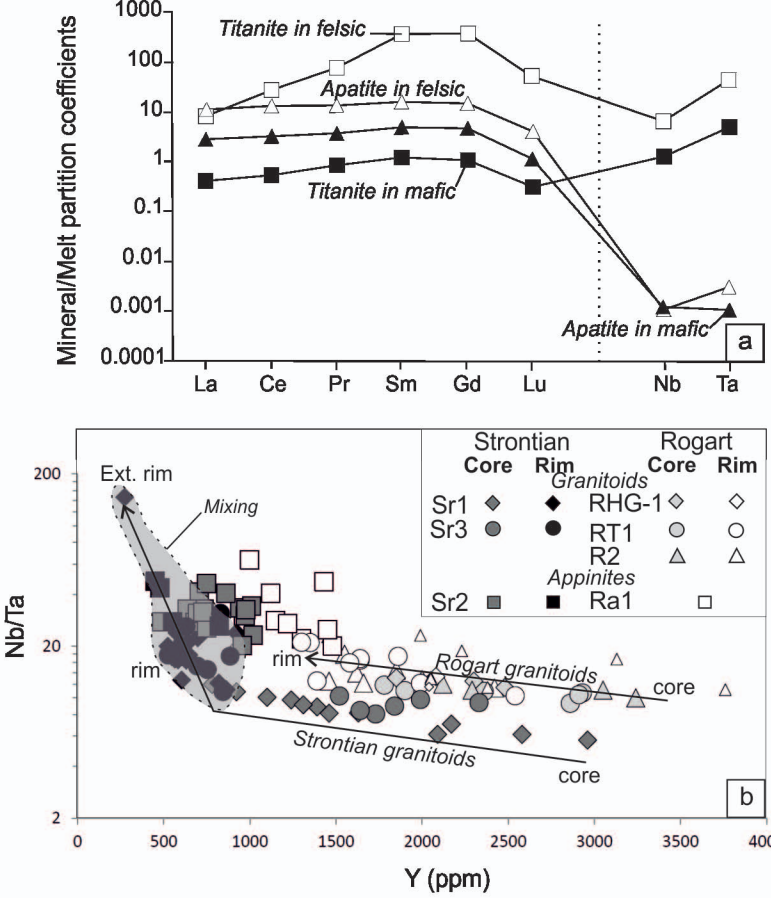

Figure 11, Bruand et al. (2013)

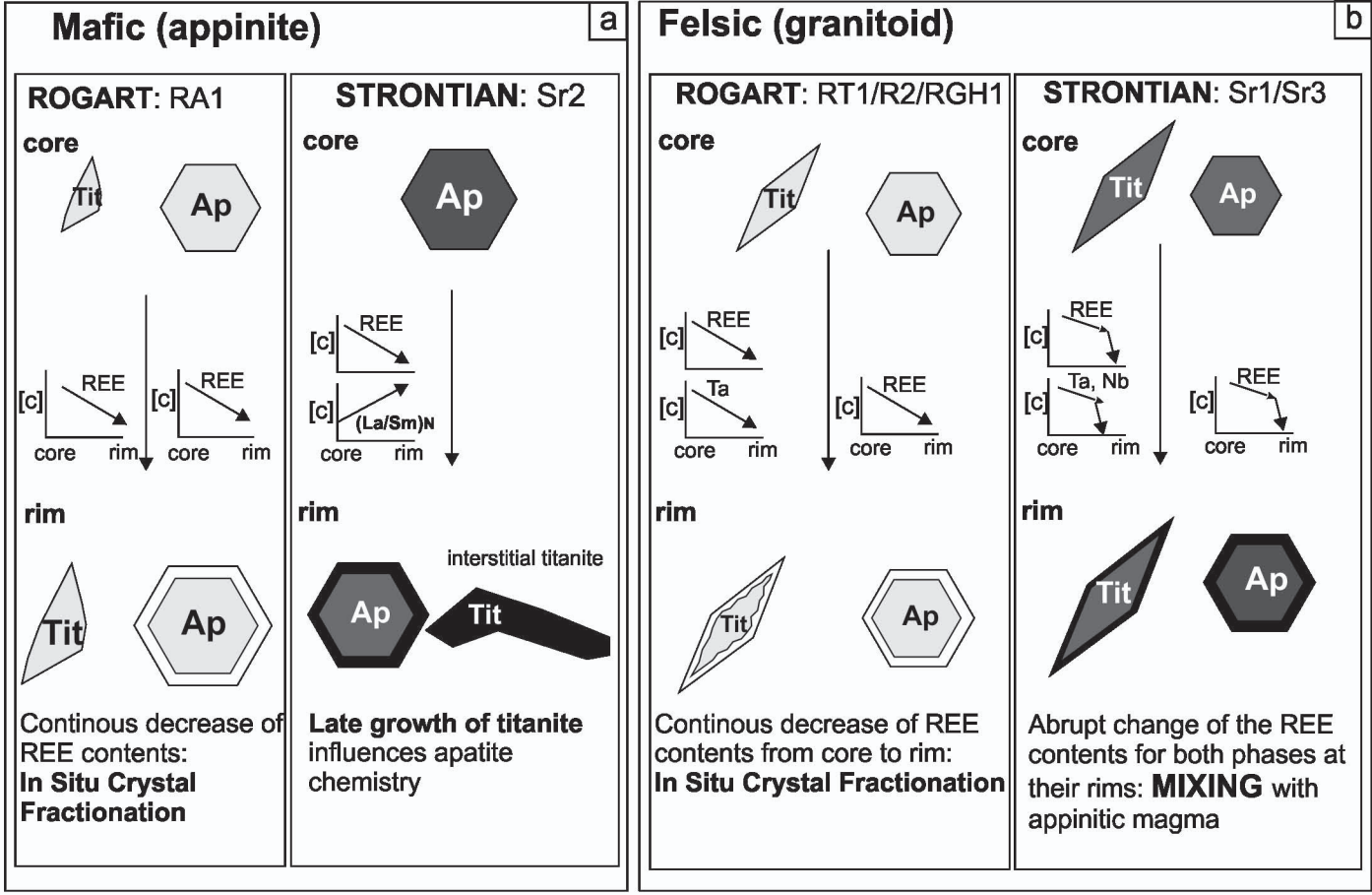

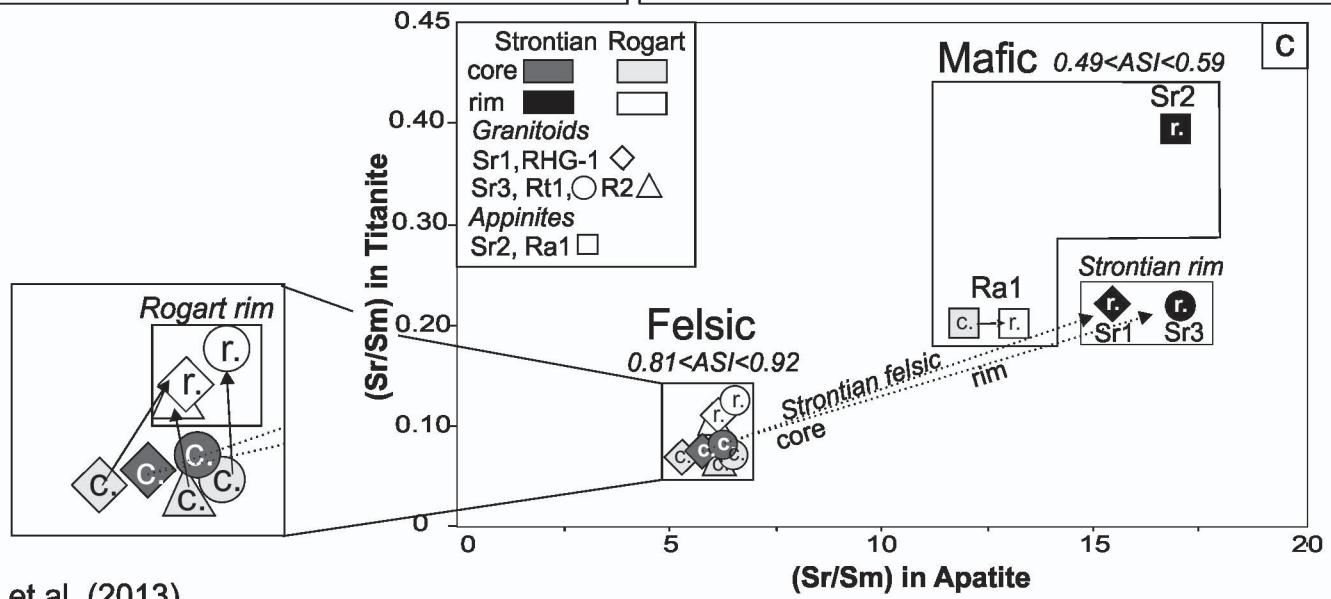

Figure 12, Bruand et al. (2013)

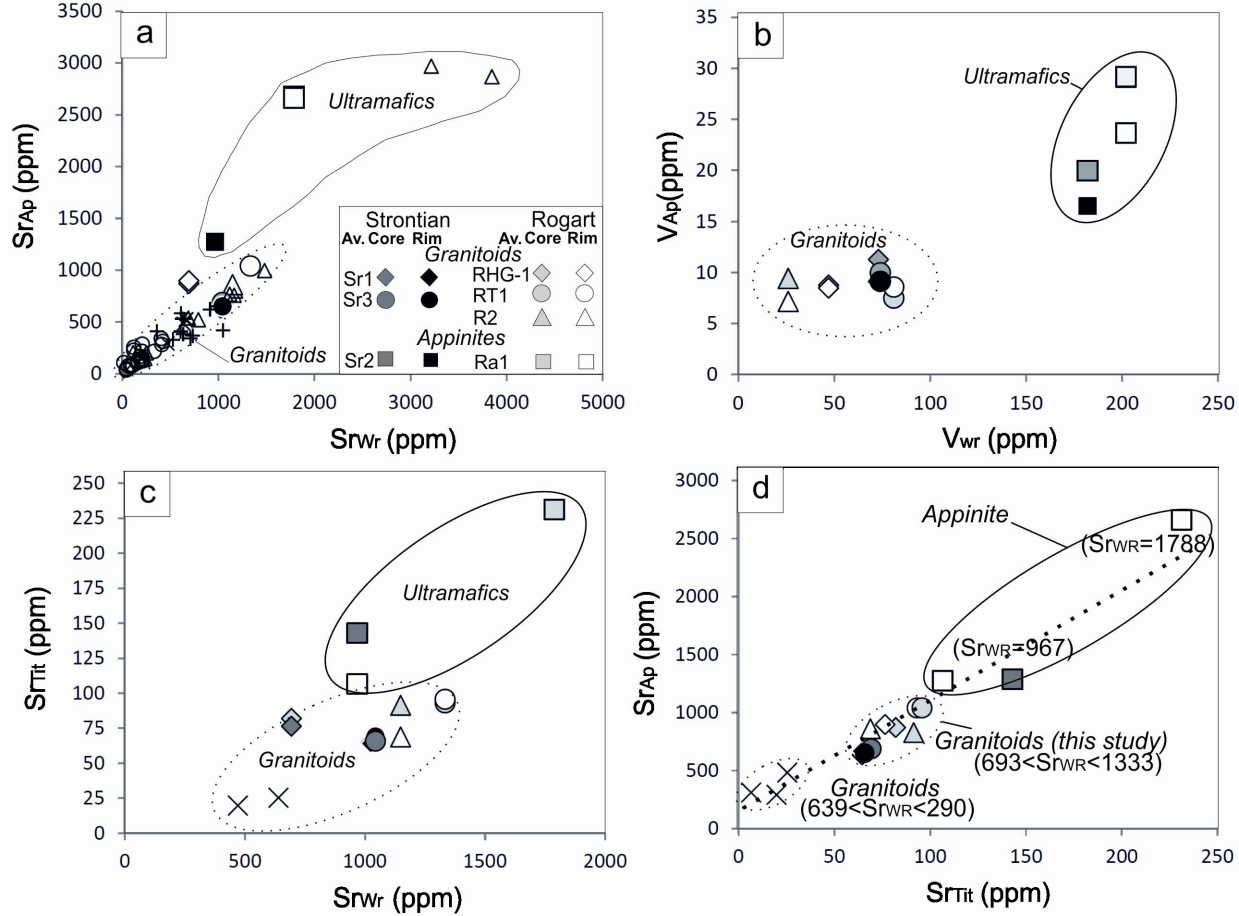

Fig. 13, Bruand et al. (2013)

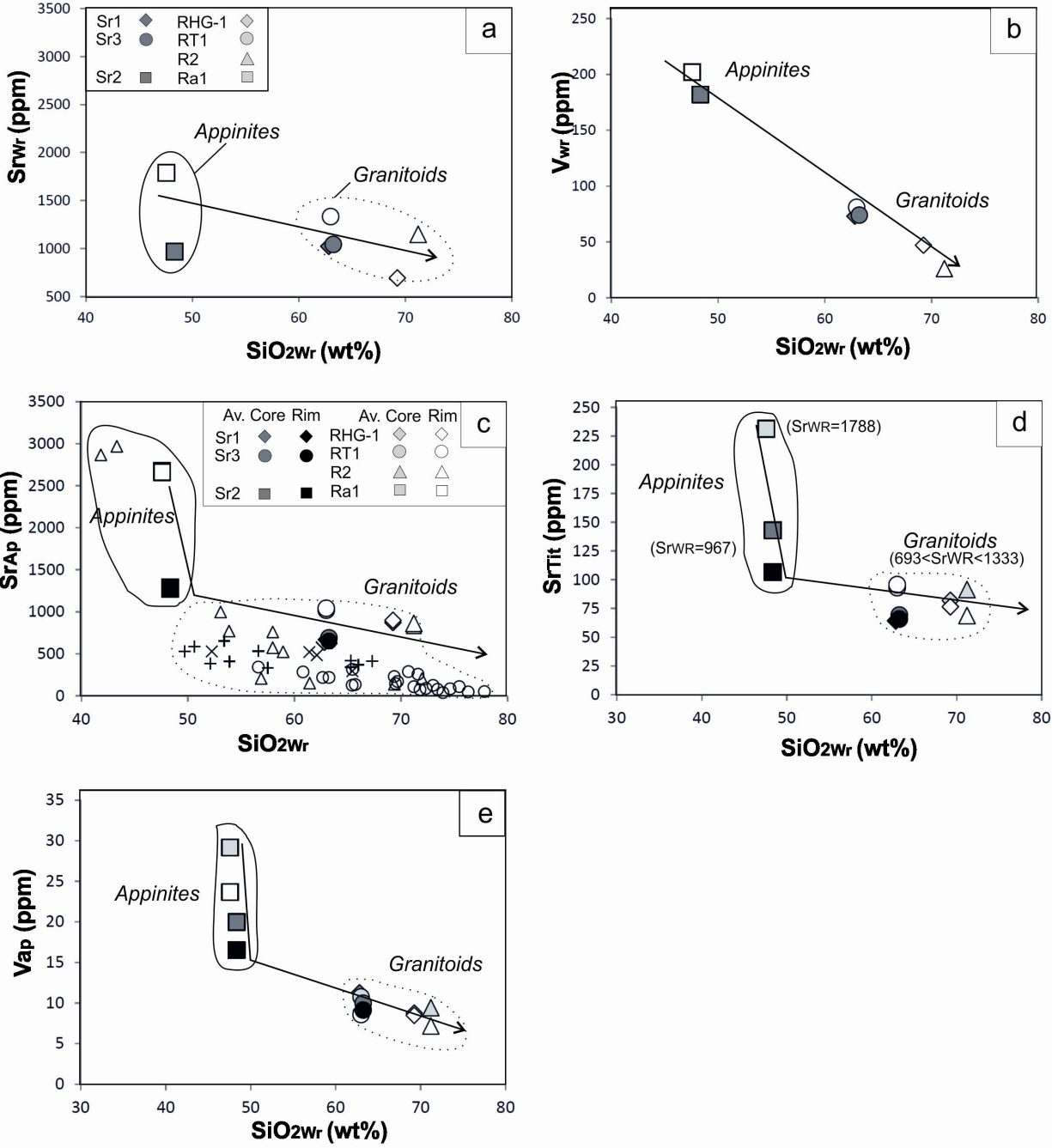

Figure 14, Bruand et al. (2013)

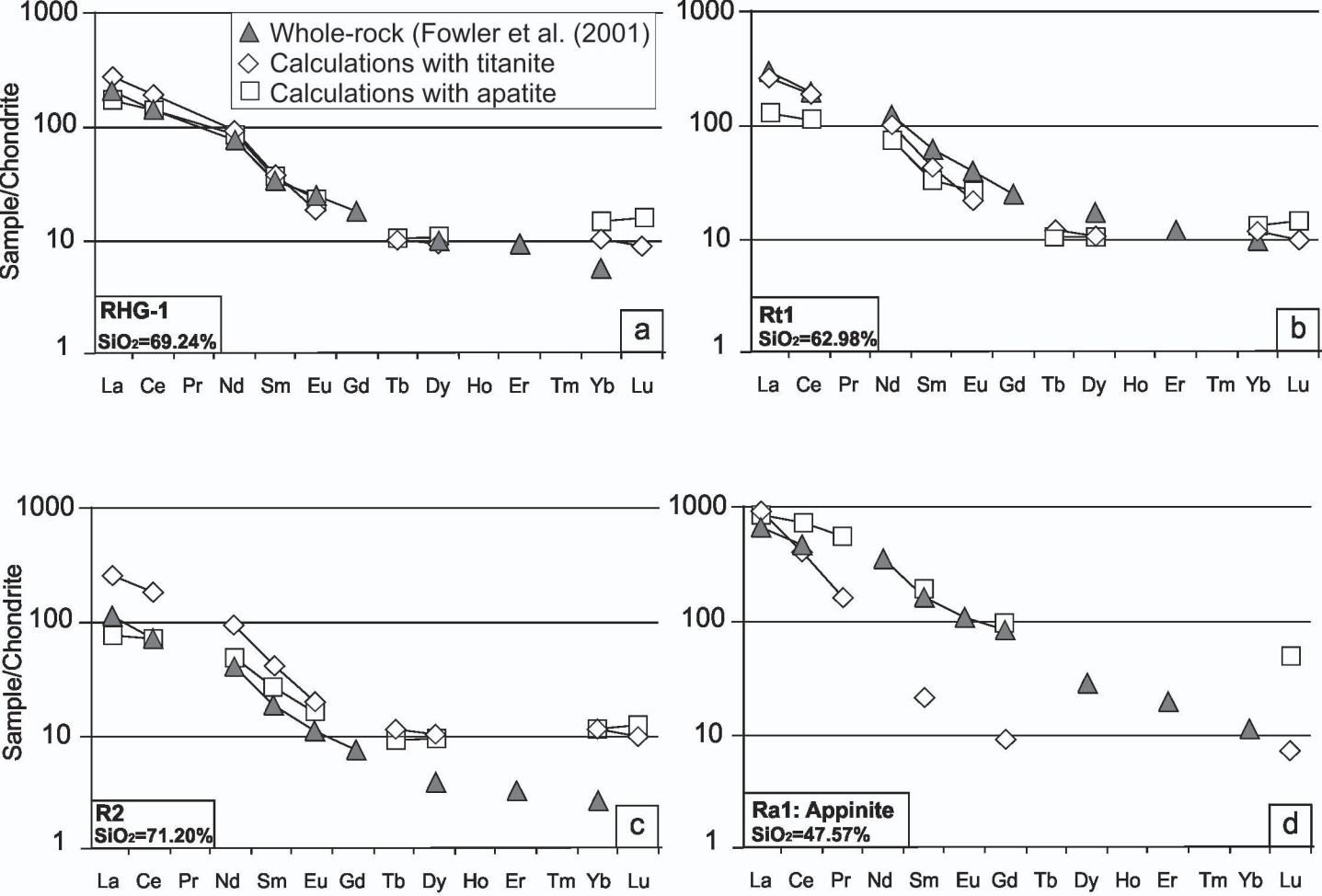

Fig. 15, Bruand et al. (2013)

Table 1: Estimated modal proportion of titanite, apatite and zircon in the Rogart and Strontian samples.

	Rock Type	**Grid Reference**	**Mineralogy**	**Titanite**	**Apatite**	**Zircon**
Strontian				*Modal proportion*		
SR1	Granodiorite	NM795611	hbl-fsp-bt-qz	2-3%	1%	<1%
SR2	Appinite	NM786611	hbl-fsp-bt +/- cal	5%	1-2%	<0.5%
SR3	Granodiorite	NM779607	hbl-fsp-bt-qz +/- aln	1-2%	<1%	<1%
Rogart						
RHG-1	Granite	NC671046	fsp-bt-qz +/- chl-cal	1-2%	1-2%	<1%
R2	Tonalite	NC709029	hbl-fsp-qz-bt-ms +/- aln	1%	<1%	<1%
RT1	Tonalite	NC741065	hbl-fsp-qz-bt-ms +/- aln	1-2%	1%	<1%
RA1	Appinite	NC702026	hbl-cpx-fsp-bt +/- cal	3%	5%	<0.3%

The grid referencing system used is the Ordnance Survey National Grid reference system using OSGB 36 datum. Mineral abbreviations are after Whitney and Evans (2010).

Table2: Representative analyses of titanite. See entire dataset in Electronic Supplementary Data

RA1 Sample - APPINITE

Mount	**SiO_2**	**CaO**	**TiO_2**	**V**	**Cr**	**Sr**	**Y**	**Zr**	**Nb**	**La**	**Ce**	**Pr**	**Nd**	**Sm**	**Eu**	**Gd**	**Tb**	**Dy**	**Ho**	**Er**	**Tm**	**Yb**	**Lu**	**Ta**	**$(Eu/Eu^*)_N$**	**$(La/Sm)_N$**
mr07d09	***28.2***	***26.4***	***29.8***	***1140***	***52***	***257***	***2170***	***731***	***1950***	***3990***	***14100***	***2250***	***11100***	***2170***	***467***	***1230***	***135***	***585***	***88***	***188***	***23***	***134***	***15***	***233***	***0.87***	***20.23***
mr30b03*	***29.9***	***26.0***	***32.2***	***1010***	***46***	***263***	***1990***	***1280***	***2110***	***5290***	***17000***	***2470***	***11300***	***2000***	***454***	***1130***	***119***	***511***	***79***	***167***	***21***	***123***	***14***	***101***	***0.92***	***29.22***
mr30c03	***30.8***	***25.7***	***32.0***	***990***	***46***	***256***	***2190***	***1330***	***2240***	***5420***	***17500***	***2520***	***11900***	***2210***	***488***	***1260***	***136***	***570***	***87***	***189***	***23***	***135***	***16***	***150***	***0.89***	***27.27***
mr30a06	32.4	27.2	33.7	1080	51	217	1300	426	652	2240	8090	1320	6390	1250	337	716	78	335	52	108	13	79	10	30	1.09	1.12
mr30a03	32.7	27.8	33.1	1140	86	219	963	362	416	1340	5190	876	4370	898	199	546	59	257	39	87	10	65	7.6	16	0.87	0.93
mr30a05	33.6	27.8	34.2	1200	90	229	1220	415	433	1670	6410	1070	5300	1070	249	646	71	315	48	103	13	78	9.3	16	0.91	0.97
mr30b05*	32.6	26.8	33.0	1210	45	213	1450	528	588	3040	10400	1620	7650	1400	328	813	88	376	57	123	14	86	10	24	0.94	1.36
RT1 Sample - GRANITOID																										
mr07c14	***28.2***	***26.9***	***30.7***	***822***	***172***	***96***	***2540***	***576***	***2500***	***3780***	***12200***	***1760***	***7350***	***1290***	***225***	***784***	***104***	***538***	***99***	***248***	***34***	***220***	***25***	***345***	***0.68***	***1.83***
mr30d13	***32.5***	***26.6***	***33.0***	***809***	***161***	***87***	***2280***	***528***	***1830***	***3200***	***10600***	***1490***	***6250***	***1070***	***191***	***681***	***90***	***466***	***85***	***218***	***30***	***194***	***23***	***168***	***0.68***	***1.87***
ap3a05*	***31.5***	***26.9***	***33.8***	***833***	***191***	***82***	***1720***	***446***	***1460***	***2330***	***7530***	***1030***	***4270***	***726***	***136***	***471***	***61***	***324***	***61***	***164***	***24***	***172***	***21***	***132***	***0.71***	***2.00***
1-mr07d06	30.1	27.6	30.8	877	200	84	1900	485	1400	2470	8210	1200	5080	896	160	525	73	390	72	187	27	187	22	127	0.71	1.72
1-mr30d14	32.1	26.7	32.5	823	197	117	2910	568	1200	3200	11800	1850	8620	1730	277	1080	141	704	121	284	37	214	23	115	0.62	1.16
1-ap3a03*	32.3	27.3	34.2	845	143	86	2360	519	1310	2930	10200	1520	6720	1230	207	777	102	520	93	229	32	194	23	120	0.65	1.49
2-mr07c13	29.2	28.8	32.4	790	223	102	1350	322	1050	1170	4040	620	2720	518	141	350	48	253	48	128	19	140	18	50	1.01	1.41
2-mr30d06	34.1	27.8	34.0	778	204	108	1860	372	1310	1610	5650	854	3850	737	180	510	68	365	69	175	26	183	24	75	0.89	1.36
2-ap3a06*	31.3	27.5	33.7	735	206	99	1580	362	1190	1640	5760	836	3740	713	166	472	62	323	60	154	22	148	18	75	**0.87**	1.44
RHG-1 Sample - GRANITOID																										
1-mr08a04*	28.0	26.7	29.4	811	191	78	1850	481	1220	2940	9330	1290	5300	883	164	549	72	381	69	171	24	160	20	93	0.72	2.08

Table 2 (Suite)

	SiO_2	CaO	TiO_2	V	Cr	Sr	Y	Zr	Nb	La	Ce	Pr	Nd	Sm	Eu	Gd	Tb	Dy	Ho	Er	Tm	Yb	Lu	Ta	$(Eu/Eu^*)_N$	$(La/Sm)_N$
1-mr08a05	27.7	27.3	30.6	751	159	89	2300	511	1080	3440	11500	1680	7380	1330	222	835	108	546	93	222	30	174	20	86	0.64	1.62
2-mr08a03*	28.5	28.3	30.8	882	224	71	924	308	1240	1250	3800	487	1910	301	80	202	28	149	29	88	14	107	16	64	0.99	2.59
2-mr08a07	27.9	27.3	30.0	783	186	82	2080	491	1160	3160	10400	1480	6320	1100	190	675	90	465	81	197	27	174	20	87	0.67	1.79
Rp-mr08a06	29.7	27.2	30.8	737	124	86	2040	539	1470	3710	11800	1630	6720	1080	192	662	85	431	77	190	26	169	20	127	0.69	2.15
R2 Sample - GRANITOID																										
mr08a12*	***27.9***	***26.0***	***30.0***	***841***	***146***	***89***	***3570***	***644***	***2220***	***3920***	***14600***	***2350***	***11100***	***2220***	***341***	***1340***	***180***	***906***	***152***	***350***	***44***	***260***	***27***	***282***	***0.60***	***1.10***
mr08a13	***28.3***	***26.9***	***29.8***	***813***	***183***	***85***	***2450***	***592***	***1860***	***3050***	***10600***	***1570***	***6810***	***1240***	***208***	***760***	***103***	***537***	***97***	***243***	***32***	***207***	***24***	***241***	***0.65***	***1.54***
1-mr08a11*	28.8	27.4	30.6	900	215	82	2290	507	1340	2520	9000	1380	5970	1110	187	692	93	485	87	221	30	202	24	121	0.65	1.42
1-mr08a14*	28.8	27.4	30.1	855	231	88	2120	483	1300	2560	8560	1250	5350	948	173	582	80	437	80	207	29	198	25	108	0.71	1.69
2-mr08a10*	28.9	28.1	31.2	821	193	65	1850	360	1400	1620	5710	862	3770	748	158	500	69	368	66	176	26	176	23	97	0.79	1.35
2-no10d14	32.8	27.9	35.5	704	219	89	1470	307	1250	1010	3830	611	2920	586	152	400	55	299	54	147	21	145	20	53	0.96	1.08
Rp-mr08a08	27.7	28.2	30.8	716	119	57.5	2050	349	1580	1440	5610	904	4250	899	177	604	81	417	77	191	28	172	21	120	0.73	1.00
Rp-mr08a09	27.8	27.9	30.9	699	104	60.1	2050	335	1690	1430	5640	917	4250	893	176	603	82	434	77	194	27	182	21	131	0.73	1.00
SR2 Sample - APPINTIE																										
no09d11	***34.7***	***28.3***	***34.9***	***789***	***250***	***168***	***951***	***1080***	***1480***	***4390***	***8380***	***932***	***3500***	***548***	***201***	***331***	***43***	***212***	***39***	***96***	***14***	***93***	***12***	***47***	***1.44***	***5.00***
no10a08*	***34.0***	***28.6***	***36.9***	***820***	***269***	***164***	***1090***	***895***	***1250***	***3870***	***7660***	***892***	***3530***	***565***	***199***	***359***	***45***	***233***	***44***	***105***	***14***	***104***	***13***	***37***	***1.35***	***4.28***
no10a10*	35.1	29.4	36.6	857	409	114	697	352	201	1880	3970	466	1920	326	108	210	28	144	27	70	10	65	8.7	6.5	1.26	3.60
no10a12	34.2	28.9	35.2	842	450	120	487	376	233	1860	3680	407	1580	258	95	155	20	104	18	46	6.7	46	6.5	8.4	1.45	4.50
2-no10a11*	34.8	29.1	35.9	855	481	127	451	337	223	1720	3370	369	1440	227	88.8	141	18	92.9	17	45	6.6	42	5.9	4.7	1.51	4.73
2-no10b06	34.1	29.2	36.4	919	522	95.7	821	431	272	1390	3130	418	1900	374	82.4	264	35	181	32	79	11	68	10	10	0.80	2.32

Table 2 (Suite)

SR1 Sample - GRANITOID

Mount	**SiO_2**	**CaO**	**TiO_2**	**V**	**Cr**	**Sr**	**Y**	**Zr**	**Nb**	**La**	**Ce**	**Pr**	**Nd**	**Sm**	**Eu**	**Gd**	**Tb**	**Dy**	**Ho**	**Er**	**Tm**	**Yb**	**Lu**	**Ta**	**$(Eu/Eu^*)_N$**	**$(La/Sm)_N$**
no08c06*	***34.6***	***27.8***	***36.5***	***859***	***96***	***72***	***2130***	***669***	***2240***	***4880***	***14800***	***1910***	***7490***	***1160***	***198***	***694***	***88***	***452***	***82***	***205***	***29***	***185***	***21***	***351***	***0.67***	***2.63***
no08d03	***33.0***	***27.8***	***34.5***	***940***	***136***	***69***	***3310***	***770***	***2060***	***4630***	***15600***	***2370***	***10700***	***1990***	***302***	***1260***	***161***	***806***	***135***	***318***	***40***	***239***	***27***	***396***	***0.58***	***1.45***
1-no08c13	33.5	28.1	35.0	851	175	65	1310	601	1030	3900	10700	1280	4680	660	120	392	49	256	47	126	19	128	17	113	0.72	3.69
1-no08c14*	33.9	28.1	34.9	887	167	68	2090	659	1620	4040	12700	1720	7030	1180	195	708	90	454	80	200	28	172	21	264	0.65	2.14
2-no08c09	32.8	28.1	35.4	774	114	64	622	471	797	2790	5410	531	1900	294	71	194	26	131	23	58	8.2	53	7.8	27	0.91	5.93
2-no08c12*	33.0	28.1	34.7	741	134	65	524	520	721	2630	5080	481	1620	235	56	146	20	102	19	50	6.9	54	8.5	36	0.92	6.99
2-no08d14	32.7	28.8	35.1	783	131	65	698	471	674	2740	5340	536	1930	314	79	214	28	150	27	72	10	73	10	30	0.93	5.45
3-no08c10	32.6	28.8	35.2	860	125	61	652	333	589	2370	4730	515	1970	332	93	217	27	146	26	62	8.5	55	7.2	20	1.06	4.46
3-no08c11*	34.0	28.8	35.4	964	125	50	273	212	265	1070	2170	220	806	117	51	80.1	10	50	9.8	26	4.1	24	3.7	1.8	1.59	5.71
SR3 Sample - GRANITOID																										
ap3e04*	***31.9***	***25.7***	***33.0***	***852***	***230***	***64.0***	***3290***	***635***	***2140***	***4770***	***16200***	***2360***	***10900***	***2060***	***310***	***1280***	***166***	***830***	***138***	***317***	***40***	***233***	***26***	***364***	***0.58***	***1.45***
mr07a05	***28.7***	***27.8***	***31.4***	***741***	***109***	***72.8***	***826***	***759***	***2110***	***4850***	***10900***	***1080***	***3420***	***411***	***82***	***234***	***29***	***147***	***29***	***76***	***12***	***86***	***13***	***260***	***0.81***	***7.37***
1-ap3e05*	32.7	26.8	33.4	835	147	62.6	1730	612	1080	3640	10700	1390	5510	854	150	542	67	349	63	162	23	155	20	134	0.67	2.66
1-no09b13	32.1	27.8	34.5	716	134	67.4	1520	512	1190	3820	8460	987	3820	615	141	420	56	299	57	143	20	133	18	116	0.85	3.88
2-mr07a03*	29.5	28.5	31.8	764	141	64.7	526	481	836	2640	5240	513	1690	231	55	149	19	101	19	49	7.3	55	8.2	47	0.90	7.14
2-ap3e03	32.4	27.9	33.9	716	119	62.8	630	470	869	2920	5560	530	1880	282	66	199	25	129	24	61	8.4	61	9.0	34	0.85	6.47
2-no09a03	34.2	28.6	37.6	787	181	58.7	844	570	1260	3210	7270	742	2490	325	63	202	27	137	27	79	12	91	14	116	0.75	6.17

(1) cores compositions, (2) rims compositions, (3) Dark external rim, (Rp) Reprecipitation feature. Analyses in bold are from Fir-tree and extremely bright sector zones. Al_2O_3, SiO_2, CaO, TiO_2 are reported in Wt% and the other elements in ppm. * are analyses reported in figure 2.

Table 3: Representative analyses of apatite. See entire dataset in Electronic Supplementary Data

RA1 Sample - APPINITE

Analysis Nb	P_2O_5	CaO	V	Sr	Y	Zr	La	Ce	Pr	Nd	Sm	Eu	Gd	Tb	Dy	Ho	Er	Tm	Yb	Lu	Pb	Th	U	$(Eu/Eu^*)_N$	$(La/Sm)_N$
1-ap04b04*	44.30	55.4	31.80	2550	236	1.6	645	1910	274	1310	221	48	137	12	56	8.6	18	2.2	14	1.8	14	36	22	0.84	1.82
1-ap04b06	42.50	54.7	39.20	2650	229	4.8	1000	2590	331	1520	244	53	142	14	55	8.8	20	2.4	13	2.2	15	37	13	0.87	2.56
1-ap04b07	41.00	53.1	35.80	2370	208	3.1	871	2350	291	1310	206	46	125	12	51	7.3	16	1.8	12	1.8	13	41	19	0.87	2.64
R-ap04b05*	44.20	55.0	7.46	2610	140	<0.26	397	1140	162	762	128	30	78	7	29	5.1	11	1.3	7	1.1	12	25	26	0.90	1.94
R-ap04d06	44.00	55.4	9.04	2730	163	0.6	565	1510	198	952	152	33	100	9	40	5.7	14	1.3	9	1.3	13	25	24	0.81	2.32
R-sp04f14	42.00	55.0	39.90	2380	324	4.0	1030	2630	373	1700	283	55	172	17	71	11.5	25	3.0	18	2.4	13	42	17	0.76	2.27
R2 Sample - GRANITOID																									
1-ap04d14*	40.60	55.1	10.40	786	334	2.1	363	1100	147	681	139	26	106	13	63	11.8	31	3.9	25	4.1	9	55	49	0.65	1.63
1-sp03c09	44.10	55.2	8.46	872	337	0.5	449	1210	163	699	129	24	93	12	57	11.3	28	3.8	23	3.8	8	33	12	0.68	2.17
2-ap04c04	46.00	55.2	7.02	862	215	0.4	309	898	113	499	93.4	20	72	8	39	7.7	19	2.4	15	2.6	7	29	18	0.73	2.07
2-ap04e04*	45.30	55.2	5.98	897	312	0.3	382	1110	150	684	136	26	102	12	58	10.8	27	3.7	21	3.5	8	37	18	0.67	1.75
2-sp03b10	42.70	55.2	9.54	870	447	0.5	554	1450	199	901	179	33	145	18	88	17.0	40	4.9	34	5.3	9	53	16	0.62	1.93
2-sp03d05	42.40	55.2	6.71	847	273	0.4	380	1030	134	612	115	23	90	11	52	10.2	26	3.1	22	3.7	8	33	15	0.68	2.06
3-ap04d13*	47.40	55.3	6.58	895	284	0.3	339	1000	131	611	117	24	93	11	55	10.5	26	3.2	21	3.5	9	31	16	0.69	1.81
RT1 Sample - GRANITOID																									
1-ap04h13	40.00	55.3	8.63	982	315	1.0	558	1550	197	844	138	33	104	12	59	11.0	28	3.4	23	3.7	7	55	48	0.83	2.53
1-ap04i10*	41.40	55.3	16.80	1060	187	0.9	355	920	120	514	84.3	21	60	7	34	6.8	17	2.0	15	2.4	7	43	33	0.89	2.63
1-sp04c05	44.50	55.0	9.27	1020	441	1.4	801	2110	279	1220	193	48	139	16	78	15.6	39	5.3	33	5.3	7	69	34	0.89	2.59

Table 3: Representative analyses of apatite. See entire dataset in Electronic Supplementary Data (Suite)

RT1 Sample - GRANITOID																								
2-ap04h14*	42.30	54.7	9.08	1050	450	1.8	926	2460	297	1290	198	53	145	16	78	15.8	40	5.1	33	6.0	9	74	31	0.96	2.92
2-ap04i09*	41.30	55.1	8.68	1070	470	2.0	935	2450	306	1300	207	52	150	17	82	16.4	43	5.6	34	6.0	9	79	38	0.90	2.82
2-ap04i11*	40.60	55.0	8.75	1020	452	2.1	871	2340	289	1230	195	51	144	16	82	16.1	40	5.7	36	5.8	8	81	35	0.92	2.79
2-sp04b05	45.50	55.0	8.44	1010	375	1.2	786	2150	273	1120	174	39	117	13	66	12.6	33	4.4	30	4.9	7	60	27	0.83	2.82
3-sp04b06	43.40	55.0	5.43	1060	134	0.2	286	798	94.9	400	60.4	15	45	5	26	4.8	12	1.4	10	1.5	5	18	15	0.90	2.96
3-sp04c06	43.00	55.0	7.05	1020	220	0.9	443	1130	145	633	99.6	24	71	8	41	7.9	20	2.6	16	2.9	6	38	32	0.88	2.78
3-sp04c08	45.50	55.0	7.13	1060	192	0.3	397	1020	131	554	86.6	22	64	7	35	6.4	17	2.1	14	2.3	6	26	26	0.91	2.86
RHG-1 Sample - GRANITOID																								
1-sp03d10	42.40	55.0	8.23	870	272	0.3	523	1290	160	701	114	23	85	9	46	8.9	23	3.2	22	3.3	8	25	13	0.73	2.86
1-sp03e07*	41.90	55.0	10.70	862	446	1.5	1050	2580	320	1290	201	40	139	16	76	15.3	40	5.2	35	5.7	8	82	42	0.73	3.26
1-sp03f05	43.30	55.0	8.35	867	339	1.1	616	1670	214	900	141	28	99	12	56	11.0	29	4.1	27	4.1	8	46	19	0.72	2.73
1-sp03f10	42.00	55.0	9.93	974	450	1.3	1470	3260	370	1410	198	39	138	16	77	15.1	38	5.2	36	5.4	10	74	24	0.72	4.64
2-ap04f06	42.60	55.2	9.37	896	433	1.2	1030	2810	320	1280	188	37	139	15	76	14.1	37	4.9	36	5.8	11	70	21	0.70	3.42
2-ap04f07	43.50	55.0	8.27	926	305	0.6	588	1540	195	818	130	27	90	11	49	9.3	25	3.3	20	3.5	8	46	16	0.77	2.82
2-sp03e06*	44.30	55.0	8.50	900	282	0.5	660	1630	195	799	122	26	84	10	47	9.6	24	3.4	21	3.6	8	48	16	0.77	3.38
2-sp03e08	42.60	55.0	9.00	894	457	1.3	1050	2470	308	1210	187	39	136	16	76	15.4	37	5.5	37	6.1	9	64	19	0.75	3.51
3-ap04f10	42.60	55.2	7.09	858	205	0.2	537	1390	165	592	94.6	19	70	8	37	7.3	18	2.4	16	2.4	9	32	21	0.70	3.54
3-sp03e10	42.80	55.0	7.59	868	183	0.2	329	852	107	460	76.7	16	58	7	30	5.8	15	2.0	14	2.1	6	27	21	0.74	2.68
3-sp03f08	42.40	55.0	8.24	972	439	1.2	1490	3230	365	1410	197	39	137	16	77	14.6	38	5.1	35	5.2	10	73	22	0.72	4.72

Table 3: Representative analyses of apatite. See entire dataset in Electronic Supplementary Data (Suite)

Analysis Nb	P_2O_5	CaO	V	Sr	Y	Zr	La	Ce	Pr	Nd	Sm	Eu	Gd	Tb	Dy	Ho	Er	Tm	Yb	Lu	Pb	Th	U	$(Eu/Eu^*)_N$	$(La/Sm)_N$
SR1 Sample	*Granodiorite*																								
1-ap04f13	42.40	55.4	10.80	572	225	1.8	2680	3310	263	869	112	29	79	8	42	8.3	21	2.4	16	2.7	11	136	47	0.93	14.94
1-ap04f14	43.80	55.4	12.40	571	211	1.7	2540	3040	249	822	103	27	77	8	38	7.4	18	2.4	17	2.8	11	125	40	0.92	15.40
1-ap04g05	41.50	55.0	8.90	697	154	1.1	2030	2510	201	664	84.8	19	59	6	29	5.5	14	1.7	12	1.8	9	62	17	0.81	14.95
1-ap04g09*	43.90	55.0	16.30	623	162	0.7	1440	2250	219	809	118	13	79	8	39	5.9	14	1.6	8	1.6	9	72	25	0.41	7.62
1-ap04g10*	43.00	55.3	8.37	676	156	1.2	1910	2490	205	726	94	18	68	7	34	6.3	14	1.8	12	1.9	10	61	18	0.67	12.69
1-sp03h09	44.70	55.0	9.35	666	194	1.2	2190	2750	249	891	119	21	82	9	41	7.8	18	2.2	14	2.1	10	80	23	0.63	11.49
1-sp03h13	46.60	55.0	12.80	653	198	1.3	1860	2820	291	1030	134	17	88	10	44	7.5	18	2.0	10	1.6	9	82	24	0.47	8.67
2-ap04g04	45.40	55.9	8.34	665	68	0.4	880	1060	82.5	274	33.1	8	24	2	11	2.3	6	0.8	5	0.9	8	40	21	0.90	16.60
2-ap04g06*	44.40	55.5	9.28	687	74.8	0.4	993	1280	98.7	333	42.2	9	30	3	14	2.9	7	0.9	6	1.0	9	46	15	0.77	14.69
2-ap04g08*	46.90	55.4	9.84	619	89.4	0.5	1080	1390	116	390	50.5	11	32	3	18	3.0	8	1.0	7	1.2	8	52	22	0.81	13.35
2-sp03h04	45.80	55.0	9.20	681	75.1	0.4	968	1130	90.7	303	37.8	8	27	3	14	2.6	6	0.9	6	1.0	8	51	20	0.80	15.99
2-sp03h11	45.30	55.0	9.15	735	84.7	0.4	1120	1400	117	396	47.6	10	33	4	16	3.1	8	0.9	6	1.0	8	50	15	0.77	14.69
2-sp03h14	43.30	55.0	9.34	700	103	0.6	1300	1620	133	464	57.6	12	39	4	20	3.7	8	1.1	7	1.3	10	75	21	0.76	14.09
2-sp03h05	43.00	55.0	9.25	634	77.9	0.4	955	1170	90.8	310	39.2	10	26	3	14	2.7	7	0.8	7	1.0	8	54	20	0.94	15.21
2-sp03h07	43.70	55.0	8.65	627	79	0.4	985	1230	97.4	326	38.8	10	27	3	14	2.8	7	0.9	6	1.0	8	54	18	0.93	15.85
SR2 Sample - APPINTIE																									
1-ap04a12*	42.10	55.5	23.50	1360	109	7.3	904	1340	112	404	50.5	13	39	4	19	3.7	9	1.2	8	1.3	8	38	15	0.90	11.18
1-ap04a14	42.60	55.1	20.00	1350	228	4.2	1410	2310	213	857	127	22	94	10	46	8.2	20	2.4	16	2.3	9	54	28	0.62	6.93

Table 3: Representative analyses of apatite. See entire dataset in Electronic Supplementary Data (Suite)

SR2 Sample – APPINTIE (Suite)																								
Analysis Nb	**P_2O_5**	**CaO**	**V**	**Sr**	**Y**	**Zr**	**La**	**Ce**	**Pr**	**Nd**	**Sm**	**Eu**	**Gd**	**Tb**	**Dy**	**Ho**	**Er**	**Tm**	**Yb**	**Lu**	**Pb**	**Th**	**U**	**$(Eu/Eu^*)_N$**	**$(La/Sm)_N$**
1-sp01b07	42.60	55.0	24.60	1340	200	5.8	1190	2090	232	897	126	22	81	9	42	7.8	19	2.3	13	2.1	8	39	11	0.66	5.90
1-sp01b08	42.30	55.0	15.70	1270	218	2.2	1050	1900	219	891	132	18	88	10	45	8.4	18	2.3	14	2.1	7	40	11	0.50	4.97
1-sp05f08	42.50	55.0	23.00	1320	242	8.3	1330	2440	261	1060	152	22	99	11	50	9.1	21	2.7	17	2.3	8	31	12	0.53	*5.46*
1-sp05f09	42.90	55.0	18.10	1310	240	5.1	1250	2230	249	1010	148	20	101	10	51	9.1	22	2.5	16	2.4	8	47	17	0.51	5.27
R-ap04a08	41.30	55.4	6.38	1490	132	0.6	947	1510	148	557	77.9	16	52	6	28	4.9	12	1.3	10	1.3	10	53	23	0.74	7.59
R-ap04a13*	44.70	55.3	20.30	1340	96.2	2.3	805	1100	96.3	348	45.1	11	32	4	18	3.4	9	1.1	7	1.1	9	55	19	0.89	11.15
R-sp01b06	43.60	55.0	23.50	1330	124	8.2	890	1200	115	429	60.1	12	45	5	23	4.6	12	1.6	10	1.6	7	30	8	0.71	9.25
R-sp05f03	47.20	55.0	12.10	1230	123	1.5	927	1280	120	445	61.4	14	44	5	24	4.6	12	1.3	9	1.5	7	47	20	0.80	9.43
SR3 Sample - GRANITOID																								
1-ap04e12	43.30	54.8	9.44	600	165	1.3	2070	2750	219	735	95.4	21	71	7	35	6.7	16	1.9	13	2.0	10	93	34	0.76	13.55
1-ap04e13	52.00	54.6	9.44	714	195	1.5	2580	3370	270	878	113	22	79	9	40	7.3	18	2.2	14	2.5	11	95	29	0.72	14.26
1-ap04e14*	43.50	54.7	9.04	728	176	1.3	2420	3130	249	824	101	21	74	7	36	6.7	16	1.9	13	2.0	9	81	22	0.73	14.96
1-sp01d13	46.20	54.8	10.10	742	186	1.4	1980	2810	261	950	129	20	86	9	42	7.8	18	2.0	13	2.0	9	69	21	0.57	9.58
2-ap04f04*	44.70	55.2	8.22	643	75.2	<0.30	946	1170	91.1	304	37.1	9	26	3	12	2.7	6	0.8	5	0.9	8	40	25	0.84	15.92
2-sp01c07	47.40	54.8	8.84	665	76.6	0.3	1020	1230	94.4	324	38.2	10	26	3	14	2.8	7	0.9	5	1.0	8	49	19	0.92	16.67
2-sp01d06	45.40	54.8	0.95	654	47.9	<0.11	664	806	67.3	228	28.5	5	22	2	9	1.8	4	0.5	3	0.5	6	8	4	0.68	14.55

For Rogart samples (1) are core composition, (2) oscillatory rim, (3) unoscillatory rim.For Strontian samples (1) correspond to core or all crystal composition, (2) rim composition. (R) are the bright rims present of appinite's apatite crystals. P_2O_5 and CaO are reported in Wt% and the other elements in ppm. * are analyses reported in figure 3.

Table 4: Analyses of zircon compositions. See entire dataset in Electronic Supplementary Data

	SiO2	P2O5	Sc	Y	Nb	La	Ce	Pr	Nd	Sm	Eu	Gd	Tb	Dy	Ho	Er	Tm	Yb	Lu	Hf	Ta	Pb	Th	U	Th/U
RT1 Sample																									
2-ap05c05	33.2	0.028	97	550	2.94	-	39	0.052	1.1	2.11	0.80	10.9	3.22	43.2	16.8	88.1	21.1	228	49.8	9250	0.95	8.4	193	360	0.5
2-ap06c06*	33.3	0.035	98	503	2.45	-	41	0.067	1.2	2.04	0.78	10.4	3.16	39.7	15.6	80.8	19.0	198	43.8	8450	0.88	9.0	192	313	0.6
2-ap06c07	33.5	0.032	99	418	2.60	0.061	34	-	0.8	1.63	0.75	8.5	2.58	34.5	12.6	67.7	15.7	166	35.5	9420	0.85	8.0	191	327	0.6
2-oc03f04*	33.2	0.033	88	440	2.02	0.090	40	0.064	1.4	1.95	0.71	9.4	2.75	36.2	13.8	68.2	16.2	170	34.6	8710	0.78	9.7	225	315	0.7
2-oc03f05	33.3	0.061	85	394	1.91	0.158	32	0.103	1.0	1.57	0.69	8.4	2.58	32.0	12.4	62.1	15.1	154	32.1	9370	0.72	7.9	176	316	0.6
3-ap06c10	33.3	0.035	101	483	2.60	0.049	39	0.084	1.0	2.09	0.80	10.1	2.91	38.4	14.6	74.8	18.3	189	41.3	9040	0.87	10.6	241	398	0.6
3-oc03e14	33.2	0.029	98	560	2.58	0.047	34	0.048	1.3	2.04	0.66	10.7	3.13	43.6	17.3	87.9	23.4	242	51.3	9090	0.96	6.6	162	300	0.5
RHG-1 Sample																									
1-ap05d04	33.2	0.0375	93	542	2.73	0.233	36.7	0.123	1.16	1.59	0.84	10.9	3.27	42.9	16.9	86.6	21.4	227	48.7	8510	1.03	9.21	189	349	0.5
1-oc03d05	33.2	0.0453	98	591	2.99	0.289	53.7	0.182	1.58	3.07	0.883	15.3	3.96	48.4	18.4	95.9	22.2	240	46.8	9560	1.13	12.7	325	421	0.8
1-oc03d07	33.2	0.0384	107	869	3.58	0.140	60.5	0.27	2.87	5.1	1.59	20.1	5.83	73.5	27.8	136	31.7	330	66.6	9170	1.19	15.8	388	491	0.8
2-ap05f07	33	0.034	81	379	2.27	0.064	30.2	0.0509	0.767	1.57	0.578	7.54	2.35	30	11.5	58.6	13.9	146	31.6	9430	0.738	8.18	175	328	0.5
2-oc03e04	33.2	0.0258	109	593	2.8	0.078	43.3	0.0686	1.02	2.37	0.807	11.2	3.6	48.2	18.9	93	23.3	244	48.6	10700	1.16	10.3	276	437	0.6
2-oc03e08*	33.2	0.0315	85	480	2.14	0.098	33.4	0.0815	0.871	1.52	0.686	8.75	3.08	36.6	14.8	76.7	18.2	189	39.3	8640	0.964	8.36	200	331	0.6
2-oc03e09*	33.2	0.0342	100	611	3.36	0.082	44.3	0.11	1.09	2.44	0.884	10.6	3.65	48.6	18.5	96.7	23.6	247	52.4	8700	1.16	9.2	208	302	0.7
3-ap05d06	32.9	0.0326	78	385	1.96	0.260	31.7	0.106	1.11	1.46	0.606	8.79	2.4	31.1	12	62.2	14.7	150	32.5	8410	0.773	11.6	199	346	0.6
R2 Sample																									
1-ap05f12*	33.2	0.034	90	581	3.6	0.064	48	0.083	1.4	2.0	1.05	11	3.5	44	17	92	22	231	51	9050	1.04	11.5	236	368	0.6
1-oc03b07	33.2	0.041	115	584	1.7	0.071	32	0.133	1.6	3.2	1.01	13	4.1	50	19	93	21	222	44	8140	0.63	7.1	160	222	0.7
2-ap05f11	33.3	0.043	94	649	3.2	-	52	0.109	1.6	3.1	1.22	15	4.2	52	20	101	24	241	52	8380	0.96	13.7	280	379	0.7
2-oc03b11	33.2	0.028	90	403	2.0	-	33	0.057	1.1	1.7	0.65	9	2.5	33	13	65	16	161	34	9280	0.81	8.9	202	364	0.6
2-oc03c04	33.2	0.022	110	593	3.0	0.132	38	0.041	1.0	1.8	0.75	11	3.4	45	18	93	24	248	53	9260	0.92	9.7	223	429	0.5
SR1 Sample																									
1-oc03f06	33	0.034	91	471	2.0	0.031	30	0.055	0.85	1.6	0.69	9	2.8	38	15	74	17	190	38.2	8320	1.12	7.6	179	313	0.6
1-oc03f09	33	0.032	90	708	1.0	0.735	36	0.318	2.57	4.0	1.47	19	5.2	64	22	108	25	240	48.8	8580	0.65	12.2	265	338	0.8
2-ap06c14*	33.3	0.034	110	537	2.2	-	43	0.041	0.71	1.7	0.79	10	3.4	43	16	83	19	197	43.6	8700	1.17	13.0	324	466	0.7
2-ap06d04*	33.1	0.030	96	447	2.1	0.072	30	0.054	0.94	1.8	0.72	10	2.7	33	14	68	17	178	40.1	7980	1.06	7.5	160	281	0.6
2-ap06d10	33	0.035	104	511	2.6	-	34	<0.0297	0.91	1.6	0.64	9	3.3	39	16	81	20	207	45.8	8220	1.25	9.3	207	377	0.5

Table 4: Analyses of zircon compositions. See entire dataset in Electronic Supplementary Data. (suite)

	SiO2	P2O5	Sc	Y	Nb	La	Ce	Pr	Nd	Sm	Eu	Gd	Tb	Dy	Ho	Er	Tm	Yb	Lu	Hf	Ta	Pb	Th	U	Th/U
SR2 Sample																									
1-ap06d13*	33.1	0.038	111	676	2.2	0.026	34	0.12	2.0	3.1	0.98	17	4.8	59	22	102	24	238	49	9320	0.97	10	236	334	0.7
1-oc04b10	33	0.072	116	1230	3.8	-	74	0.25	3.4	5.5	2.82	29	8.4	109	41	202	49	480	99	9610	1.53	60	1230	1340	0.9
2-oc04a07	33	0.061	117	1080	4.5	-	105	0.24	4.1	6.5	2.97	31	8.9	101	35	167	37	362	73	9170	2.08	123	2690	1780	1.5
2-oc04b07	33	0.064	108	1110	5.2	0.077	114	0.30	4.3	6.4	3.19	32	8.9	103	36	166	38	364	71	9170	2.39	177	3520	2240	1.6
3-oc04b05	33.2	0.038	100	932	1.1	0.249	39	0.54	7.2	7.5	3.01	26	7.6	84	30	143	34	332	66	8770	0.69	32	712	601	1.2
3-oc04b11	33	0.030	99	818	3.2	-	66	0.15	2.2	4.5	1.78	19	5.7	71	26	128	30	307	67	11000	1.64	56	1160	2170	0.5
3-oc04b12	33	0.057	135	1270	5.4	0.099	91	0.26	3.8	5.4	2.28	27	7.8	103	41	208	50	502	101	8390	2.19	64	1320	1260	1.0
SR3 Sample																									
1-ap06g05*	33.1	0.024	93	433	2.3	0.059	33	0.05	0.66	1.4	0.80	8.3	2.9	35	14	69	17	173	35	8010	0.91	9.3	219	359	0.6
1-oc03a06	33	0.037	121	724	2.9	0.068	42	0.12	1.87	2.9	1.07	14.5	4.6	60	23	111	27	265	55	8600	1.28	14.8	380	530	0.7
2-ap06g08	33.2	0.036	94	397	2.4	0.087	30	0.09	0.74	1.9	0.57	8.2	2.3	31	12	63	15	157	33	7790	0.80	8.2	185	327	0.6
2-ap06g09	33	0.038	87	349	1.9	0.081	30	0.06	0.84	1.4	0.64	7.7	2.2	28	11	54	13	131	27	7010	0.80	9.7	211	340	0.6
2-oc03b04	33	0.032	96	441	2.0	0.077	28	0.04	0.92	1.6	0.59	7.4	2.6	34	13	68	17	180	38	7500	1.01	7.8	158	278	0.6
3-oc03a05	33	0.035	112	514	2.1	0.055	39	0.09	0.88	1.9	0.84	9.9	3.2	41	16	76	19	194	40	8220	1.04	13.5	328	439	0.7
3-oc04d05	33	0.043	87	629	1.0	0.502	32	0.22	2.29	3.7	1.09	15.5	4.8	57	20	95	24	230	48	8100	0.73	11.1	244	326	0.7

(1), (2) and (3) correspond to analyses from cores (1) toward external rims (3). SiO_2 and P_2O_5 are reported in Wt% and the other elements in ppm. * are analyses reported in figure 4.

Electronic Appendix 1: LA-ICP-MS analytical results for international reference materials (NIST 610, NIST 612, Durango, 91500).

Element	Mass	NIST 610							NIST 612						
		This study (ppm)	n	SD (ppm)	RSD (%)	Literature Value (ppm)	SD ppm	RSD%	This study (ppm)	n	SD (ppm)	RSD (%)	Literature Value (ppm)	SD ppm	RSD%
Sc	45	441.1	**214**	3.1	0.7	441.1	9.6	2.2	41.0	**84**	0.5	1.2	41.1	4.1	10.0
Ti	47	433.8	**214**	5.6	1.3	434.0	14.7	3.4	48.1	**84**	1.5	3.0	48.1	3.0	6.3
V	51	441.7	**214**	3.3	0.8	441.7	42.7	9.7	39.2	**84**	0.5	1.2	39.2	3.8	9.6
Cr	53	405.2	**214**	2.9	0.7	405.2	32.3	8.0	39.9	**84**	0.6	1.5	39.9	15.2	38.0
Mn	55	433.3	**214**	3	0.6	433.3	31.8	7.3	38.4	**84**	0.6	1.5	38.4	1.0	2.6
Co	59	405.0	**214**	3.3	0.8	405	22.9	5.7	35.3	**84**	0.6	1.6	35.3	2.4	6.9
Zn	66	456.3	**214**	10.1	2.2	456.3	19.2	4.2	37.9	**84**	1.4	3.6	37.9	3.9	10.2
Ga	69	438.1	**214**	3.9	0.9	438.1	11.3	2.6	36.2	**84**	0.7	1.9	36.2	2.0	5.6
Rb	85	431.1	**214**	3.9	0.9	431.1	11.4	2.6							
Sr	88	497.4	**214**	4.7	0.9	497.4	18.3	3.7							
Y	89	449.9	**214**	4.4	1.0	449.9	19.3	4.3	38.2	**84**	0.9	2.4	38.3	2.1	5.6
Zr	90	439.9	**214**	4.6	1.0	439.9	7.8	1.8							
Nb	93	419.4	**214**	4.4	1.0	419.4	57.6	13.7	38.1	**84**	0.8	2.2	38.1	0.9	2.3
Sn	118	396.3	**214**	4.5	1.1	396.3	17.8	4.5	38.0	**84**	1.0	2.6	38.0	1.8	4.6
Sb	121	368.5	**214**	4.6	1.2	368.5	27.5	7.5							
Ba	137	424.1	**214**	5.0	1.2	424.1	29.3	6.9							
La	139	457.4	**214**	4.6	1.0	457.4	72.4	15.8	35.8	**84**	0.8	2.3	35.8	2.2	6.0
Ce	140	447.8	**214**	4.6	1.0	447.8	16.8	3.8	38.3	**84**	0.9	2.3	38.4	1.6	4.3
Pr	141	429.8	**214**	4.5	1.0	429.8	30	7.0	37.2	**84**	0.9	2.4	37.2	0.9	2.5
Nd	146	430.8	**214**	4.7	1.1	430.8	37.5	8.7	35.2	**84**	0.8	2.3	35.2	2.4	6.9
Sm	147	450.5	**214**	4.9	1.1	450.5	20.6	4.6	36.7	**84**	1.0	2.6	36.7	2.6	7.2
Eu	153	461.1	**214**	4.7	1.0	461.1	52.1	11.3	34.4	**84**	0.7	2.2	34.4	1.6	4.6
Gd	158	419.9	**214**	4.5	1.1	419.9	25.2	6.0	36.9	**84**	1.0	2.8	37.0	1.1	2.9
Tb	159	442.8	**214**	4.6	1.0	442.8	22.4	5.1	35.9	**84**	0.8	2.3	35.9	2.7	7.5
Dy	163	426.5	**214**	4.1	1.0	426.5	18	4.2	36.0	**84**	0.9	2.5	36.0	0.8	2.3
Ho	165	449.4	**214**	4.8	1.1	449.4	24.6	5.5	37.9	**84**	0.9	2.5	37.9	1.1	2.9
Er	166	426.0	**214**	4.5	1.1	426	23.9	5.6	37.4	**84**	0.9	2.5	37.4	1.5	4.0

Tm	169	420.1	**214**	4.2	1.0	420.1	19.2	4.6	37.5	**84**	0.9	2.5	37.6	1.3	3.3
Yb	172	461.5	**214**	4.8	1.0	461.5	30.6	6.6	39.9	**84**	1.0	2.5	40.0	2.9	7.2
Lu	175	434.7	**214**	4.2	1.0	434.7	31	7.1	37.7	**84**	0.9	2.3	37.7	2.0	5.2
Hf	178	417.7	**214**	4.2	1.0	417.7	28.2	6.8	34.8	**84**	0.9	2.6	34.8	3.7	10.5
Ta	181	376.6	**214**	3.5	0.9	376.6	77.6	20.6	39.8	**84**	0.9	2.3	39.8	2.2	5.4
Pb	208	413.3	**214**	4.1	1.0	413.3	15.4	3.7	39.0	**84**	0.9	2.2	39.0	1.8	4.7
Th	232	450.6	**214**	4.0	0.9	450.6	27.8	6.2	37.2	**84**	0.8	2.1	37.2	0.7	1.9
U	238	457.1	**214**	4.2	0.9	457.1	13.6	3.0	37.2	**84**	0.6	1.7	37.2	1.2	3.3

α Pearce et al. (1997)

* Marks et al. (2012)

φ Wiedenbeck et al. (2004)

β SiO_2 value used as internal standard has been determine by EPMA

DURANGO						91500					
This study (ppm)	n	SD (ppm)	RSD (%)	Literature Value (ppm)ϕ	RSD (%)	This study (ppm)β	n	SD (ppm)	RSD (%)	Literature Value (ppm)*	RSD %
0.22	**12**	0.02	9.6	0.11	18	80	**22**	6.1	8		
				26	25	5.9	**22**	0.99	17		
24	**32**	3.8	16	36	23	0.05	**3**	0.02	42		
				-		1.3	**7**	0.19	14		
94	**32**	3.0	3.1	114	3.5	-	**-**	-			
						0.04	**2**	0.01	24		
9.2	**32**	2.8	31								
0.1	**4**	0.01	6.3	0.04	15						
445	**32**	16	3.6	500	2.5						
400	**32**	24	6.1	410	15	148	**22**	5	4	140	10
0.5	**32**	0.1	23	0.4	25						
						0.93	**22**	0.20	22	0.79	8
						0.10	**14**	0.02	19		
1.2	**32**	0.3	26	1.8	8.5						
3007	**32**	261	8.7	3310	11.5	-	**-**	-		0.006	54
3584	**32**	259	7.2	4430	7.5	2.58	**22**	0.11	4	2.56	10
284	**32**	19	6.6	320	5.5	0.017	**11**	0.003	17	0.024	63
925	**32**	57	6.2	870	6	0.21	**22**	0.04	19	0.24	16
117	**32**	6.0	5.1	120	9	0.43	**22**	0.05	11	0.5	15
15	**32**	0.9	6.2	16.9	3.5	0.23	**22**	0.02	8	0.24	12
98	**32**	6.9	7.1	103	11.5	2.34	**22**	0.15	6	2.21	11
12	**32**	0.7	6.2	13.5	14	0.86	**22**	0.04	5	0.86	8
65	**32**	4.7	7.3	68	15	12.14	**22**	0.51	4	11.8	7
13	**32**	0.8	5.8	15	16.5	4.97	**22**	0.22	4	4.84	7
33	**32**	2.2	6.6	35	17	27.03	**22**	1.1	4	24.6	10

4.2	**32**	0.3	6.0	5	16	6.97	**22**	0.31	5	6.89	5
26	**32**	1.9	7.4	27	15	73.7	**22**	3	4	73.9	5
3.4	**32**	0.2	6.9	3.8	10.5	14.3	**22**	0.61	4	13.1	8
						5275	**22**	142	3	-	-
						0.52	**22**	0.03	6	-	-
0.5	**32**	0.1	13	0.7	14.5	3	**22**	0.17	5	-	-
182	**32**	16	8.5	175	12	29.7	**22**	1	4	29.9	7
9.1	**32**	1.1	12	12.4	21	82	**22**	3	4	80	10

Electronic Appendix 2: Analyses of titanite compositions

RA1 Sample

Mount	**SiO_2**	**CaO**	**TiO_2**	**V**	**Cr**	**Sr**	**Y**	**Zr**	**Nb**	**La**	**Ce**	**Pr**	**Nd**	**Sm**	**Eu**	**Gd**	**Tb**	**Dy**	**Ho**	**Er**	**Tm**	**Yb**	**Lu**	**Hf**	**Ta**	**Pb**	**Th**	**U**	**$(Eu/Eu^*)_N$**	**$(La/Sm)_N$**
mr07d09	***28.2***	***26.4***	***29.8***	***1140***	***52***	***257***	***2170***	***731***	***1950***	***3990***	***14100***	***2250***	***11100***	***2170***	***467***	***1230***	***135***	***585***	***88***	***188***	***23***	***134***	***15***	***63***	***233***	***47***	***876***	***285***	***0.87***	***20.23***
mr07d10	***29.0***	***26.6***	***30.3***	***1140***	***56***	***277***	***1700***	***519***	***1430***	***3960***	***13500***	***2120***	***10000***	***1860***	***395***	***1010***	***110***	***463***	***68***	***144***	***17***	***100***	***11***	***47***	***145***	***40***	***686***	***222***	***0.88***	***26.95***
mr07d13	***28.6***	***27.6***	***31.3***	***1050***	***68***	***287***	***1400***	***597***	***1410***	***2230***	***8310***	***1410***	***6850***	***1310***	***362***	***733***	***80***	***353***	***55***	***115***	***15***	***95***	***11***	***46***	***33***	***37***	***768***	***523***	***1.13***	***16.01***
mr30b03*	***29.9***	***26.0***	***32.2***	***1010***	***46***	***263***	***1990***	***1280***	***2110***	***5290***	***17000***	***2470***	***11300***	***2000***	***454***	***1130***	***119***	***511***	***79***	***167***	***21***	***123***	***14***	***82***	***101***	***55***	***1160***	***565***	***0.92***	***29.22***
mr30b04	***31.4***	***26.0***	***32.8***	***1040***	***49***	***265***	***2030***	***1290***	***2140***	***5350***	***17400***	***2560***	***11700***	***2030***	***469***	***1150***	***121***	***521***	***80***	***171***	***21***	***126***	***14***	***84***	***99***	***60***	***1180***	***583***	***0.94***	***28.84***
mr30c03	***30.8***	***25.7***	***32.0***	***990***	***46***	***256***	***2190***	***1330***	***2240***	***5420***	***17500***	***2520***	***11900***	***2210***	***488***	***1260***	***136***	***570***	***87***	***189***	***23***	***135***	***16***	***86***	***150***	***65***	***1290***	***636***	***0.89***	***27.27***
mr30a06	32.4	27.2	33.7	1080	51	217	1300	426	652	2240	8090	1320	6390	1250	337	716	78	335	52	108	13	79	10	34	30	31	421	231	1.09	1.12
mr30a07	31.7	27.1	33.9	1070	57	249	1480	361	1030	2220	8620	1420	6890	1350	336	786	86	369	57	127	16	98	12	33	51	40	783	315	0.99	1.03
mr07d12	30.1	27.6	31.4	1110	72	265	1430	362	579	2010	7700	1350	6790	1370	345	794	87	378	58	124	15	90	10	23	12	32	588	253	1.01	0.92
mr30a03	32.7	27.8	33.1	1140	86	219	963	362	416	1340	5190	876	4370	898	199	546	59	257	39	87	10	65	7.6	36	16	24	305	217	0.87	0.93
mr30a04	32.4	27.8	33.1	1180	88	223	1150	348	402	1470	5870	1010	5050	1050	241	630	69	300	46	97	12	75	9.0	29	14	22	351	209	0.90	0.87
mr30a05	33.6	27.8	34.2	1200	90	229	1220	415	433	1670	6410	1070	5300	1070	249	646	71	315	48	103	13	78	9.3	37	16	26	396	232	0.91	0.97
mr30b05*	32.6	26.8	33.0	1210	45	213	1450	528	588	3040	10400	1620	7650	1400	328	813	88	376	57	123	14	86	10	38	24	30	499	227	0.94	1.36
mr07d11	29.4	28.3	31.0	1160	138	229	999	322	264	1330	5150	900	4490	876	253	501	55	244	38	86	11	68	8.6	21	4.2	23	406	260	1.16	0.95
mr07d14	28.8	28.0	30.8	1050	74	238	1120	424	493	1470	5740	995	5070	1040	267	606	65	286	44	98	12	73	8.7	33	12	18	279	248	1.03	0.88

RT1 Sample

Mount																														
mr07c14	***28.2***	***26.9***	***30.7***	***822***	***172***	***95.8***	***2540***	***576***	***2500***	***3780***	***12200***	***1760***	***7350***	***1290***	***225***	***784***	***104***	***538***	***99***	***248***	***34***	***220***	***25***	***43***	***345***	***35***	***874***	***101***	***0.68***	***1.83***
mr07d03	***29.4***	***26.7***	***29.6***	***849***	***652***	***90.8***	***2620***	***645***	***1650***	***3100***	***10900***	***1690***	***7490***	***1430***	***240***	***871***	***119***	***612***	***108***	***262***	***35***	***216***	***24***	***50***	***192***	***22***	***510***	***77***	***0.66***	***1.35***
mr07d07	***28.1***	***27.0***	***30.6***	***806***	***132***	***95***	***2310***	***627***	***2760***	***3650***	***11900***	***1680***	***7060***	***1200***	***210***	***734***	***97***	***500***	***91***	***228***	***32***	***212***	***25***	***53***	***398***	***38***	***884***	***104***	***0.68***	***1.90***
mr30d09	***31.7***	***27.0***	***32.8***	***837***	***171***	***93.2***	***2320***	***618***	***2050***	***3220***	***10700***	***1540***	***6600***	***1170***	***196***	***745***	***96***	***497***	***90***	***225***	***31***	***202***	***24***	***42***	***234***	***28***	***639***	***91***	***0.64***	***1.72***
mr30d13	***32.5***	***26.6***	***33.0***	***809***	***161***	***86.6***	***2280***	***528***	***1830***	***3200***	***10600***	***1490***	***6250***	***1070***	***191***	***681***	***90***	***466***	***85***	***218***	***30***	***194***	***23***	***36***	***168***	***33***	***784***	***92***	***0.68***	***1.87***
ap3a05*	***31.5***	***26.9***	***33.8***	***833***	***191***	***82.3***	***1720***	***446***	***1460***	***2330***	***7530***	***1030***	***4270***	***726***	***136***	***471***	***61***	***324***	***61***	***164***	***24***	***172***	***21***	***30***	***132***	***23***	***525***	***96***	***0.71***	***2.00***
1-mr07d05	29.0	27.8	31.3	877	208	81	1780	457	1400	2290	7780	1100	4620	791	148	486	66	356	66	176	25	174	21	32	118	20	479	94.4	0.73	1.81
1-mr07d06	30.1	27.6	30.8	877	200	84	1900	485	1400	2470	8210	1200	5080	896	160	525	73	390	72	187	27	187	22	34	127	23	480	90.7	0.71	1.72
1-mr30d07	32.3	27.4	33.2	870	191	89	2860	580	1060	3000	11000	1720	7900	1540	253	974	130	660	118	278	36	223	25	37	114	20	448	74.1	0.63	1.22
1-mr30d10	32.3	26.8	32.9	837	221	102	2930	570	1090	3090	11400	1760	8300	1650	270	1050	135	692	121	286	37	225	26	35	102	19	436	68.7	0.63	1.17
1-mr30d14	32.1	26.7	32.5	823	197	117	2910	568	1200	3200	11800	1850	8620	1730	277	1080	141	704	121	284	37	214	23	35	115	19	413	65.9	0.62	1.16
1-ap3a03*	32.3	27.3	34.2	845	143	86	2360	519	1310	2930	10200	1520	6720	1230	207	777	102	520	93	229	32	194	23	35	120	20	460	76.8	0.65	1.49

RT1 Sample (Suite)

Mount	**SiO_2**	**CaO**	**TiO_2**	**V**	**Cr**	**Sr**	**Y**	**Zr**	**Nb**	**La**	**Ce**	**Pr**	**Nd**	**Sm**	**Eu**	**Gd**	**Tb**	**Dy**	**Ho**	**Er**	**Tm**	**Yb**	**Lu**	**Hf**	**Ta**	**Pb**	**Th**	**U**	**$(Eu/Eu^*)_N$**	**$(La/Sm)_N$**
2-mr07c13	29.2	28.8	32.4	790	223	102	1350	322	1050	1170	4040	620	2720	518	141	350	48	253	48	128	19	140	18	27	50.1	18	397	205	1.01	1.41
2-mr07d04	30.3	28.4	31.5	842	185	96	1390	396	1630	2490	7570	1020	4100	672	142	412	54	283	53	134	19	132	17	30	130	29	635	118	0.82	2.31
2-mr07d08	29.9	28.0	30.7	870	235	92	2540	529	1080	2870	10100	1590	7090	1360	230	841	113	585	105	252	33	209	24	36	105	22	465	84.8	0.66	1.32
2-mr30d06	34.1	27.8	34.0	778	204	108	1860	372	1310	1610	5650	854	3850	737	180	510	68	365	69	175	26	183	24	27	75.2	20	463	127	0.89	1.36
2-mr30d08	32.6	28.1	33.7	736	209	98	1300	317	1170	1200	4270	645	2910	541	142	367	47	250	47	122	18	123	17	25	55.6	19	418	180	0.97	1.39
2-mr30d11	32.0	27.6	34.0	795	226	94	1640	389	1120	1870	6160	880	3790	684	150	463	61	317	59	154	22	156	20	26	67.6	22	509	113	0.81	1.71
2-mr30d12	32.4	27.8	33.6	776	216	92	1640	376	1100	1780	5900	865	3760	685	154	460	61	317	59	157	23	161	20	27	65.1	21	499	119	0.84	1.62
2-ap3a04	32.9	28.0	34.4	843	227	84	1990	495	1130	2550	8430	1200	5100	885	164	579	77	398	74	190	27	184	22	35	93.1	25	548	91.1	0.70	1.80
2-ap3a06*	31.3	27.5	33.7	735	206	99	1580	362	1190	1640	5760	836	3740	713	166	472	62	323	60	154	22	148	18	26	74.5	20	469	131	**0.87**	1.44

RHG-1 Sample

Mount																														
1-mr08a04*	28.0	26.7	29.4	811	191	78	1850	481	1220	2940	9330	1290	5300	883	164	549	72	381	69	171	24	160	20	33	93	19	435	80	0.72	2.08
1-mr07b14	27.6	27.1	30.1	858	250	80	2480	489	1320	2590	9370	1470	6610	1250	208	785	107	550	96	236	32	214	23	32	115	18	412	77	0.64	1.29
1-mr08a05	27.7	27.3	30.6	751	159	89	2300	511	1080	3440	11500	1680	7380	1330	222	835	108	546	93	222	30	174	20	33	86	17	392	67	0.64	1.62
2-mr08a03*	28.5	28.3	30.8	882	224	71	924	308	1240	1250	3800	487	1910	301	80	202	28	149	29	88	14	107	16	23	64	25	558	145	0.99	2.59
2-mr08a07	27.9	27.3	30.0	783	186	82	2080	491	1160	3160	10400	1480	6320	1100	190	675	90	465	81	197	27	174	20	33	87	18	407	70	0.67	1.79
Rp-mr07b13	27.1	26.9	30.6	811	149	86	2350	506	2030	3280	11100	1620	6900	1230	212	764	101	517	91	229	30	193	23	36	224	33	787	99	0.67	1.67
Rp-mr08a06	29.7	27.2	30.8	737	124	86	2040	539	1470	3710	11800	1630	6720	1080	192	662	85	431	77	190	26	169	20	38	127	22	486	77	0.69	2.15

R2 Sample

Mount																														
mr08a12*	***27.9***	***26.0***	***30.0***	***841***	***146***	***89***	***3570***	***644***	***2220***	***3920***	***14600***	***2350***	***11100***	***2220***	***341***	***1340***	***180***	***906***	***152***	***350***	***44***	***260***	***27***	***45***	***282***	***28***	***681***	***79***	***0.60***	***1.10***
mr08a13	***28.3***	***26.9***	***29.8***	***813***	***183***	***85***	***2450***	***592***	***1860***	***3050***	***10600***	***1570***	***6810***	***1240***	***208***	***760***	***103***	***537***	***97***	***243***	***32***	***207***	***24***	***47***	***241***	***27***	***618***	***88***	***0.65***	***1.54***
ap3c04	***33.2***	***27.5***	***35.8***	***825***	***143***	***110***	***1530***	***404***	***2180***	***3530***	***10400***	***1320***	***5140***	***779***	***143***	***490***	***60***	***297***	***54***	***144***	***21***	***139***	***18***	***31***	***197***	***31***	***722***	***91***	***0.71***	***2.83***
ap3c05	***33.6***	***27.4***	***33.7***	***854***	***165***	***76***	***2020***	***479***	***1310***	***2450***	***8510***	***1290***	***5550***	***984***	***160***	***627***	***83***	***433***	***78***	***200***	***27***	***180***	***20***	***33***	***120***	***19***	***387***	***78***	***0.62***	***1.55***
ap3c06	***32.3***	***27.0***	***33.0***	***869***	***201***	***73***	***1640***	***451***	***1350***	***2280***	***7130***	***973***	***4040***	***685***	***122***	***452***	***58***	***307***	***57***	***154***	***24***	***162***	***21***	***31***	***110***	***24***	***511***	***94***	***0.67***	***2.08***
no10d07	***33.1***	***27.9***	***36.2***	***920***	***147***	***151***	***3010***	***666***	***2290***	***5040***	***16600***	***2510***	***11200***	***2140***	***317***	***1190***	***156***	***740***	***123***	***287***	***35***	***198***	***22***	***47***	***243***	***35***	***598***	***66***	***0.61***	***1.47***
no10d05	***32.6***	***27.9***	***35.1***	***830***	***186***	***117***	***3570***	***810***	***1780***	***4020***	***14200***	***2320***	***11000***	***2250***	***345***	***1380***	***185***	***917***	***153***	***348***	***45***	***258***	***28***	***58***	***265***	***22***	***552***	***68***	***0.60***	***1.12***
1-mr08a11*	28.8	27.4	30.6	900	215	82	2290	507	1340	2520	9000	1380	5970	1110	187	692	93	485	87	221	30	202	24	34	121	21	461	84	0.65	1.42
1-mr08a14*	28.8	27.4	30.1	855	231	88	2120	483	1300	2560	8560	1250	5350	948	173	582	80	437	80	207	29	198	25	32	108	21	464	92	0.71	1.69

R2 Sample

Mount	**SiO_2**	**CaO**	**TiO_2**	**V**	**Cr**	**Sr**	**Y**	**Zr**	**Nb**	**La**	**Ce**	**Pr**	**Nd**	**Sm**	**Eu**	**Gd**	**Tb**	**Dy**	**Ho**	**Er**	**Tm**	**Yb**	**Lu**	**Hf**	**Ta**	**Pb**	**Th**	**U**	**$(Eu/Eu^*)_N$**	**$(La/Sm)_N$**
1-ap3c03	32.2	27.5	33.4	795	221	87	2000	474	1140	2760	9350	1320	5590	951	176	631	79	414	72	186	26	170	20	31	89	21	484	78	0.69	1.81
2-mr08a10*	28.9	28.1	31.2	821	193	65	1850	360	1400	1620	5710	862	3770	748	158	500	69	368	66	176	26	176	23	30	97	21	472	128	0.79	1.35
2-no10d09	32.4	27.9	34.7	837	190	67	1460	403	1300	1860	5830	804	3250	535	106	341	47	260	50	140	22	156	20	27	104	22	453	123	0.76	2.17
2-no10d10	32.0	27.9	34.9	719	227	80	1550	320	1330	1190	4200	653	2980	583	131	392	54	292	55	146	22	158	21	28	74	19	447	140	0.84	1.27
2-no10d14	32.8	27.9	35.5	704	219	89	1470	307	1250	1010	3830	611	2920	586	152	400	55	299	54	147	21	145	20	26	53	18	423	175	0.96	1.08
Rp-no10e03	30.8	27.9	33.8	734	140	78	1990	303	1390	854	3520	617	3090	737	191	551	74	384	71	174	25	183	24	24	60.3	18	358	343	0.91	3.17
Rp-no10e04	31.4	27.9	35.2	758	152	72.8	3130	340	1730	934	4200	789	4180	1150	227	863	126	651	117	274	38	232	28	26	103	18	371	311	0.69	2.73
Rp-no10d03	33.2	27.9	35.6	803	141	77.9	3760	379	1920	1260	5030	916	4900	1420	223	1090	159	835	147	350	46	284	32	29	172	22	431	282	0.55	0.55
Rp-no10d12	32.4	27.9	35.6	733	95	76.3	2230	296	1800	899	3840	688	3580	905	207	687	93	473	86	211	27	178	23	29	96	32	448	482	0.80	0.62
Rp-mr08a08	27.7	28.2	30.8	716	119	57.5	2050	349	1580	1440	5610	904	4250	899	177	604	81	417	77	191	28	172	21	30	120	22	504	141	0.73	1.00
Rp-mr08a09	27.8	27.9	30.9	699	104	60.1	2050	335	1690	1430	5640	917	4250	893	176	603	82	434	77	194	27	182	21	30	131	22	507	146	0.73	1.00
In-situ																														
1-no10d06	33.6	27.9	35.9	907	224	106	3240	654	1300	3250	11500	1920	9150	1890	295	1160	157	768	134	319	39	242	27	39	130	20	426	70.1	0.61	1.07
1-no10d13	33.0	27.9	35.1	916	179	93.5	3050	610	1440	3100	11000	1780	8310	1670	265	1030	139	695	122	292	38	225	25	37	130	22	446	71.9	0.62	1.16
2-no10c11	31.7	27.5	33.5	731	164	43.1	1620	352	1660	1430	4730	648	2730	501	114	335	51	274	56	151	24	163	21	34	119	18	481	144	0.85	1.78
2-no10c12	32.6	27.9	34.4	849	189	70.4	1660	438	1510	1970	6330	908	3710	616	118	386	53	289	58	160	24	178	23	31	124	23	520	101	0.74	2.00
2-no10d04	32.3	27.9	34.4	779	190	66.8	2420	444	1290	1920	6730	1020	4600	954	145	653	92	479	87	226	31	213	26	33	113	23	550	142	0.56	1.26
Rp-no10d08	33.3	27.9	35.3	877	202	74.5	2380	510	1460	2380	8260	1280	5690	1080	184	700	98	501	89	223	32	192	22	33	127	19	415	82.6	0.65	1.38

SR1 Sample

Mount																														
mr07b08	***28.2***	***26.7***	***30.4***	***808***	***102***	***74***	***1850***	***769***	***2960***	***5190***	***15000***	***1870***	***7030***	***1020***	***177***	***600***	***75***	***381***	***69***	***174***	***24***	***162***	***19***	***62***	***548***	***46***	***1120***	***120***	***0.69***	***3.18***
mr07b09	***29.0***	***26.9***	***31.2***	***871***	***120***	***91***	***1820***	***573***	***2390***	***5150***	***15100***	***1980***	***7920***	***1220***	***195***	***694***	***85***	***418***	***72***	***171***	***23***	***150***	***18***	***47***	***346***	***37***	***826***	***100***	***0.65***	***2.64***
mr07b11	***28.1***	***26.4***	***30.4***	***811***	***83***	***70***	***2080***	***632***	***2340***	***4720***	***14400***	***1900***	***7500***	***1150***	***197***	***684***	***88***	***438***	***79***	***200***	***28***	***182***	***21***	***45***	***409***	***43***	***1030***	***115***	***0.68***	***2.56***
ap3c07	***33.4***	***26.4***	***33.9***	***800***	***95***	***77***	***1880***	***689***	***2580***	***5110***	***14600***	***1800***	***6960***	***1020***	***172***	***612***	***76***	***378***	***68***	***176***	***26***	***163***	***21***	***52***	***434***	***43***	***1040***	***114***	***0.66***	***3.13***
ap3c13	***33.9***	***28.3***	***34.9***	***955***	***126***	***84***	***2570***	***742***	***2410***	***4890***	***15800***	***2190***	***9630***	***1680***	***247***	***1010***	***128***	***622***	***103***	***239***	***32***	***188***	***21***	***53***	***350***	***35***	***832***	***110***	***0.58***	***1.82***
1-mr07b06	29.0	27.4	30.7	861	170	63	1460	574	1010	3630	10500	1330	5020	733	132	437	55	287	53	138	20	139	18	35	124	26	626	107	0.71	3.09
1-ap3c08	32.4	27.5	33.6	781	159	66	781	623	890	3720	8430	858	2870	353	73	223	27	136	26	70	10	80	12	38	74	29	703	113	0.79	6.58
1-ap3c09	33.5	27.6	34.6	826	146	67	922	594	1270	3870	9330	997	3400	421	81	265	32	160	31	83	13	97	14	38	117	29	662	115	0.74	5.74
1-ap3c10	32.6	27.0	32.7	818	202	61	1390	605	1010	3680	10400	1270	4760	696	122	434	53	272	50	132	19	135	18	38	114	28	650	102	0.68	3.30
1-ap3c14	33.8	28.1	34.3	823	210	67	1240	654	1040	4030	10700	1250	4610	629	113	385	47	234	45	115	17	120	16	41	107	28	691	108	0.70	4.00

SR1 Sample

Mount	**SiO_2**	**CaO**	**TiO_2**	**V**	**Cr**	**Sr**	**Y**	**Zr**	**Nb**	**La**	**Ce**	**Pr**	**Nd**	**Sm**	**Eu**	**Gd**	**Tb**	**Dy**	**Ho**	**Er**	**Tm**	**Yb**	**Lu**	**Hf**	**Ta**	**Pb**	**Th**	**U**	**$(Eu/Eu^*)_N$**	**$(La/Sm)_N$**
2-mr07b07	27.7	28.0	31.2	736	148	64	575	514	733	2790	5680	559	1870	250	59	162	21	109	20	54	8.3	59	9.1	34	41	27	674	120	0.90	6.97
2-mr07b10	28.7	28.1	31.6	756	157	67	642	507	727	2800	5560	551	1910	283	68	185	24	125	23	61	9.0	63	10	34	35	31	700	141	0.91	6.18
2-mr07b12	29.6	27.7	31.2	812	148	65	863	540	955	3940	9480	1020	3420	420	84	247	30	155	30	80	12	89	12	36	86	28	664	106	0.79	5.86
2-ap3c11	32.7	27.9	33.5	743	129	63	565	554	714	2740	5440	530	1800	244	57	166	21	105	20	53	7.5	57	8.4	36	43	29	697	117	0.86	7.01
2-ap3c12	33.4	27.9	34.6	801	120	65	922	390	674	2840	5650	631	2550	442	110	299	39	201	36	89	12	81	10	28	28	29	687	140	0.92	4.01
In-situ																														
no08a03	***35.9***	***28.4***	***38.6***	***796***	***94***	***102***	***679***	***553***	***2150***	***5640***	***11200***	***1030***	***3130***	***345***	***74***	***212***	***24***	***117***	***23***	***57***	***10***	***67***	***11***	***44***	***164***	***38***	***1000***	***126***	***0.84***	***10.21***
no08a07	***36.0***	***28.6***	***35.7***	***801***	***132***	***69.7***	***542***	***532***	***1060***	***3190***	***6250***	***566***	***1840***	***256***	***53***	***147***	***19***	***99***	***17***	***44***	***7***	***45***	***8***	***31***	***56***	***34***	***673***	***122***	***0.83***	***7.78***
no08c04	***34.2***	***27.8***	***36.5***	***870***	***124***	***74.1***	***2350***	***709***	***2630***	***5060***	***15500***	***2100***	***8390***	***1390***	***233***	***821***	***106***	***520***	***91***	***229***	***30***	***192***	***23***	***50***	***480***	***43***	***1040***	***120***	***0.66***	***2.27***
no08c06*	***34.6***	***27.8***	***36.5***	***859***	***96***	***71.7***	***2130***	***669***	***2240***	***4880***	***14800***	***1910***	***7490***	***1160***	***198***	***694***	***88***	***452***	***82***	***205***	***29***	***185***	***21***	***46***	***351***	***44***	***1040***	***121***	***0.67***	***2.63***
no08d03	***33.0***	***27.8***	***34.5***	***940***	***136***	***68.9***	***3310***	***770***	***2060***	***4630***	***15600***	***2370***	***10700***	***1990***	***302***	***1260***	***161***	***806***	***135***	***318***	***40***	***239***	***27***	***49***	***396***	***32***	***864***	***116***	***0.58***	***1.45***
no08d04	***33.4***	***27.8***	***36.3***	***943***	***112***	***74.2***	***3660***	***912***	***3420***	***5750***	***19300***	***2840***	***12800***	***2400***	***352***	***1500***	***196***	***967***	***157***	***373***	***47***	***270***	***30***	***68***	***708***	***42***	***1130***	***126***	***0.57***	***1.50***
no08d05	***33.0***	***27.8***	***34.1***	***938***	***188***	***62.1***	***3050***	***662***	***1310***	***3930***	***13500***	***2050***	***9110***	***1750***	***261***	***1100***	***149***	***739***	***125***	***292***	***37***	***224***	***25***	***45***	***214***	***24***	***611***	***99***	***0.57***	***1.40***
no08d06	***34.7***	***28.1***	***35.3***	***924***	***117***	***73.9***	***3450***	***924***	***2960***	***5400***	***18000***	***2690***	***11900***	***2220***	***324***	***1380***	***183***	***897***	***151***	***344***	***44***	***254***	***28***	***74***	***601***	***38***	***969***	***119***	***0.56***	***1.52***
1-no08c07	33.9	28.1	35.9	814	127	68	1100	567	1430	4390	11200	1260	4370	569	109	328	40	200	39	101	15	106	14	36	142	30	729	116	0.77	4.82
1-no08c13	33.5	28.1	35.0	851	175	65	1310	601	1030	3900	10700	1280	4680	660	120	392	49	256	47	126	19	128	17	39	113	28	664	118	0.72	3.69
1-no08c14*	33.9	28.1	34.9	887	167	68	2090	659	1620	4040	12700	1720	7030	1180	195	708	90	454	80	200	28	172	21	45	264	32	756	110	0.65	2.14
1-no08d07	34.9	28.1	35.0	958	158	62	2960	645	1210	3770	13100	1970	8870	1680	253	1080	144	720	122	284	37	226	25	44	213	28	629	105	0.57	1.40
1-no08d08	33.7	28.1	34.5	887	185	64	2170	624	1140	3740	11900	1660	7000	1190	195	722	95	480	86	217	29	191	23	40	162	28	684	111	0.64	1.96
1-no08d10	34.5	28.8	34.8	879	171	65	1630	640	1110	4030	11700	1450	5570	834	148	513	64	327	60	158	22	157	20	41	136	29	693	114	0.69	3.02
1-no08d12	33.4	28.1	35.4	949	173	57	2580	562	1140	3140	11000	1630	7300	1400	217	881	118	608	107	264	34	206	23	39	186	24	587	105	0.60	1.40
2-no08a05	33.5	28.7	35.4	785	132	65	611	536	1020	3050	6230	603	1930	245	59	152	19	104	21	56	8.5	67	10	41	57	28	650	129	0.93	7.77
2-no08a06	33.8	28.9	35.9	818	137	69	646	615	844	3310	6730	646	2090	279	67	170	24	114	22	59	9.1	68	9.6	40	48	31	743	125	0.93	7.41
2-no08a08	33.8	28.9	34.6	707	115	65	604	605	1060	3180	6660	647	2080	264	60	175	21	118	21	60	8.7	70	9.9	45	83	30	756	127	0.85	7.52
2-no08c03	32.6	28.1	35.6	747	116	61	618	457	808	2560	5000	482	1650	256	62	172	23	123	23	60	9.1	67	9.6	29	27	27	635	132	0.90	6.24
2-no08c05	32.9	28.1	35.2	729	129	64	576	494	759	2710	5130	493	1720	262	62	170	22	117	22	55	8.3	61	9.2	33	32	30	715	127	0.89	6.46
2-no08c09	32.8	28.1	35.4	774	114	64	622	471	797	2790	5410	531	1900	294	71	194	26	131	23	58	8.2	53	7.8	29	27	39	721	138	0.91	5.93
2-no08c12*	33.0	28.1	34.7	741	134	65	524	520	721	2630	5080	481	1620	235	56	146	20	102	19	50	6.9	54	8.5	33	36	30	704	121	0.92	6.99
2-no08d09	32.3	28.8	34.8	738	140	68	583	560	776	2950	5860	564	1920	266	62	171	22	119	22	58	8.0	63	9.4	41	47	28	755	128	0.88	6.93
2-no08d11	33.7	28.8	35.5	766	149	67	631	558	805	3100	6290	614	2080	276	64	181	23	120	22	58	8.8	67	10	39	49	30	756	128	0.87	7.01
2-no08d13	32.5	28.1	34.0	761	127	65	820	552	1030	3930	9200	951	3210	390	80	237	28	149	28	78	12	88	13	37	85	30	714	115	0.80	6.29

SR1 Sample(Suite)

In-situ	**SiO_2**	**CaO**	**TiO_2**	**V**	**Cr**	**Sr**	**Y**	**Zr**	**Nb**	**La**	**Ce**	**Pr**	**Nd**	**Sm**	**Eu**	**Gd**	**Tb**	**Dy**	**Ho**	**Er**	**Tm**	**Yb**	**Lu**	**Hf**	**Ta**	**Pb**	**Th**	**U**	**$(Eu/Eu^*)_N$**	**$(La/Sm)_N$**
2-no08d14	32.7	28.8	35.1	783	131	65	698	471	674	2740	5340	536	1930	314	79	214	28	150	27	72	10	73	10	34	30	27	727	150	0.93	5.45
3-no08c10	32.6	28.8	35.2	860	125	61	652	333	589	2370	4730	515	1970	332	93	217	27	146	26	62	8.5	55	7.2	26	20	26	594	211	1.06	4.46
3-no08c11*	34.0	28.8	35.4	964	125	50	273	212	265	1070	2170	220	806	117	51	80.1	10	50	9.8	26	4.1	24	3.7	16	1.8	5.1	56.1	240	1.59	5.71

SR2 Sample

Mount																														
mr07a12	***28.9***	***28.0***	***32.3***	***787***	***247***	***164***	***1020***	***878***	***1160***	***3500***	***6770***	***773***	***3040***	***516***	***166***	***333***	***43***	***219***	***41***	***103***	***14***	***87***	***12***	***44***	***32***	***30***	***687***	***157***	***1.22***	***4.24***
mr07a14	***28.7***	***27.7***	***31.6***	***788***	***276***	***157***	***1450***	***672***	***1250***	***3310***	***7420***	***949***	***4130***	***790***	***184***	***508***	***67***	***340***	***61***	***144***	***19***	***110***	***14***	***56***	***71***	***32***	***699***	***74***	***0.89***	***2.62***
mr07b03	***28.8***	***27.7***	***31.5***	***790***	***267***	***157***	***1240***	***688***	***1130***	***3470***	***7850***	***1000***	***4190***	***725***	***188***	***451***	***57***	***288***	***51***	***122***	***16***	***98***	***12***	***49***	***56***	***35***	***798***	***78***	***1.00***	***2.99***
mr07a11	28.8	28.4	32.6	919	276	195	707	487	532	3290	6170	687	2600	414	133	248	32	160	29	69	9.0	61	8.3	27	13	24	456	105	1.27	4.96
mr07b04	29.2	28.0	31.8	784	301	179	1020	306	528	2950	6290	773	3210	563	135	345	45	227	40	102	14	89	11	21	23	19	336	57	0.93	3.27
2-mr07a13	29.5	28.8	32.4	851	375	133	478	316	242	1670	3330	378	1490	236	83	155	20	101	19	48	6.4	43	6.1	13	5.6	11	187	60	1.33	4.42
In-Situ																														
no09d06	***34.6***	***28.3***	***40.3***	***946***	***274***	***210***	***1190***	***1440***	***1250***	***3660***	***7170***	***810***	***3290***	***574***	***179***	***373***	***50***	***260***	***47***	***119***	***16***	***111***	***14***	***56***	***37***	***124***	***754***	***158***	***1.18***	***3.98***
no09d08	***34.0***	***28.3***	***35.5***	***813***	***300***	***156***	***827***	***708***	***869***	***3280***	***6450***	***705***	***2710***	***429***	***157***	***265***	***34***	***180***	***32***	***83***	***11***	***79***	***11***	***33***	***16***	***28***	***603***	***125***	***1.42***	***4.77***
no09d10	***33.8***	***29.2***	***36.2***	***818***	***245***	***152***	***804***	***899***	***1210***	***3620***	***6640***	***717***	***2630***	***401***	***155***	***247***	***32***	***166***	***30***	***79***	***11***	***78***	***11***	***43***	***25***	***88***	***2320***	***280***	***1.50***	***5.64***
no09d11	***34.7***	***28.3***	***34.9***	***789***	***250***	***168***	***951***	***1080***	***1480***	***4390***	***8380***	***932***	***3500***	***548***	***201***	***331***	***43***	***212***	***39***	***96***	***14***	***93***	***12***	***53***	***47***	***99***	***2390***	***220***	***1.44***	***5.00***
no10a08*	***34.0***	***28.6***	***36.9***	***820***	***269***	***164***	***1090***	***895***	***1250***	***3870***	***7660***	***892***	***3530***	***565***	***199***	***359***	***45***	***233***	***44***	***105***	***14***	***104***	***13***	***43***	***37***	***38***	***893***	***129***	***1.35***	***4.28***
no10a09	***32.8***	***27.9***	***35.5***	***828***	***255***	***161***	***1100***	***889***	***1220***	***3750***	***7580***	***875***	***3510***	***587***	***193***	***361***	***46***	***242***	***44***	***114***	***15***	***100***	***13***	***44***	***34***	***37***	***864***	***140***	***1.28***	***3.99***
no10a13	***35.4***	***28.9***	***36.0***	***849***	***311***	***135***	***756***	***720***	***727***	***3030***	***6010***	***662***	***2520***	***383***	***148***	***246***	***31***	***161***	***29***	***73***	***11***	***73***	***10***	***35***	***14***	***61***	***1450***	***164***	***1.47***	***4.94***
no10a14	***33.5***	***28.6***	***36.1***	***799***	***313***	***120***	***782***	***329***	***423***	***2250***	***5020***	***594***	***2400***	***396***	***131***	***247***	***32***	***169***	***30***	***80***	***11***	***73***	***10***	***24***	***15***	***14***	***305***	***57***	***1.28***	***3.55***
no10b04	***34.4***	***28.6***	***37.8***	***838***	***250***	***162***	***896***	***1020***	***1360***	***4150***	***7970***	***868***	***3240***	***488***	***176***	***293***	***36***	***181***	***34***	***84***	***12***	***81***	***11***	***46***	***36***	***90***	***2180***	***212***	***1.42***	***5.31***
no10b09	***34.2***	***28.6***	***37.1***	***823***	***277***	***166***	***1240***	***835***	***1180***	***3750***	***7530***	***892***	***3650***	***618***	***174***	***410***	***53***	***276***	***48***	***125***	***16***	***103***	***13***	***54***	***46***	***43***	***1010***	***119***	***1.05***	***3.79***
no10b10	***32.5***	***28.6***	***36.6***	***815***	***286***	***170***	***1210***	***834***	***1160***	***3560***	***7290***	***875***	***3620***	***630***	***168***	***386***	***51***	***267***	***49***	***116***	***16***	***96***	***12***	***51***	***45***	***41***	***936***	***115***	***1.04***	***3.53***
no09d03	34.4	29.1	36.9	790	313	133	734	316	344	2230	4520	516	2080	354	130	226	30	156	29	72	10	67	8.7	19	11	22	317	62.6	1.40	3.93
no09d04	34.6	28.9	36.5	821	341	143	940	660	741	2820	5710	673	2670	458	161	305	39	212	38	99	13	86	12	41	22	34	743	194	1.31	3.85
no09d05	34.5	29.1	35.2	841	430	133	748	416	264	2070	4320	508	2040	357	122	227	30	158	29	72	10	67	8.7	24	10	18	373	83.2	1.31	3.62
no09d07	35.3	29.1	35.6	894	594	133	794	409	289	1690	3640	442	1890	363	109	252	33	175	33	78	10	71	8.7	27	10	12	230	49.4	1.10	2.91
no09d12	34.2	29.2	36.0	773	344	124	635	324	328	2100	4240	494	2010	345	121	214	28	147	27	65	10	67	8.6	21	10	23	499	67.7	1.36	3.80
no09d13	33.3	28.9	35.0	802	359	134	1010	635	709	2880	6190	730	3010	521	165	322	40	220	40	92	14	88	12	32	21	60	641	95.9	1.23	3.45
no09d14	34.3	29.1	37.0	791	337	132	680	327	342	2190	4450	504	2060	345	122	226	30	151	29	70	10	66	8.6	22	13	19	396	62.6	1.33	3.96

SR2 Sample

In-Situ	**SiO_2**	**CaO**	**TiO_2**	**V**	**Cr**	**Sr**	**Y**	**Zr**	**Nb**	**La**	**Ce**	**Pr**	**Nd**	**Sm**	**Eu**	**Gd**	**Tb**	**Dy**	**Ho**	**Er**	**Tm**	**Yb**	**Lu**	**Hf**	**Ta**	**Pb**	**Th**	**U**	**$(Eu/Eu^*)_N$**	**$(La/Sm)_N$**
no10a06	34.8	28.7	36.7	825	323	157	974	621	1090	3430	6710	774	3110	497	177	318	41	217	39	99	13	80	11	42	36	29	586	83.4	1.36	4.31
no10a07	34.9	28.5	36.3	816	319	160	978	658	1100	3580	7000	805	3170	510	180	329	41	220	40	99	13	85	12	44	34	27	601	82.6	1.34	4.38
no10a10*	35.1	29.4	36.6	857	409	114	697	352	201	1880	3970	466	1920	326	108	210	28	144	27	70	10	65	8.7	18	6.5	14	280	46.9	1.26	3.60
no10a12	34.2	28.9	35.2	842	450	120	487	376	233	1860	3680	407	1580	258	95	155	20	104	18	46	6.7	46	6.5	18	8.4	28	607	91.2	1.45	4.50
no10b05	33.4	28.9	37.9	798	320	128	750	308	373	2280	4730	558	2230	376	128	232	31	156	29	74	10	64	9.1	19	15	20	391	58.4	1.32	3.79
no10b08	33.2	28.9	36.6	857	549	130	749	354	196	1920	4110	500	2050	358	108	228	30	153	28	69	9.2	67	9.2	17	4.2	13	235	46.8	1.15	3.35
no10b11	34.7	28.9	37.6	927	346	196	859	488	544	3660	7070	809	3160	495	153	302	37	190	33	80	11	73	9.2	25	13	26	520	85.2	1.21	4.62
no10b12	33.5	28.9	36.4	699	383	141	956	602	628	2670	5330	631	2620	448	134	292	38	203	37	94	13	83	12	73	31	23	498	60.3	1.13	3.72
no10b13	32.9	28.9	35.7	709	411	121	727	389	308	1790	3730	452	1880	323	101	218	29	148	28	71	10	64	8.8	35	10	10	192	44.9	1.16	3.46
2-no10a11*	34.8	29.1	35.9	855	481	127	451	337	223	1720	3370	369	1440	227	89	141	18	93	17	45	6.6	42	5.9	17	4.7	10	163	49.4	1.51	4.73
2-no10b06	34.1	29.2	36.4	919	522	95.7	821	431	272	1390	3130	418	1900	374	82	264	35	181	32	79	11	68	10	28	10	6.1	84.1	16.2	0.80	2.32
2-no10b07	34.1	29.2	36.9	924	588	92.3	588	130	112	1100	2330	293	1310	256	61	181	24	128	23	59	7.5	48	6.7	15	6.2	5.3	61.2	12.6	0.86	2.68
2-no10b14	33.3	28.9	34.9	855	598	84.6	551	124	102	1090	2330	296	1300	252	61	173	23	116	22	56	7.2	48	6.7	11	3.7	5.7	87.3	15.4	0.88	2.70

SR3 Sample

Mount																														
mr07a08	***28.7***	***27.3***	***31.2***	***812***	***116***	***74.6***	***1110***	***735***	***2330***	***5310***	***12900***	***1400***	***4730***	***588***	***110***	***333***	***40***	***206***	***39***	***105***	***15***	***110***	***15***	***53***	***333***	***44***	***1070***	***134***	***0.76***	***5.64***
mr07a09	***28.3***	***27.5***	***30.6***	***797***	***137***	***65.8***	***729***	***570***	***1290***	***3780***	***8580***	***868***	***2860***	***339***	***70***	***196***	***25***	***125***	***24***	***68***	***11***	***89***	***13***	***33***	***122***	***28***	***693***	***126***	***0.82***	***6.96***
ap3e04*	***31.9***	***25.7***	***33.0***	***852***	***230***	***64.0***	***3290***	***635***	***2140***	***4770***	***16200***	***2360***	***10900***	***2060***	***310***	***1280***	***166***	***830***	***138***	***317***	***40***	***233***	***26***	***45***	***364***	***37***	***894***	***92***	***0.58***	***1.45***
ap3e07	***31.6***	***26.7***	***34.5***	***767***	***91***	***75.6***	***1350***	***805***	***2670***	***5890***	***14400***	***1570***	***5400***	***666***	***124***	***420***	***49***	***242***	***46***	***121***	***18***	***125***	***17***	***57***	***418***	***49***	***1280***	***138***	***0.71***	***5.52***
mr07a05	***28.7***	***27.8***	***31.4***	***741***	***109***	***72.8***	***826***	***759***	***2110***	***4850***	***10900***	***1080***	***3420***	***411***	***82***	***234***	***29***	***147***	***29***	***76***	***12***	***86***	***13***	***62***	***260***	***41***	***1080***	***142***	***0.81***	***7.37***
1-ap3e05*	32.7	26.8	33.4	835	147	62.6	1730	612	1080	3640	10700	1390	5510	854	150	542	67	349	63	162	23	155	20	38	134	26	637	100	0.67	2.66
2-mr07a03*	29.5	28.5	31.8	764	141	64.7	526	481	836	2640	5240	513	1690	231	55	149	19	101	19	49	7.3	55	8.2	32	47	27	639	118	0.90	7.14
2-mr07a04	29.1	28.4	31.5	764	136	63.9	576	526	745	2840	5800	577	1880	255	60	161	21	112	21	57	7.9	60	8.9	33	44	27	678	120	0.90	6.95
2-mr07a06	28.7	28.1	32.3	782	85	71.9	885	475	1260	3950	7550	782	2950	485	116	319	40	205	36	85	11	68	9.1	34	72	53	1330	162	0.90	5.09
2-mr07a07	28.1	28.5	32.0	778	145	67.3	586	542	695	2660	5250	509	1740	261	61	171	21	114	21	59	8	60	10	34	37	28	725	132	0.87	6.36
2-ap3e03	32.4	27.9	33.9	716	119	62.8	630	470	869	2920	5560	530	1880	282	66	199	25	129	24	61	8.4	61	9.0	31	34	32	745	117	0.85	6.47
In Situ																														
no09b07	***31.8***	***27.1***	***34.3***	***776***	***180***	***76.4***	***2840***	***574***	***1330***	***3840***	***11700***	***1650***	***7090***	***1310***	***229***	***849***	***119***	***638***	***112***	***270***	***36***	***209***	***25***	***32***	***163***	***18***	***483***	***74***	***0.66***	***1.83***
no09b12	***31.6***	***27.0***	***33.1***	***778***	***197***	***68.6***	***2010***	***569***	***1060***	***3420***	***9280***	***1230***	***4870***	***822***	***148***	***544***	***75***	***413***	***73***	***191***	***25***	***169***	***20***	***33***	***114***	***22***	***521***	***79***	***0.67***	***2.60***
no09a10	***31.9***	***27.5***	***36.2***	***770***	***181***	***55.7***	***2170***	***874***	***2670***	***3390***	***9940***	***1310***	***5060***	***836***	***141***	***557***	***78***	***409***	***79***	***200***	***28***	***189***	***22***	***77***	***425***	***28***	***696***	***98***	***0.63***	***2.53***

SR3 Sample

In Situ	**SiO_2**	**CaO**	**TiO_2**	**V**	**Cr**	**Sr**	**Y**	**Zr**	**Nb**	**La**	**Ce**	**Pr**	**Nd**	**Sm**	**Eu**	**Gd**	**Tb**	**Dy**	**Ho**	**Er**	**Tm**	**Yb**	**Lu**	**Hf**	**Ta**	**Pb**	**Th**	**U**	**$(Eu/Eu^*)_N$**	**$(La/Sm)_N$**
1-no09b13	32.1	27.8	34.5	716	134	67.4	1520	512	1190	3820	8460	987	3820	615	141	420	56	299	57	143	20	133	18	32	116	36	981	100	0.85	3.88
1-no09a04	32.8	27.5	35.9	769	186	61.4	1640	567	1470	3400	9280	1110	4220	672	121	428	59	316	59	147	22	144	18	37	174	25	613	95	0.69	3.16
1-no09a06	32.0	27.4	36.6	771	114	78.5	2330	587	1690	4340	12100	1570	6280	1090	200	718	96	491	89	226	30	180	21	37	180	26	679	88	0.69	2.49
1-no09b06	33.6	27.8	36.0	740	95	73.1	1990	538	1360	4320	10100	1230	4940	882	198	594	81	425	78	193	26	162	21	35	139	43	1190	112	0.83	3.06
1-no09b08	32.7	27.7	35.2	721	101	71.9	1840	546	1380	4410	9880	1180	4740	795	176	541	72	392	71	182	25	164	21	35	154	46	1170	105	0.82	3.46
2-no09a03	34.2	28.6	37.6	787	181	58.7	844	570	1260	3210	7270	742	2490	325	63	202	27	137	27	79	12	91	14	38	116	26	575	102	0.75	6.17
2-no09a05	33.4	28.9	38.3	759	141	62.5	753	511	803	2830	5930	604	2120	315	64	210	28	146	27	71	11	79	11	36	55	22	536	95	0.76	5.61
2-no09a07	33.6	28.7	38.6	745	78	68.6	829	469	1150	3540	6540	660	2460	381	90	266	34	172	31	76	10	72	11	28	37	23	577	119	0.86	5.80
2-no09a08	33.8	28.9	37.0	793	144	67.7	604	471	722	2190	4020	389	1370	211	53	147	20	108	22	57	8.8	67	10	30	36	21	484	115	0.91	6.48
2-no09b05	33.5	28.9	36.4	829	165	69.8	695	518	897	2680	5480	538	1930	246	57	176	23	115	25	63	9.7	74	12	29	59	21	510	102	0.84	6.80

(1) cores compositions, (2) rims compositions (Rp) Reprecipitation feature. Analyses in bold are from Fir-tree and extremely bright sector zones. Al_2O_3, SiO_2, CaO, TiO_2 are reported in Wt% and the other elements in ppm. * are analyses reported in figure 2.

Electronic Appendix 3: Analyses of apatite compositions.

RA1 Sample Appinite

Analysis Nb	P_2O_5	CaO	V	Sr	Y	Zr	La	Ce	Pr	Nd	Sm	Eu	Gd	Tb	Dy	Ho	Er	Tm	Yb	Lu	Pb	Th	U	$(Eu/Eu^*)_N$	$(La/Sm)_N$	La/Sm	Ce/Th
1-ap04b04*	44.30	55.4	31.80	2550	236	1.6	645	1910	274	1310	221	48	137	12	56	8.6	18	2.2	14	1.8	14	36	22	0.84	1.82	2.9	53
1-ap04b06	42.50	54.7	39.20	2650	229	4.8	1000	2590	331	1520	244	53	142	14	55	8.8	20	2.4	13	2.2	15	37	13	0.87	2.56	4.1	71
1-ap04b07	41.00	53.1	35.80	2370	208	3.1	871	2350	291	1310	206	46	125	12	51	7.3	16	1.8	12	1.8	13	41	19	0.87	2.64	4.2	58
1-ap04d07	41.00	54.5	35.50	2660	236	3.8	741	2050	273	1260	209	44	138	12	52	8.4	18	2.2	13	1.7	13	37	16	0.79	2.21	3.5	56
1-ap04d08	39.80	55.1	38.50	2800	227	4.0	822	2250	307	1370	220	51	135	12	51	8.5	18	2.3	13	1.7	14	45	22	0.90	2.33	3.7	50
1-ap04d09	39.40	54.9	36.40	2830	206	4.2	779	2100	288	1280	205	47	124	12	45	7.3	17	2.0	11	1.7	15	41	10	0.90	2.37	3.8	51
1-ap04d10	40.50	55.0	35.60	2750	219	1.9	791	2200	289	1310	195	47	129	12	51	8.1	17	1.9	12	1.7	13	49	38	0.91	2.53	4.1	45
1-ap3h13	44.70	55.5	7.63	2900	173	0.4	579	1520	210	969	158	35	103	10	38	6.5	13	1.6	10	1.4	14	35	34	0.84	2.29	3.7	44
1-ap3h14	43.70	55.2	33.10	2730	237	3.1	768	2060	287	1350	220	47	144	13	54	8.5	18	2.1	13	1.9	15	36	11	0.81	2.18	3.5	58
1-ap3i04	44.50	55.4	18.50	2600	169	2.0	558	1490	206	984	159	34	100	10	39	6.1	14	1.4	9	1.4	12	31	19	0.81	2.19	3.5	49
1-ap3i05	42.20	54.4	36.50	2470	286	4.2	1090	2860	380	1750	281	57	169	16	64	10.2	22	2.7	15	2.3	13	44	20	0.79	2.42	3.9	65
1-ap3i06	43.80	54.5	38.10	2630	289	4.9	1270	3270	415	1840	290	60	171	16	66	10.0	21	2.5	16	2.2	15	40	11	0.82	2.73	4.4	82
1-ap3i07	42.40	54.8	36.00	2650	265	4.0	1070	2670	368	1660	263	52	165	16	61	10.0	21	2.4	15	2.0	13	42	13	0.76	2.54	4.1	63
1-ap3i08	39.30	55.2	6.71	2470	165	0.3	672	1680	234	1040	171	32	99	9	36	5.8	11	1.5	7	1.1	11	36	32	0.75	2.45	3.9	47
1-ap3i10	39.30	55.0	36.90	2870	304	4.4	1200	2970	406	1830	290	67	178	17	68	10.5	24	2.7	17	2.5	15	46	18	0.90	2.58	4.1	65
1-ap3i11	40.30	55.1	34.10	2830	315	4.4	1200	3060	411	1860	292	69	186	17	67	10.9	25	2.7	18	2.3	17	56	37	0.91	2.57	4.1	55
1-ap3i12	39.60	54.7	37.40	3030	341	5.1	1300	3200	431	1970	316	70	197	19	75	12.0	26	3.2	18	2.9	17	56	31	0.86	2.57	4.1	58
1-ap3i13	44.70	55.3	6.66	2660	160	0.4	621	1540	212	954	148	32	93	9	34	6.0	12	1.4	9	1.2	11	29	25	0.84	2.62	4.2	53
1-sp04d12	40.20	55.0	42.90	2920	334	5.8	1300	3390	462	2060	344	71	192	19	76	12.2	26	2.9	18	2.4	17	39	8	0.84	2.36	3.8	86
1-sp04f06	41.00	55.0	35.80	2780	248	4.3	959	2480	339	1590	260	56	151	14	58	9.2	19	2.3	15	2.0	17	49	30	0.86	2.30	3.7	51
1-sp04f08	41.40	55.0	31.40	2550	255	2.4	765	2060	290	1340	218	53	135	13	54	9.0	20	2.5	15	2.3	14	41	29	0.94	2.19	3.5	50
1-sp04f09	40.10	55.0	46.00	2630	350	6.1	1070	2880	407	1930	329	71	201	20	82	13.0	28	3.3	20	2.9	15	51	19	0.84	2.03	3.3	57
1-sp04f11	42.10	55.0	31.40	2600	242	2.0	640	1870	264	1250	208	50	131	12	53	8.7	20	2.4	14	2.1	14	48	40	0.93	1.92	3.1	39
1-sp04f12	42.20	55.0	12.50	2620	191	1.2	536	1490	211	993	167	41	102	10	41	6.6	15	1.7	11	1.7	15	39	26	0.95	2.00	3.2	38
1-sp04f05	41.20	55.0	7.57	2600	221	0.6	578	1570	240	1140	198	41	131	12	50	8.2	18	2.0	11	1.9	12	34	22	0.78	1.82	2.9	46
1-sp04f13	42.60	55.0	6.60	2410	198	0.7	614	1600	227	1020	159	32	99	10	42	7.0	15	1.9	10	1.6	11	30	13	0.77	2.41	3.9	53
R-ap04b05*	44.20	55.0	7.46	2610	140	<0.26	397	1140	162	762	128	30	78	7	29	5.1	11	1.3	7	1.1	12	25	26	0.90	1.94	3.1	46
R-ap04d06	44.00	55.4	9.04	2730	163	0.6	565	1510	198	952	152	33	100	9	40	5.7	14	1.3	9	1.3	13	25	24	0.81	2.32	3.7	61
R-sp04d13	41.70	55.0	33.70	2860	232	2.7	763	2050	288	1320	230	48	140	13	54	8.3	18	2.1	12	1.7	14	34	16	0.81	2.07	3.3	61
R-sp04d14	41.90	55.0	32.40	2760	229	3.2	791	2110	296	1370	233	46	144	14	54	8.3	18	2.1	12	1.7	14	35	10	0.76	2.12	3.4	60

RA1 Sample

Analysis Nb	P_2O_5	CaO	V	Sr	Y	Zr	La	Ce	Pr	Nd	Sm	Eu	Gd	Tb	Dy	Ho	Er	Tm	Yb	Lu	Pb	Th	U	$(Eu/Eu^*)_N$	$(La/Sm)_N$	La/Sm	Ce/Th
R-sp04f04	40.40	55.0	31.50	2630	282	1.3	652	1920	282	1400	245	51	162	15	65	10.6	23	2.8	15	2.2	14	52	42	0.78	1.66	2.7	37
R-sp04f10	42.40	55.0	11.70	2660	185	0.8	498	1360	196	943	154	37	99	9	38	6.5	15	1.6	10	1.7	12	30	25	0.93	2.02	3.2	45
R-sp04f14	42.00	55.0	39.90	2380	324	4.0	1030	2630	373	1700	283	55	172	17	71	11.5	25	3.0	18	2.4	13	42	17	0.76	2.27	3.6	63

R2 Sample

Analysis Nb	P_2O_5	CaO	V	Sr	Y	Zr	La	Ce	Pr	Nd	Sm	Eu	Gd	Tb	Dy	Ho	Er	Tm	Yb	Lu	Pb	Th	U	$(Eu/Eu^*)_N$	$(La/Sm)_N$	La/Sm	Ce/Th
1-ap04d14*	40.60	55.1	10.40	786	334	2.1	363	1100	147	681	139	26	106	13	63	11.8	31	3.9	25	4.1	9	55	49	0.65	1.63	2.6	20
1-sp03c09	44.10	55.2	8.46	872	337	0.5	449	1210	163	699	129	24	93	12	57	11.3	28	3.8	23	3.8	8	33	12	0.68	2.17	3.5	37
2-ap04c04	46.00	55.2	7.02	862	215	0.4	309	898	113	499	93.4	20	72	8	39	7.7	19	2.4	15	2.6	7	29	18	0.73	2.07	3.3	31
2-ap04c05	45.80	54.9	8.11	876	501	1.0	637	1800	240	1090	201	41	166	19	98	18.2	46	5.8	36	5.8	10	64	23	0.68	1.98	3.2	28
2-ap04d11	43.20	54.8	5.57	839	259	0.4	318	940	121	545	108	22	89	10	49	9.4	24	3.0	19	3.0	8	30	23	0.68	1.84	2.9	31
2-ap04d12	42.20	55.0	6.62	836	359	0.4	408	1300	161	727	146	28	123	15	70	13.0	33	3.8	28	4.2	9	41	30	0.64	1.75	2.8	32
2-ap04e04*	45.30	55.2	5.98	897	312	0.3	382	1110	150	684	136	26	102	12	58	10.8	27	3.7	21	3.5	8	37	18	0.67	1.75	2.8	30
2-sp03b10	42.70	55.2	9.54	870	447	0.5	554	1450	199	901	179	33	145	18	88	17.0	40	4.9	34	5.3	9	53	16	0.62	1.93	3.1	27
2-sp03b13	43.30	55.2	9.04	868	593	0.8	630	1770	241	1080	218	38	169	22	106	20.3	50	6.7	43	6.7	9	64	22	0.60	1.80	2.9	28
2-sp03c07	42.70	55.2	6.48	866	293	0.3	417	1100	142	625	115	21	89	11	53	10.4	25	3.4	20	3.3	8	33	13	0.64	2.26	3.6	33
2-sp03d04	44.70	55.2	6.69	853	264	0.4	366	980	130	584	111	22	90	11	51	9.4	24	3.2	20	3.5	8	33	15	0.66	2.06	3.3	30
2-sp03d05	42.40	55.2	6.71	847	273	0.4	380	1030	134	612	115	23	90	11	52	10.2	26	3.1	22	3.7	8	33	15	0.68	2.06	3.3	31
3-ap04d13*	47.40	55.3	6.58	895	284	0.3	339	1000	131	611	117	24	93	11	55	10.5	26	3.2	21	3.5	9	31	16	0.69	1.81	2.9	32
ap04e05	44.10	55.3	5.98	850	288	<0.165	375	1110	141	638	125	23	100	11	58	10.4	26	3.3	19	3.2	9	26	14	0.62	1.87	3.0	43
ap04e06	45.00	55.3	5.75	858	333	0.4	392	1120	148	684	135	24	111	13	64	11.7	30	3.8	22	3.4	8	27	16	0.59	1.81	2.9	41
ap04e07	43.00	55.3	4.92	818	258	<0.197	364	1070	130	573	107	21	89	10	48	9.0	23	3.1	19	3.3	8	24	39	0.66	2.12	3.4	46
ap3h10	47.40	55.6	6.79	807	520	1.5	549	1630	228	1000	198	43	156	18	88	17.5	43	5.5	37	6.7	8	84	128	0.75	1.73	2.8	19
ap3h11	44.10	55.6	6.18	801	338	0.2	393	1120	151	686	129	23	104	12	64	11.7	30	3.8	23	3.7	8	31	22	0.60	1.90	3.0	37
ap3h12	43.20	55.5	4.34	780	311	0.5	369	1090	149	647	122	22	100	12	62	10.9	30	3.4	22	3.4	7	24	31	0.62	1.89	3.0	46
sp03c04	43.30	55.2	6.34	825	260	0.3	353	952	126	566	104	23	83	10	47	9.3	23	2.8	19	3.3	8	34	29	0.76	2.12	3.4	28
sp03c05	43.00	55.2	8.31	881	398	0.6	495	1400	186	859	165	32	133	16	78	14.7	37	4.7	30	4.9	8	55	20	0.66	1.87	3.0	25
sp03c06	41.90	55.2	12.40	850	394	0.8	447	1300	175	792	159	32	125	15	72	14.0	34	4.5	30	4.7	8	47	34	0.69	1.76	2.8	28
sp03c10	42.80	55.2	5.88	841	250	0.3	336	947	127	561	106	24	83	10	46	8.7	22	2.8	18	3.0	7	30	30	0.76	1.98	3.2	31
sp03c11	44.60	55.2	6.19	831	258	0.3	329	937	123	563	106	22	83	10	47	9.4	23	2.9	18	3.3	7	31	41	0.70	1.94	3.1	31
sp03d06	42.30	55.2	7.30	770	236	0.3	395	983	124	547	97.5	26	78	9	42	8.7	21	2.7	18	3.1	7	48	29	0.90	2.53	4.1	21
sp03d07	43.50	55.2	8.76	811	374	0.8	546	1390	183	827	149	35	119	13	68	13.7	33	4.1	28	4.9	8	58	25	0.80	2.29	3.7	24

RT1 Sample

Analysis Nb	P_2O_5	CaO	V	Sr	Y	Zr	La	Ce	Pr	Nd	Sm	Eu	Gd	Tb	Dy	Ho	Er	Tm	Yb	Lu	Pb	Th	U	$(Eu/Eu^*)_N$	$(La/Sm)_N$	La/Sm	Ce/Th
1-ap04h12	40.30	55.2	7.23	1000	313	1.4	547	1550	191	851	136	29	103	12	56	11.1	27	3.4	23	3.7	9	79	60	0.76	2.51	4.0	20
1-ap04h13	40.00	55.3	8.63	982	315	1.0	558	1550	197	844	138	33	104	12	59	11.0	28	3.4	23	3.7	7	55	48	0.83	2.53	4.0	28
1-ap04i10*	41.40	55.3	16.80	1060	187	0.9	355	920	120	514	84.3	21	60	7	34	6.8	17	2.0	15	2.4	7	43	33	0.89	2.63	4.2	22
1-sp04c05	44.50	55.0	9.27	1020	441	1.4	801	2110	279	1220	193	48	139	16	78	15.6	39	5.3	33	5.3	7	69	34	0.89	2.59	4.2	30
1-sp04c14	44.10	55.0	11.40	1020	423	1.9	894	2450	304	1270	192	46	136	16	76	14.9	37	4.8	33	5.5	7	79	27	0.87	2.91	4.7	31
1-sp04d09	41.40	55.0	11.20	1030	459	1.5	857	2260	297	1260	197	50	138	17	81	15.9	42	5.4	35	6.0	7	74	26	0.92	2.72	4.4	31
2-ap04h14*	42.30	54.7	9.08	1050	450	1.8	926	2460	297	1290	198	53	145	16	78	15.8	40	5.1	33	6.0	9	74	31	0.96	2.92	4.7	33
2-ap04i05	36.20	54.8	7.75	1030	414	1.9	783	2100	265	1110	178	44	133	15	71	14.2	36	4.5	30	5.0	8	71	52	0.87	2.75	4.4	30
2-ap04i06	39.70	55.1	9.61	1060	496	1.8	945	2500	325	1340	211	52	159	19	87	17.0	45	5.8	38	5.9	9	82	48	0.87	2.80	4.5	30
2-ap04i09*	41.30	55.1	8.68	1070	470	2.0	935	2450	306	1300	207	52	150	17	82	16.4	43	5.6	34	6.0	9	79	38	0.90	2.82	4.5	31
2-ap04i11*	40.60	55.0	8.75	1020	452	2.1	871	2340	289	1230	195	51	144	16	82	16.1	40	5.7	36	5.8	8	81	35	0.92	2.79	4.5	29
2-sp04b05	45.50	55.0	8.44	1010	375	1.2	786	2150	273	1120	174	39	117	13	66	12.6	33	4.4	30	4.9	7	60	27	0.83	2.82	4.5	36
2-sp04b07	44.00	55.0	11.00	1070	418	2.0	978	2740	329	1350	201	48	136	15	75	13.8	36	5.0	32	5.2	7	77	25	0.88	3.04	4.9	36
2-sp04c09	44.30	55.0	9.04	1000	423	1.5	797	2100	270	1150	186	47	132	16	79	14.9	40	5.0	33	5.4	7	75	36	0.91	2.68	4.3	28
2-sp04c11	44.50	55.0	10.20	1040	424	1.6	936	2320	290	1220	188	50	135	16	78	14.8	39	5.2	31	5.6	8	86	34	0.96	3.11	5.0	27
2-sp04d08	43.10	55.0	11.00	1060	386	1.4	777	2090	269	1110	172	45	119	14	70	13.8	33	4.4	31	4.8	7	73	30	0.95	2.82	4.5	29
3-sp04b06	43.40	55.0	5.43	1060	134	0.2	286	798	94.9	400	60.4	15	45	5	26	4.8	12	1.4	10	1.5	5	18	15	0.90	2.96	4.7	44
3-sp04c06	43.00	55.0	7.05	1020	220	0.9	443	1130	145	633	99.6	24	71	8	41	7.9	20	2.6	16	2.9	6	38	32	0.88	2.78	4.4	30
3-sp04c08	45.50	55.0	7.13	1060	192	0.3	397	1020	131	554	86.6	22	64	7	35	6.4	17	2.1	14	2.3	6	26	26	0.91	2.86	4.6	39
3-sp04c10	44.90	55.0	7.03	1030	216	0.6	469	1180	151	628	96.9	26	70	8	40	8.0	20	2.5	16	2.6	6	42	35	0.95	3.02	4.8	28
ap04h11	40.30	55.3	5.94	1020	170	0.6	324	845	112	473	75.8	17	58	6	33	5.6	14	1.7	11	1.9	6	24	28	0.78	2.67	4.3	35
ap04i12	43.80	55.2	13.60	1040	437	1.6	814	2400	314	1250	199	50	140	15	77	15.3	42	5.1	39	5.0	9	79	33	0.90	2.55	4.1	31
sp04c04	45.10	55.0	9.77	1060	464	1.8	1090	2780	355	1450	218	51	152	17	83	16.5	42	5.5	37	5.7	8	80	25	0.85	3.12	5.0	35

RHG-1 Sample

Analysis Nb																											
1-ap04f05	43.00	55.0	12.40	868	431	1.4	1020	2540	296	1190	190	41	139	15	75	14.8	38	4.8	35	5.6	10	77	29	0.76	3.35	5.4	33
1-ap04f08	42.70	55.0	7.87	829	442	0.9	820	2180	276	1180	190	39	138	16	78	14.3	39	5.1	33	5.3	9	87	65	0.74	2.70	4.3	25
1-ap04f09	43.60	55.0	8.28	856	389	0.9	647	1730	210	893	145	34	109	12	61	12.5	33	4.3	30	4.6	8	63	47	0.83	2.79	4.5	27
1-ap04f11	43.70	55.1	8.93	891	386	0.9	1320	3290	369	1400	198	37	140	15	70	13.0	35	4.6	31	4.4	10	75	24	0.68	4.16	6.7	44
1-sp03d10	42.40	55.0	8.23	870	272	0.3	523	1290	160	701	114	23	85	9	46	8.9	23	3.2	22	3.3	8	25	13	0.73	2.86	4.6	52

RHG-1 Sample (suite)

Analysis Nb	P_2O_5	CaO	V	Sr	Y	Zr	La	Ce	Pr	Nd	Sm	Eu	Gd	Tb	Dy	Ho	Er	Tm	Yb	Lu	Pb	Th	U	$(Eu/Eu^*)_N$	$(La/Sm)_N$	La/Sm	Ce/Th
1-sp03d12	45.20	55.0	0.44	900	77.6	<0.087	236	547	62.4	250	35.8	7	26	3	13	2.5	6	0.8	6	0.8	7	2	1	0.70	4.12	6.6	275
1-sp03e05	41.50	55.0	9.51	802	507	1.1	664	1940	278	1220	201	43	149	17	87	17.0	44	6.1	40	6.6	8	79	62	0.75	2.06	3.3	24
1-sp03e07*	41.90	55.0	10.70	862	446	1.5	1050	2580	320	1290	201	40	139	16	76	15.3	40	5.2	35	5.7	8	82	42	0.73	3.26	5.2	32
1-sp03e11	40.30	55.0	9.63	864	399	1.5	1080	2540	304	1200	178	36	122	14	65	13.1	33	4.6	31	5.0	8	72	25	0.74	3.79	6.1	36
1-sp03f05	43.30	55.0	8.35	867	339	1.1	616	1670	214	900	141	28	99	12	56	11.0	29	4.1	27	4.1	8	46	19	0.72	2.73	4.4	36
1-sp03f10	42.00	55.0	9.93	974	450	1.3	1470	3260	370	1410	198	39	138	16	77	15.1	38	5.2	36	5.4	10	74	24	0.72	4.64	7.4	44
1-sp03f11	42.40	55.0	10.90	882	473	1.2	964	2460	309	1270	197	41	137	15	81	15.0	41	5.4	37	5.9	8	70	24	0.76	3.06	4.9	35
2-ap04f06	42.60	55.2	9.37	896	433	1.2	1030	2810	320	1280	188	37	139	15	76	14.1	37	4.9	36	5.8	11	70	21	0.70	3.42	5.5	40
2-ap04f07	43.50	55.0	8.27	926	305	0.6	588	1540	195	818	130	27	90	11	49	9.3	25	3.3	20	3.5	8	46	16	0.77	2.82	4.5	34
2-ap04f12	43.10	55.1	8.52	888	359	1.0	1200	2850	345	1240	183	34	122	14	67	13.6	34	4.1	30	4.5	10	60	21	0.69	4.09	6.6	48
2-sp03d09	42.30	55.0	9.89	895	433	1.2	1050	2480	308	1260	199	39	139	16	73	14.6	38	5.4	35	5.9	9	69	19	0.72	3.29	5.3	36
2-sp03d13	47.00	55.0	7.99	910	331	0.8	894	2140	243	959	147	28	103	12	55	10.8	28	4.3	25	4.2	9	62	26	0.70	3.80	6.1	35
2-sp03d14	43.00	55.0	8.57	877	443	1.4	1180	2800	336	1310	196	37	133	16	74	14.3	37	5.1	36	5.6	9	67	23	0.69	3.76	6.0	42
2-sp03e04	43.40	55.0	9.01	904	279	0.4	545	1380	184	736	114	23	79	10	46	9.1	24	3.4	22	3.5	8	44	13	0.75	2.99	4.8	31
2-sp03e06*	44.30	55.0	8.50	900	282	0.5	660	1630	195	799	122	26	84	10	47	9.6	24	3.4	21	3.6	8	48	16	0.77	3.38	5.4	34
2-sp03e08	42.60	55.0	9.00	894	457	1.3	1050	2470	308	1210	187	39	136	16	76	15.4	37	5.5	37	6.1	9	64	19	0.75	3.51	5.6	39
2-sp03e12	41.90	55.0	9.64	874	381	1.2	1150	2600	315	1200	174	33	117	14	64	12.1	33	4.7	29	4.8	9	63	19	0.71	4.13	6.6	41
2-sp03e13	39.80	55.0	8.45	851	302	0.9	997	2120	249	979	136	27	95	11	52	10.0	26	3.2	24	3.8	9	56	16	0.71	4.58	7.3	38
2-sp03f04	42.60	55.0	8.63	883	261	0.4	576	1390	172	696	107	24	80	9	44	8.5	23	3.1	21	3.4	8	44	15	0.79	3.36	5.4	32
2-sp03f07	41.90	55.0	7.62	903	374	0.8	784	1980	247	997	150	31	104	13	61	11.6	31	4.4	29	4.9	8	52	19	0.76	3.26	5.2	38
2-sp03f09	44.00	55.0	9.56	988	450	1.5	1470	3360	373	1430	208	39	138	16	76	14.9	39	4.9	35	5.3	11	77	25	0.70	4.41	7.1	44
2-sp03f12	42.00	55.0	7.96	924	271	0.6	664	1560	185	745	109	23	78	9	45	9.1	21	3.2	22	3.3	8	41	13	0.75	3.80	6.1	38
3-ap04f10	42.60	55.2	7.09	858	205	0.2	537	1390	165	592	94.6	19	70	8	37	7.3	18	2.4	16	2.4	9	32	21	0.70	3.54	5.7	44
3-sp03e10	42.80	55.0	7.59	868	183	0.2	329	852	107	460	76.7	16	58	7	30	5.8	15	2.0	14	2.1	6	27	21	0.74	2.68	4.3	32
3-sp03e14	41.20	55.0	7.86	865	272	0.6	777	1730	200	800	118	25	85	9	45	9.0	22	3.1	21	3.3	8	56	20	0.77	4.11	6.6	31
3-sp03f06	43.00	55.0	7.83	884	239	0.3	474	1220	154	638	97	20	71	8	40	8.1	20	2.7	19	3.0	8	37	19	0.74	3.05	4.9	33
3-sp03f08	42.40	55.0	8.24	972	439	1.2	1490	3230	365	1410	197	39	137	16	77	14.6	38	5.1	35	5.2	10	73	22	0.72	4.72	7.6	44
sp03d08	42.00	55.0	7.71	882	200	0.3	455	1070	130	535	81	21	61	7	33	6.6	18	2.4	16	2.8	7	39	29	0.90	3.51	5.6	27
sp03d11	43.90	55.0	8.53	904	225	0.3	659	1540	169	671	97.9	18	67	8	38	7.6	18	2.6	17	2.6	9	33	11	0.66	4.20	6.7	47
sp03f13	42.20	55.0	9.76	874	400	1.7	1050	2290	266	1060	160	39	116	13	64	13.2	33	4.6	31	5.3	12	148	156	0.88	4.10	6.6	15

SR1 Sample *Granodiorite*

Analysis Nb	**P_2O_5**	**CaO**	**V**	**Sr**	**Y**	**Zr**	**La**	**Ce**	**Pr**	**Nd**	**Sm**	**Eu**	**Gd**	**Tb**	**Dy**	**Ho**	**Er**	**Tm**	**Yb**	**Lu**	**Pb**	**Th**	**U**	**$(Eu/Eu^*)_N$**	**$(La/Sm)_N$**	**La/Sm**	**Ce/Th**
1-ap04f13	42.40	55.4	10.80	572	225	1.8	2680	3310	263	869	112	29	79	8	42	8.3	21	2.4	16	2.7	11	136	47	0.93	14.94	24	24
1-ap04f14	43.80	55.4	12.40	571	211	1.7	2540	3040	249	822	103	27	77	8	38	7.4	18	2.4	17	2.8	11	125	40	0.92	15.40	25	24
1-ap04g05	41.50	55.0	8.90	697	154	1.1	2030	2510	201	664	84.8	19	59	6	29	5.5	14	1.7	12	1.8	9	62	17	0.81	14.95	24	40
1-ap04g09*	43.90	55.0	16.30	623	162	0.7	1440	2250	219	809	118	13	79	8	39	5.9	14	1.6	8	1.6	9	72	25	0.41	7.62	12	31
1-ap04g10*	43.00	55.3	8.37	676	156	1.2	1910	2490	205	726	94	18	68	7	34	6.3	14	1.8	12	1.9	10	61	18	0.67	12.69	20	41
1-sp03h09	44.70	55.0	9.35	666	194	1.2	2190	2750	249	891	119	21	82	9	41	7.8	18	2.2	14	2.1	10	80	23	0.63	11.49	18	35
1-sp03h13	46.60	55.0	12.80	653	198	1.3	1860	2820	291	1030	134	17	88	10	44	7.5	18	2.0	10	1.6	9	82	24	0.47	8.67	14	34
2-ap04g04	45.40	55.9	8.34	665	68	0.4	880	1060	82.5	274	33.1	8	24	2	11	2.3	6	0.8	5	0.9	8	40	21	0.90	16.60	27	27
2-ap04g06*	44.40	55.5	9.28	687	74.8	0.4	993	1280	98.7	333	42.2	9	30	3	14	2.9	7	0.9	6	1.0	9	46	15	0.77	14.69	24	28
2-ap04g08*	46.90	55.4	9.84	619	89.4	0.5	1080	1390	116	390	50.5	11	32	3	18	3.0	8	1.0	7	1.2	8	52	22	0.81	13.35	21	27
2-sp03h04	45.80	55.0	9.20	681	75.1	0.4	968	1130	90.7	303	37.8	8	27	3	14	2.6	6	0.9	6	1.0	8	51	20	0.80	15.99	26	22
2-sp03h11	45.30	55.0	9.15	735	84.7	0.4	1120	1400	117	396	47.6	10	33	4	16	3.1	8	0.9	6	1.0	8	50	15	0.77	14.69	24	28
2-sp03h14	43.30	55.0	9.34	700	103	0.6	1300	1620	133	464	57.6	12	39	4	20	3.7	8	1.1	7	1.3	10	75	21	0.76	14.09	23	22
2-sp03h05	43.00	55.0	9.25	634	77.9	0.4	955	1170	90.8	310	39.2	10	26	3	14	2.7	7	0.8	7	1.0	8	54	20	0.94	15.21	24	22
2-sp03h07	43.70	55.0	8.65	627	79	0.4	985	1230	97.4	326	38.8	10	27	3	14	2.8	7	0.9	6	1.0	8	54	18	0.93	15.85	25	23
SR2 Sample	*Appinite*																										
Analysis Nb																											
1-ap04a04	42.50	55.0	25.50	1380	264	7.4	1130	2450	289	1200	179	20	113	13	59	10.0	24	2.7	16	2.1	8	37	11	0.43	3.94	6	66
1-ap04a05	44.60	55.0	26.10	1400	275	9.8	1240	2630	316	1300	183	22	117	13	57	10.2	24	2.7	16	2.3	8	35	9	0.45	4.23	7	75
1-ap04a06	41.80	55.0	22.70	1350	268	7.8	1220	2920	315	1300	187	24	113	13	59	10.3	24	2.7	16	2.2	7	32	9	0.50	4.07	7	92
1-ap04a09	39.90	54.7	20.60	1300	104	3.9	868	1220	110	405	54.3	12	41	4	21	3.9	9	1.1	7	1.3	7	41	14	0.75	9.98	16	30
1-ap04a10	41.20	54.9	19.60	1330	287	3.4	1110	2560	303	1290	190	23	125	13	61	10.8	26	3.2	20	2.5	7	44	10	0.46	3.65	6	58
1-ap04a11	42.10	54.9	24.70	1350	256	7.5	1130	2460	282	1190	174	22	107	12	54	9.5	22	2.7	17	2.1	7	31	8	0.48	4.06	6	78
1-ap04a12*	42.10	55.5	23.50	1360	109	7.3	904	1340	112	404	50.5	13	39	4	19	3.7	9	1.2	8	1.3	8	38	15	0.90	11.18	18	35
1-ap04a14	42.60	55.1	20.00	1350	228	4.2	1410	2310	213	857	127	22	94	10	46	8.2	20	2.4	16	2.3	9	54	28	0.62	6.93	11	42
1-ap04d05	40.30	54.5	21.90	1270	256	3.4	1320	2640	289	1180	168	25	115	12	57	10.2	22	2.7	17	2.4	9	48	16	0.54	4.91	8	55
1-ap3h04	40.70	55.4	11.30	1390	180	1.6	1120	1770	183	748	107	19	76	8	38	7.1	17	1.9	11	1.9	7	57	20	0.64	6.54	10	31
1-ap3h05	43.60	55.3	17.80	1440	181	3.1	1240	2030	205	795	115	20	80	8	35	7.2	17	1.9	12	1.8	8	42	19	0.65	6.73	11	48
1-ap3h06	42.70	55.2	18.80	1410	178	2.5	1180	1940	192	745	102	19	74	8	36	6.5	17	1.8	12	1.8	8	53	19	0.68	7.22	12	37
1-ap3h07	44.30	55.4	24.40	1380	240	8.9	1140	2120	241	981	146	20	101	11	53	9.3	21	2.7	16	2.1	8	28	8	0.51	4.88	8	76
1-ap3h08	43.40	55.0	25.10	1350	225	6.7	1160	2180	241	1010	146	21	100	10	48	8.6	22	2.6	15	2.0	9	40	13	0.52	4.96	8	54

SR2 Sample (Suite) *Appinite*

Analysis Nb	P_2O_5	CaO	V	Sr	Y	Zr	La	Ce	Pr	Nd	Sm	Eu	Gd	Tb	Dy	Ho	Er	Tm	Yb	Lu	Pb	Th	U	$(Eu/Eu^*)_N$	$(La/Sm)_N$	La/Sm	Ce/Th
1-ap3h09	44.40	55.2	17.60	1340	217	4.6	1030	1900	224	939	137	19	97	10	46	8.2	19	2.2	14	1.9	8	40	12	0.50	4.69	8	47
1-ap3g04	39.90	55.6	16.00	1350	274	4.6	1180	2030	232	995	162	20	115	12	59	10.8	25	3.0	18	2.5	7	46	15	0.45	4.55	7	44
1-ap3g05	40.70	55.4	10.90	1230	271	2.0	952	1750	213	973	163	20	111	12	57	10.5	25	2.9	16	2.4	6	47	13	0.45	3.65	6	37
1-ap3g06	39.50	55.2	26.00	1350	192	9.5	1140	1850	193	801	116	18	83	9	41	7.4	18	2.2	13	1.8	8	29	8	0.55	6.14	10	64
1-ap3g07	41.40	55.3	22.50	1360	199	8.6	1160	1880	201	827	123	18	86	9	43	7.7	18	2.2	13	1.8	8	30	9	0.54	5.89	9	63
1-sp01b04	42.30	55.0	24.40	1360	235	6.8	1000	1760	207	891	139	16	94	11	50	9.0	21	2.5	15	2.2	9	46	18	0.44	4.49	7	38
1-sp01b05	44.10	55.0	7.19	1280	208	1.2	815	1390	165	736	121	11	86	10	45	8.3	20	2.3	14	2.0	9	60	27	0.34	4.21	7	23
1-sp01b07	42.60	55.0	24.60	1340	200	5.8	1190	2090	232	897	126	22	81	9	42	7.8	19	2.3	13	2.1	8	39	11	0.66	5.90	9	54
1-sp01b08	42.30	55.0	15.70	1270	218	2.2	1050	1900	219	891	132	18	88	10	45	8.4	18	2.3	14	2.1	7	40	11	0.50	4.97	8	48
1-sp01b10	43.20	55.0	19.00	1320	261	6.6	1280	2630	311	1220	172	28	105	12	54	10.0	23	3.0	17	2.3	8	41	12	0.64	4.65	7	64
1-sp01b11	43.90	55.0	20.40	1330	255	8.0	1270	2590	303	1200	167	28	105	12	55	9.6	22	2.8	16	2.2	8	40	11	0.63	4.75	8	65
1-sp01b12	43.00	55.0	20.70	1250	203	7.0	923	1460	161	668	108	15	80	9	43	8.3	19	2.3	14	2.0	7	41	10	0.48	5.34	9	35
1-sp01b13	41.50	55.0	26.70	1300	219	9.8	1050	1670	186	771	118	18	87	10	48	9.0	20	2.5	15	2.3	7	31	8	0.55	5.56	9	55
1-sp01b14	42.40	55.0	24.80	1330	212	4.6	1120	1890	210	839	124	15	85	9	44	8.1	20	2.5	13	2.1	9	55	22	0.44	5.64	9	34
1-sp01c05	44.30	55.0	27.30	1350	228	9.5	1270	2140	239	974	143	19	95	11	48	9.0	20	2.4	15	2.2	7	26	7	0.48	5.55	9	82
1-sp01c06	46.20	55.0	21.40	1260	206	7.2	1030	1780	204	822	124	17	83	10	45	8.3	18	2.3	13	1.8	7	22	6	0.50	5.19	8	80
1-sp05a03	44.20	55.0	19.70	1270	202	1.6	985	1760	204	827	122	16	79	9	42	7.8	19	2.1	14	2.1	9	72	22	0.50	5.04	8	25
1-sp05a04	44.30	55.0	14.90	1120	202	2.6	671	1430	169	742	119	15	81	9	42	7.9	18	2.4	14	1.8	7	41	12	0.45	3.52	6	35
1-sp05a06	45.20	55.0	15.10	1320	238	1.8	1190	2260	262	1090	156	21	99	11	50	9.2	21	2.4	14	2.0	9	52	17	0.50	4.76	8	44
1-sp05a07	46.20	55.0	18.30	1210	236	3.2	1100	2220	261	1090	156	20	98	11	50	8.4	21	2.6	15	2.3	7	36	13	0.50	4.40	7	63
1-sp05b05	44.20	55.0	19.70	1220	192	7.0	1280	2150	225	892	125	23	82	9	41	7.8	18	2.1	14	2.0	6	31	10	0.69	6.39	10	70
1-sp05b06	44.30	55.0	15.90	1280	211	5.0	1430	2200	228	894	127	24	83	9	44	8.2	18	2.3	15	2.3	7	59	25	0.70	7.03	11	37
1-sp05b07	44.20	55.0	21.90	1240	267	5.4	1060	2250	273	1200	182	22	115	12	60	10.1	23	2.8	17	2.3	8	40	13	0.46	3.64	6	56
1-sp05b08	42.80	55.0	26.70	1310	305	5.9	746	1580	212	973	175	21	122	14	66	12.0	28	3.3	20	2.9	8	48	13	0.43	2.66	4	33
1-sp05b09	45.00	55.0	19.10	1160	215	4.8	863	1650	201	881	138	15	91	10	46	8.3	20	2.4	14	2.0	6	34	10	0.41	3.91	6	48
1-sp05b10	44.10	55.0	5.81	1160	201	1.8	792	1500	177	798	124	14	84	9	44	7.8	18	2.1	12	1.7	6	35	10	0.41	3.99	6	43
1-sp05b14	44.10	55.0	9.64	1080	208	1.2	813	1740	208	876	126	17	86	9	43	7.9	18	2.4	13	2.1	5	40	9	0.50	4.03	6	44
1-sp05c07	44.40	55.0	29.60	1240	148	9.9	1260	2050	205	784	105	22	67	7	32	6.0	14	1.7	11	1.5	7	29	8	0.78	7.49	12	72
1-sp05d04	49.20	55.0	15.90	1130	251	2.9	733	1570	204	965	158	17	106	12	56	10.0	23	2.7	16	2.3	7	55	18	0.40	2.90	5	29
1-sp05d05	47.60	55.0	27.10	1260	196	9.3	856	1290	140	627	107	13	78	9	44	7.8	19	2.3	14	2.1	8	30	7	0.44	5.00	8	43
1-sp05d06	46.70	55.0	18.80	1210	211	3.6	953	1440	163	736	119	14	85	10	46	8.6	20	2.4	15	2.1	9	70	23	0.42	5.00	8	21

SR2 Sample (Suite) *Appinite*

Analysis Nb	P_2O_5	CaO	V	Sr	Y	Zr	La	Ce	Pr	Nd	Sm	Eu	Gd	Tb	Dy	Ho	Er	Tm	Yb	Lu	Pb	Th	U	$(Eu/Eu^*)_N$	$(La/Sm)_N$	La/Sm	Ce/Th
1-sp05d10	44.60	55.0	21.80	1200	186	3.6	915	1640	175	754	113	15	79	8	40	7.0	17	2.1	12	1.8	7	38	16	0.47	5.06	8	43
1-sp05d11	42.90	55.0	14.70	1280	264	3.7	1260	2400	277	1140	171	21	110	12	58	10.4	23	2.9	17	2.4	7	51	17	0.46	4.60	7	47
1-sp05d12	42.60	55.0	21.50	1280	285	5.3	1330	2640	307	1270	184	23	116	13	63	10.9	26	2.9	17	2.5	7	44	15	0.48	4.51	7	60
1-sp05d13	43.20	55.0	21.80	1290	260	3.4	1230	2380	284	1170	170	20	108	12	55	10.1	22	2.7	15	2.3	8	60	17	0.46	4.52	7	40
1-sp05d14	41.70	55.0	17.30	1280	224	4.9	1170	1790	185	800	124	18	90	10	48	9.2	21	2.4	16	2.3	7	53	18	0.51	5.89	9	34
1-sp05e03	45.40	55.0	15.70	1300	318	2.5	1170	2680	325	1350	200	24	124	14	68	12.0	29	3.3	20	2.6	8	53	23	0.47	3.65	6	50
1-sp05e04	43.80	55.0	24.00	1250	262	3.1	1200	2500	301	1190	173	21	108	12	55	10.0	23	2.7	16	2.2	6	34	12	0.48	4.33	7	73
1-sp05e05	45.50	55.0	5.50	1300	255	1.4	1160	2470	289	1200	175	20	109	12	55	10.0	23	2.8	15	2.1	8	51	20	0.45	4.14	7	49
1-sp05e06	44.20	55.0	17.70	1260	284	5.1	1280	2720	318	1310	188	22	118	13	61	10.8	25	3.1	17	2.2	7	44	14	0.46	4.25	7	61
1-sp05e08	43.40	55.0	25.30	1320	253	5.8	1300	2540	294	1200	172	22	105	11	54	9.7	23	2.7	16	2.2	8	34	11	0.50	4.72	8	76
1-sp05e09	45.80	55.0	21.60	1250	243	2.0	1030	2060	248	1040	155	19	98	11	53	9.1	22	2.7	15	2.1	7	43	15	0.46	4.15	7	47
1-sp05e11	43.40	55.0	23.60	1300	206	7.2	1190	2070	225	913	129	19	86	10	44	7.8	19	2.1	13	1.9	8	31	10	0.56	5.76	9	66
1-sp05e12	42.90	55.0	19.40	1220	190	3.6	947	1640	178	752	112	14	75	8	41	7.5	17	2.0	12	1.9	8	45	12	0.47	5.28	8	37
1-sp05f04	43.80	55.0	20.70	1310	257	3.8	1340	2430	275	1120	160	22	103	11	56	9.8	23	2.9	17	2.4	9	47	19	0.53	5.23	8	51
1-sp05f05	45.00	55.0	21.10	1210	243	4.6	1210	2220	255	1040	151	21	100	11	52	9.5	22	2.7	16	2.2	7	45	20	0.51	5.00	8	50
1-sp05f06	45.70	55.0	22.00	1230	231	2.2	1040	1970	232	976	142	19	92	10	49	8.8	21	2.7	15	2.1	8	44	17	0.49	4.57	7	44
1-sp05f07	43.60	55.0	18.60	1310	249	4.8	1290	2380	263	1070	153	22	102	11	53	9.4	24	2.7	16	2.3	9	48	17	0.53	5.27	8	49
1-sp05f08	42.50	55.0	23.00	1320	242	8.3	1330	2440	261	1060	152	22	99	11	50	9.1	21	2.7	17	2.3	8	31	12	0.53	*5.46*	9	80
1-sp05f09	42.90	55.0	18.10	1310	240	5.1	1250	2230	249	1010	148	20	101	10	51	9.1	22	2.5	16	2.4	8	47	17	0.51	5.27	8	47
R-ap04a08	41.30	55.4	6.38	1490	132	0.6	947	1510	148	557	77.9	16	52	6	28	4.9	12	1.3	10	1.3	10	53	23	0.74	7.59	12	29
R-ap04a13*	44.70	55.3	20.30	1340	96.2	2.3	805	1100	96.3	348	45.1	11	32	4	18	3.4	9	1.1	7	1.1	9	55	19	0.89	11.15	18	20
R-sp01b06	43.60	55.0	23.50	1330	124	8.2	890	1200	115	429	60.1	12	45	5	23	4.6	12	1.6	10	1.6	7	30	8	0.71	9.25	15	41
R-sp01b09	41.90	55.0	18.00	1320	119	2.6	823	1110	105	396	54.9	12	41	5	22	4.4	11	1.4	9	1.6	7	44	17	0.75	9.36	15	25
R-sp01c04	45.70	55.0	22.70	1310	140	3.3	865	1250	116	433	65	12	49	5	27	5.4	12	1.6	10	1.6	8	43	13	0.63	8.31	13	29
R-sp05a05	43.10	55.0	15.60	1200	139	1.0	729	1090	113	472	74.1	11	55	6	28	5.3	13	1.5	10	1.5	8	54	16	0.55	6.14	10	20
R-sp05b03	43.10	55.0	22.20	1220	172	2.1	1080	1540	152	595	86.7	16	63	7	34	6.4	16	1.9	13	2.0	9	80	30	0.64	7.78	12	19
R-sp05b04	44.60	55.0	12.60	1210	129	0.8	754	1070	102	407	57.3	11	44	5	24	4.7	12	1.5	10	1.7	8	72	20	0.69	8.22	13	15
R-sp05c04	43.30	55.0	15.60	1130	166	2.0	862	1650	174	715	106	16	66	7	35	6.2	15	1.9	11	1.6	6	39	11	0.57	5.08	8	43
R-sp05c05	44.60	55.0	22.40	1140	192	1.5	830	1610	186	764	113	16	80	8	39	7.2	17	2.1	13	2.0	7	52	11	0.51	4.59	7	31
R-sp05d09	45.70	55.0	4.86	1350	80.6	<0.16	602	878	81.7	311	42.5	8	29	3	14	2.7	8	0.9	5	0.8	7	7	4	0.66	8.85	14	117
R-sp05f03	47.20	55.0	12.10	1230	123	1.5	927	1280	120	445	61.4	14	44	5	24	4.6	12	1.3	9	1.5	7	47	20	0.80	9.43	15	28

SR2 Sample (Suite)			*Appinite*																							
Analysis Nb	**P_2O_5**	**CaO**	**V**	**Sr**	**Y**	**Zr**	**La**	**Ce**	**Pr**	**Nd**	**Sm**	**Eu**	**Gd**	**Tb**	**Dy**	**Ho**	**Er**	**Tm**	**Yb**	**Lu**	**Pb**	**Th**	**U**	**$(Eu/Eu^*)_N$**	**$(La/Sm)_N$**	**La/Sm**	**Ce/Th**
R-sp05f11	45.40	55.0	15.10	1220	165	1.1	853	1280	132	548	85.8	13	63	7	35	6.2	15	1.8	11	1.7	8	52	18	0.52	6.21	10	25
SR3 Sample	*Granodiorite*																										
1-ap04c07	44.90	54.8	9.24	695	155	0.9	1860	2620	228	824	107	18	77	8	34	6.1	15	1.9	11	1.8	9	59	18	0.59	10.86	17	44
1-ap04e08	44.70	54.9	9.95	622	188	1.4	1980	2890	241	894	118	20	88	9	43	7.9	19	2.1	13	2.0	9	82	27	0.58	10.48	17	35
1-ap04e09	43.70	54.8	13.40	654	155	0.9	1770	2410	202	711	93.2	18	68	7	34	6.1	15	1.7	12	1.9	9	64	20	0.68	11.86	19	38
1-ap04e10	44.70	55.0	10.30	758	190	1.0	2410	3240	284	998	125	23	89	9	41	7.4	19	2.4	16	2.3	10	82	22	0.65	12.04	19	40
1-ap04e11	44.80	55.0	10.80	640	178	1.2	1930	2580	229	820	111	18	80	8	40	7.1	16	1.9	12	2.0	9	78	22	0.59	10.86	17	33
1-ap04e12	43.30	54.8	9.44	600	165	1.3	2070	2750	219	735	95.4	21	71	7	35	6.7	16	1.9	13	2.0	10	93	34	0.76	13.55	22	30
1-ap04e13	52.00	54.6	9.44	714	195	1.5	2580	3370	270	878	113	22	79	9	40	7.3	18	2.2	14	2.5	11	95	29	0.72	14.26	23	35
1-ap04e14*	43.50	54.7	9.04	728	176	1.3	2420	3130	249	824	101	21	74	7	36	6.7	16	1.9	13	2.0	9	81	22	0.73	14.96	24	39
1-sp01d05	45.00	54.8	9.27	710	176	1.1	2250	2940	232	759	97.1	20	66	7	34	6.8	17	2.1	14	2.2	9	77	22	0.77	14.47	23	38
1-sp01d13	46.20	54.8	10.10	742	186	1.4	1980	2810	261	950	129	20	86	9	42	7.8	18	2.0	13	2.0	9	69	21	0.57	9.58	15	40
1-sp01d14	44.70	54.8	9.29	761	194	1.5	2370	3220	270	913	115	22	80	9	40	7.7	18	2.1	15	2.3	10	87	25	0.70	12.87	21	37
1-sp03b04*	42.50	54.8	10.90	681	181	1.7	1980	2700	250	882	126	20	92	10	43	7.9	18	2.3	12	2.0	8	73	20	0.57	9.81	16	37
1-sp03b07	42.60	54.8	9.50	696	194	1.6	2330	3200	281	969	128	21	85	9	42	7.9	19	2.3	14	2.3	10	87	24	0.62	11.37	18	37
1-sp03b08	41.50	54.8	9.07	645	174	1.0	2020	2620	219	746	94.8	20	65	7	35	6.6	15	1.9	13	2.3	9	75	25	0.77	13.31	21	35
2-ap04f04*	44.70	55.2	8.22	643	75.2	<0.30	946	1170	91.1	304	37.1	9	26	3	12	2.7	6	0.8	5	0.9	8	40	25	0.84	15.92	25	29
2-sp01c07	47.40	54.8	8.84	665	76.6	0.3	1020	1230	94.4	324	38.2	10	26	3	14	2.8	7	0.9	5	1.0	8	49	19	0.92	16.67	27	25
2-sp01c08	46.40	54.8	7.86	583	63.9	0.2	775	976	79	256	31.7	8	23	2	11	2.3	6	0.7	5	0.9	7	25	42	0.89	15.27	24	39
2-sp01c09	46.40	54.8	8.06	696	79.3	0.5	1070	1270	102	341	41.1	10	29	3	15	2.8	7	1.0	6	0.9	8	49	17	0.86	16.26	26	26
2-sp01c10	46.90	54.8	9.00	668	93.5	0.6	1210	1440	117	391	48.2	11	35	4	17	3.5	8	1.0	6	1.2	9	70	22	0.83	15.68	25	21
2-sp01c14	47.60	54.8	8.69	660	76.1	0.4	992	1230	93.9	312	37.3	9	26	3	14	2.6	6	0.8	5	1.0	7	45	19	0.91	16.61	27	27
2-sp01d04	45.20	54.8	8.75	631	82.2	0.3	911	1130	93.4	313	38.8	9	28	3	15	2.9	7	0.9	6	0.9	8	53	23	0.83	14.66	23	21
2-sp01d06	45.40	54.8	0.95	654	47.9	<0.11	664	806	67.3	228	28.5	5	22	2	9	1.8	4	0.5	3	0.5	6	8	4	0.68	14.55	23	101
2-sp01d08	44.60	54.8	8.40	703	83.5	0.3	1130	1320	108	356	44.5	11	30	3	15	3.0	7	1.0	6	1.0	8	51	19	0.90	15.86	25	26
2-sp01d09	44.40	54.8	8.89	675	78.9	0.3	1050	1280	99.6	321	39.1	10	28	3	14	3.1	7	0.9	6	1.0	9	54	19	0.92	16.77	27	24
2-sp01d10	43.60	54.8	9.16	631	62.2	0.2	739	944	74.8	248	30	8	22	2	11	2.2	5	0.8	5	0.8	8	39	19	0.89	15.38	25	24
2-sp01d11	44.20	54.8	7.89	608	56	0.3	703	862	66.9	220	26.4	7	18	2	9	1.9	5	0.6	4	0.9	8	32	28	0.93	16.63	27	27
2-sp03b06	41.10	54.8	8.76	650	90.5	0.6	1180	1450	121	391	47.6	12	33	4	17	3.4	8	1.0	7	1.3	8	68	24	0.90	15.48	25	21
2-sp03b09	41.10	54.8	24.50	659	92.9	0.5	960	1250	109	360	46.9	10	34	4	17	3.4	9	1.0	6	1.2	9	64	34	0.78	12.78	20	20

For Rogart samples (1) are core composition, (2) oscillatory rim, (3) unoscillatory rim.For Strontian samples (1) correspond to core or all crystal composition, (2) rim composition. (R) are the bright rims present of appinite's apatite crystals. P_2O_5 and CaO are reported in Wt% and the other elements in ppm. * are analyses reported in figure 3.

Electronic Appendix 4: Analyses of zircon compositions

RT1 Sample

	SiO2	P2O5	Sc	Y	Nb	La	Ce	Pr	Nd	Sm	Eu	Gd	Tb	Dy	Ho	Er	Tm	Yb	Lu	Hf	Ta	Pb	Th	U	Ce/Ce*	Eu/Eu*	Σ REE	Th/U
2-ap05c05	33.2	0.028	97	550	2.94	-	39	0.052	1.1	2.11	0.80	10.9	3.22	43.2	16.8	88.1	21.1	228	49.8	9250	0.95	8.4	193	360	-	0.51	505	0.5
2-ap05c07	33.2	0.041	108	883	2.96	0.030	48	0.228	3.4	5.23	1.99	21.3	6.15	75.0	27.4	136	32.1	331	69.8	9630	0.88	12.0	304	395	139	0.57	758	0.8
2-ap06b09	33.6	0.037	108	517	2.34	0.111	49	0.154	1.8	2.19	0.83	11.1	3.42	42.6	16.1	78.8	18.3	188	40.1	9440	0.96	11.5	281	346	91	0.51	453	0.8
2-ap06b10	33.4	0.032	118	620	3.58	-	42	0.072	1.1	2.14	0.92	11.6	3.59	47.1	18.8	98.3	24.0	256	57.2	9660	1.17	9.1	209	369	-	0.56	563	0.6
2-ap06c04	33.2	0.031	100	461	2.68	0.060	36	0.054	0.9	1.90	0.63	9.0	2.86	36.1	14.0	72.4	17.8	186	41.5	8920	0.83	8.4	185	330	155	0.46	419	0.6
2-ap06c06	33.3	0.035	98	503	2.45	-	41	0.067	1.2	2.04	0.78	10.4	3.16	39.7	15.6	80.8	19.0	198	43.8	8450	0.88	9.0	192	313	-	0.52	455	0.6
2-ap06c07	33.5	0.032	99	418	2.60	0.061	34	-	0.8	1.63	0.75	8.5	2.58	34.5	12.6	67.7	15.7	166	35.5	9420	0.85	8.0	191	327	-	0.61	381	0.6
2-oc03f04	33.2	0.033	88	440	2.02	0.090	40	0.064	1.4	1.95	0.71	9.4	2.75	36.2	13.8	68.2	16.2	170	34.6	8710	0.78	9.7	225	315	126	0.51	395	0.7
2-oc03f05	33.3	0.061	85	394	1.91	0.158	32	0.103	1.0	1.57	0.69	8.4	2.58	32.0	12.4	62.1	15.1	154	32.1	9370	0.72	7.9	176	316	61	0.58	354	0.6
2-oc04d08	33.2	0.052	85	818	1.60	0.283	43	0.234	3.9	5.85	1.98	24.3	6.40	76.2	26.3	128	29.0	284	55.9	8440	0.63	12.9	280	291	41	0.51	685	1.0
2-oc04d12	33.2	0.028	86	421	1.98	0.161	36	0.077	1.0	1.80	0.68	8.3	2.60	34.2	13.4	67.3	16.1	170	34.0	9260	0.88	9.2	208	327	78	0.54	386	0.6
2-oc04d13	33.2	0.025	99	601	2.94	-	36	0.035	0.8	2.16	0.93	11.3	3.40	46.6	18.2	98.4	24.1	265	55.8	9110	1.11	6.6	174	339	-	0.58	563	0.5
3-ap06c10	33.3	0.035	101	483	2.60	0.049	39	0.084	1.0	2.09	0.80	10.1	2.91	38.4	14.6	74.8	18.3	189	41.3	9040	0.87	10.6	241	398	150	0.53	432	0.6
3-oc03e14	33.2	0.029	98	560	2.58	0.047	34	0.048	1.3	2.04	0.66	10.7	3.13	43.6	17.3	87.9	23.4	242	51.3	9090	0.96	6.6	162	300	175	0.43	518	0.5
oc03e11	33.2	0.029	95	610	3.10	-	37	0.110	0.9	2.23	0.74	10.4	3.61	45.7	18.5	96.2	23.7	255	54.3	8200	1.03	7.6	181	326	-	0.47	548	0.6
oc03e12	33.2	0.034	88	490	2.45	0.163	44	0.113	1.4	2.24	0.88	11.2	3.22	39.9	15.0	75.8	17.8	183	37.5	8430	0.78	10.4	250	345	78	0.53	432	0.7

RHG-1 Sample

	SiO2	P2O5	Sc	Y	Nb	La	Ce	Pr	Nd	Sm	Eu	Gd	Tb	Dy	Ho	Er	Tm	Yb	Lu	Hf	Ta	Pb	Th	U	Ce/Ce*	Eu/Eu*	Σ REE	Th/U
1-ap05d04	33.2	0.038	93	542	2.73	0.233	36.7	0.123	1.16	1.59	0.84	10.9	3.27	42.9	16.9	86.6	21.4	227	48.7	8510	1.03	9.21	189	349	52	0.62	498	0.5
1-oc03d05	33.2	0.045	98	591	2.99	0.289	53.7	0.182	1.58	3.07	0.88	15.3	3.96	48.4	18.4	95.9	22.2	240	46.8	9560	1.13	12.7	325	421	57	0.39	550	0.8
1-oc03d07	33.2	0.038	107	869	3.58	0.140	60.5	0.27	2.87	5.1	1.59	20.1	5.83	73.5	27.8	136	31.7	330	66.6	9170	1.19	15.8	388	491	75	0.48	762	0.8
2-ap05d07	33.2	0.021	102	589	3.26	-	33.2	0.027	0.76	1.66	0.76	10.6	3.37	46.1	17.5	91	22.3	238	50.8	8900	0.96	6.89	158	332	-	0.55	516	0.5
2-ap05e06	33.4	0.043	86	495	2.6	0.237	34	0.076	1.07	1.2	0.69	9.19	2.95	38.9	14.8	78.4	19	207	45	7820	0.79	7.2	142	271	62	0.64	452	0.5
2-ap05e09	33.3	0.031	98	517	3.11	-	49.6	0.113	1.4	2.51	0.82	10.6	3.12	42	15.5	77.2	18.6	191	41.7	9650	1.01	14.5	361	519	-	0.49	454	0.7
2-ap05e10	33.3	0.028	92	531	2.8	-	38.4	0.087	1.15	1.91	0.86	11.1	3.5	42.8	16.5	82.9	20	208	44.4	8760	0.92	10.5	217	375	-	0.57	472	0.6
2-ap05e11	32.4	0.053	87	505	2.91	0.175	34.4	0.098	1.21	1.82	0.69	9.59	3.03	37.1	15.4	79.5	19.1	206	46.1	8490	0.96	8.2	178	341	64	0.50	454	0.5
2-ap05e13	33.3	0.031	107	861	5.12	-	62.9	0.127	1.7	4	1.33	17.2	5.32	66.5	26.8	134	33	345	73.5	9070	1.45	14.4	333	498	-	0.49	771	0.7
2-ap05f07	33	0.034	81	379	2.27	0.064	30.2	0.051	0.77	1.57	0.58	7.54	2.35	30	11.5	58.6	13.9	146	31.6	9430	0.74	8.18	175	328	128	0.51	335	0.5
2-oc03e04	33.2	0.026	109	593	2.8	0.078	43.3	0.069	1.02	2.37	0.81	11.2	3.6	48.2	18.9	93	23.3	244	48.6	10700	1.16	10.3	276	437	143	0.48	538	0.6

RHG-1 Sample (Suite)

	SiO2	P2O5	Sc	Y	Nb	La	Ce	Pr	Nd	Sm	Eu	Gd	Tb	Dy	Ho	Er	Tm	Yb	Lu	Hf	Ta	Pb	Th	U	Ce/Ce*	Eu/Eu*	Σ REE	Th/U
2-oc03e05	33.2	0.03	98	737	2.25	0.117	40.7	0.165	1.85	3.76	1.21	16.6	4.99	59.8	22.9	117	28.7	278	58.5	9170	1.02	9.55	237	363	71	0.47	634	0.7
2-oc03e06	33.2	0.019	97	400	1.92	-	26.4	0.045	0.33	1.35	0.65	6.47	2.2	30.7	12.3	62.7	15.9	166	35	9930	0.74	5.36	133	271	-	0.67	360	0.5
2-oc03e07	33.2	0.025	105	613	2.72	0.036	35.7	-	0.98	2.36	0.83	10.9	3.33	45.8	18.8	96.3	24.3	255	53.3	9280	1.04	7.55	181	333	-	0.50	548	0.5
2-oc03e08	33.2	0.032	85	480	2.14	0.098	33.4	0.082	0.87	1.52	0.69	8.75	3.08	36.6	14.8	76.7	18.2	189	39.3	8640	0.96	8.36	200	331	91	0.57	423	0.6
2-oc03e09	33.2	0.034	100	611	3.36	0.082	44.3	0.11	1.09	2.44	0.88	10.6	3.65	48.6	18.5	96.7	23.6	247	52.4	8700	1.16	9.2	208	302	114	0.53	550	0.7
2-oc03e10	33.2	0.035	110	723	3.82	-	44.5	0.087	1.38	2.35	0.99	12.1	4.4	55.6	22	115	28.2	289	62.1	9800	1.18	9.53	240	421	-	0.56	638	0.6
3-ap05d06	32.9	0.033	78	385	1.96	0.260	31.7	0.106	1.11	1.46	0.61	8.79	2.4	31.1	12	62.2	14.7	150	32.5	8410	0.77	11.6	199	346	46	0.52	349	0.6

R2 Sample

1-ap05f12	33.2	0.034	90	581	3.6	0.064	48	0.083	1.4	2.0	1.05	11	3.5	44	17	92	22	231	51	9050	1.04	11.5	236	368	158	0.70	523	0.6
1-oc03b07	33.2	0.041	115	584	1.7	0.071	32	0.133	1.6	3.2	1.01	13	4.1	50	19	93	21	222	44	8140	0.63	7.1	160	222	79	0.49	503	0.7
1-oc03c05	33.2	0.044	112	682	3.8	0.119	48	0.069	1.5	2.4	1.10	13	4.3	51	22	109	27	283	58	8790	1.21	8.9	227	382	128	0.60	620	0.6
2-ap05f11	33.3	0.043	94	649	3.2	-	52	0.109	1.6	3.1	1.22	15	4.2	52	20	101	24	241	52	8380	0.96	13.7	280	379	-	0.54	567	0.7
2-ap05f14	33.3	0.048	100	797	3.2	-	44	0.156	1.7	3.7	1.53	18	5.2	61	24	121	29	300	65	9020	0.91	12.1	270	423	-	0.57	675	0.6
2-ap06a05	33.2	0.024	111	489	2.2	-	38	0.038	1.2	1.9	0.69	9	2.9	40	15	73	18	194	41	9700	0.80	9.4	223	401	-	0.50	436	0.6
2-ap06a07	33.4	0.036	101	533	2.7	0.213	41	0.097	1.1	2.3	0.86	12	3.6	44	17	82	19	190	40	8830	0.82	16.7	346	520	69	0.51	452	0.7
2-ap06b05	33.4	0.034	111	591	3.2	0.130	36	0.136	1.2	2.0	0.77	11	3.4	44	18	93	23	238	52	8800	1.14	8.1	183	349	65	0.51	523	0.5
2-ap06b08	33.1	0.036	119	964	3.0	0.028	49	0.269	3.0	5.3	1.80	24	7.0	82	30	150	34	345	71	9530	0.96	14.7	343	499	136	0.49	802	0.7
2-oc03b11	33.2	0.028	90	403	2.0	-	33	0.057	1.1	1.7	0.65	9	2.5	33	13	65	16	161	34	9280	0.81	8.9	202	364	-	0.52	369	0.6
2-oc03b12	33.2	0.040	96	506	2.4	0.247	45	0.148	1.2	2.3	0.84	11	3.4	41	16	78	20	196	41	8570	1.04	10.3	251	347	57	0.51	455	0.7
2-oc03b13	33.2	0.032	106	568	3.1	-	40	0.082	1.2	2.1	0.89	10	3.4	45	18	89	22	233	50	8760	1.05	8.3	195	326	-	0.58	515	0.6
2-oc03c04	33.2	0.022	110	593	3.0	0.132	38	0.041	1.0	1.8	0.75	11	3.4	45	18	93	24	248	53	9260	0.92	9.7	223	429	125	0.53	536	0.5

SR1 Sample

	SiO2	P2O5	Sc	Y	Nb	La	Ce	Pr	Nd	Sm	Eu	Gd	Tb	Dy	Ho	Er	Tm	Yb	Lu	Hf	Ta	Pb	Th	U	Ce/Ce*	Eu/Eu*	Σ REE	Th/U
1-oc03f06	33	0.034	91	471	2.0	0.031	30	0.055	0.85	1.6	0.69	9	2.8	38	15	74	17	190	38.2	8320	1.12	7.6	179	313	175	0.57	416	0.6
1-oc03f09	33	0.032	90	708	1.0	0.735	36	0.318	2.57	4.0	1.47	19	5.2	64	22	108	25	240	48.8	8580	0.65	12.2	265	338	18	0.52	577	0.8
2-ap06c12	33.2	0.035	110	609	3.0	-	38	0.035	0.75	2.2	0.68	11	3.4	48	19	97	23	240	52.3	8260	1.40	10.6	230	385	-	0.43	535	0.6
2-ap06c14	33.3	0.034	110	537	2.2	-	43	0.041	0.71	1.7	0.79	10	3.4	43	16	83	19	197	43.6	8700	1.17	13.0	324	466	-	0.59	462	0.7
2-ap06d04	33.1	0.030	96	447	2.1	0.072	30	0.054	0.94	1.8	0.72	10	2.7	33	14	68	17	178	40.1	7980	1.06	7.5	160	281	114	0.53	395	0.6
2-ap06d10	33	0.035	104	511	2.6	-	34	<0.0297	0.91	1.6	0.64	9	3.3	39	16	81	20	207	45.8	8220	1.25	9.3	207	377	-	0.51	457	0.5

SR1 Sample (Suite)

	SiO2	P2O5	Sc	Y	Nb	La	Ce	Pr	Nd	Sm	Eu	Gd	Tb	Dy	Ho	Er	Tm	Yb	Lu	Hf	Ta	Pb	Th	U	Ce/Ce*	Eu/Eu*	Σ REE	Th/U
2-oc03f07	33	0.024	91	384	1.6	0.139	29	0.069	0.73	1.3	0.56	8	2.6	31	13	64	15	157	32.9	8580	0.93	7.1	179	296	71	0.41	354	0.6
2-oc03f14	33	0.024	92	718	2.2	0.072	33	0.074	1.71	2.9	1.12	16	4.7	60	22	105	26	256	49.8	8030	0.90	10.2	240	363	109	0.54	578	0.7
2-ap06d12	33	0.032	100	449	2.2	0.112	30	0.061	0.85	1.6	0.50	8	2.6	35	14	70	18	184	39.6	7940	1.09	7.4	164	291	87	0.50	404	0.6
oc03f11	33	0.042	101	593	2.9	0.174	38	0.136	1.17	1.9	0.76	10	3.5	47	18	94	22	235	50	8070	1.18	10.1	231	368	60	0.53	522	0.6

SR2 Sample

1-ap06d13	33.1	0.038	111	676	2.2	0.026	34	0.12	2.0	3.1	0.98	17	4.8	59	22	102	24	238	49	9320	0.97	10	236	334	79	0.42	556	0.7
1-ap06e04	33.2	0.059	118	1240	6.1	0.038	140	0.31	4.2	8.2	3.89	38	10.0	117	40	182	39	385	80	9180	2.57	199	4340	2590	314	0.52	1047	1.7
1-ap06e05	33	0.039	110	870	2.2	0.044	37	0.13	3.0	4.6	1.70	22	6.4	76	28	133	30	303	63	8400	1.00	13	342	452	120	0.67	708	0.8
1-oc04b08	33	0.071	116	828	1.8	-	44	0.13	1.7	3.3	1.43	16	5.6	69	26	130	32	347	70	8470	0.86	33	699	785	-	0.59	747	0.9
1-oc04b10	33	0.072	116	1230	3.8	-	74	0.25	3.4	5.5	2.82	29	8.4	109	41	202	49	480	99	9610	1.53	60	1230	1340	-	0.68	1103	0.9
2-oc04a07	33	0.061	117	1080	4.5	-	105	0.24	4.1	6.5	2.97	31	8.9	101	35	167	37	362	73	9170	2.08	123	2690	1780	-	0.64	933	1.5
2-oc04b07	33	0.064	108	1110	5.2	0.077	114	0.30	4.3	6.4	3.19	32	8.9	103	36	166	38	364	71	9170	2.39	177	3520	2240	182	0.68	947	1.6
2-oc04b09	33	0.037	120	1310	5.9	0.095	108	0.30	4.6	6.6	3.10	35	9.5	112	41	201	47	493	106	10700	2.59	91	1930	3730	155	0.63	1167	0.5
3-ap06d14	33	0.035	115	1220	6.2	0.030	112	0.20	3.4	6.2	3.55	33	8.8	104	38	178	42	422	92	11700	2.87	123	2750	4080	342	0.75	1044	0.7
3-ap06e08	32.9	0.054	105	920	4.5	0.075	92	0.21	3.6	5.8	2.78	26	7.2	84	30	140	31	302	63	8970	2.01	111	2290	1740	179	0.69	787	1.3
3-ap06e10	33	0.056	128	905	2.8	-	40	0.28	2.9	4.6	1.98	16	5.0	67	28	141	33	341	73	6820	0.71	20	453	531	-	0.70	754	0.9
3-oc04a04	33.2	0.073	118	1050	3.1	0.099	57	0.09	2.1	3.7	1.97	22	6.4	85	33	167	40	407	87	10300	1.50	42	946	1510	147	0.67	911	0.6
3-oc04a06	33	0.076	119	1330	4.1	-	73	0.15	2.4	5.5	2.74	28	8.4	105	41	210	50	517	111	10100	1.71	62	1270	2230	-	0.67	1154	0.6
3-oc04b05	33.2	0.038	100	932	1.1	0.249	39	0.54	7.2	7.5	3.01	26	7.6	84	30	143	34	332	66	8770	0.69	32	712	601	26	0.66	780	1.2
3-oc04b06	33.2	0.044	102	1080	1.1	0.180	40	0.65	8.9	9.2	3.68	31	8.4	100	35	165	37	368	74	7720	0.70	35	781	606	28	0.67	881	1.3
3-oc04b11	33	0.030	99	818	3.2	-	66	0.15	2.2	4.5	1.78	19	5.7	71	26	128	30	307	67	11000	1.64	56	1160	2170	-	0.58	728	0.5
3-oc04b12	33	0.057	135	1270	5.4	0.099	91	0.26	3.8	5.4	2.28	27	7.8	103	41	208	50	502	101	8390	2.19	64	1320	1260	136	0.57	1142	1.0

SR3 Sample

	SiO2	P2O5	Sc	Y	Nb	La	Ce	Pr	Nd	Sm	Eu	Gd	Tb	Dy	Ho	Er	Tm	Yb	Lu	Hf	Ta	Pb	Th	U	Ce/Ce*	Eu/Eu*	Σ REE	Th/U
1-ap06g05	33.1	0.024	93	433	2.3	0.059	33	0.05	0.66	1.4	0.80	8.3	2.9	35	14	69	17	173	35	8010	0.91	9.3	219	359	141	0.72	391	0.6
1-oc03a06	33	0.037	121	724	2.9	0.068	42	0.12	1.87	2.9	1.07	14.5	4.6	60	23	111	27	265	55	8600	1.28	14.8	380	530	110	0.51	608	0.7
1-oc04c05	33	0.044	107	592	2.7	0.467	46	0.19	1.50	2.9	0.86	12.6	3.6	47	19	92	23	242	46	8530	1.41	13.9	340	493	37	0.44	537	0.7
1-oc04c07	33	0.030	91	371	1.1	0.530	25	0.10	0.94	1.1	0.44	7.6	2.4	31	11	56	15	146	30	8210	0.76	6.4	135	227	25	0.46	326	0.6
2-ap06f11	33.3	0.027	92	436	2.5	-	34	0.04	1.07	1.8	0.64	8.3	2.8	35	13	69	16	167	35	8340	0.96	10.3	236	382	-	0.50	383	0.6

SR3 Sample (Suite)

	SiO2	P2O5	Sc	Y	Nb	La	Ce	Pr	Nd	Sm	Eu	Gd	Tb	Dy	Ho	Er	Tm	Yb	Lu	Hf	Ta	Pb	Th	U	Ce/Ce*	Eu/Eu*	Σ REE	Th/U
2-ap06f12	33.1	0.034	105	594	3.3	-	37	0.07	1.12	1.8	0.88	9.9	3.6	46	18	92	23	238	50	7910	1.19	9.7	229	375	-	0.64	521	0.6
2-ap06f13	33.1	0.033	97	470	2.8	0.039	36	0.06	0.89	2.0	0.76	10.3	2.8	40	15	71	18	178	38	8100	1.06	9.5	230	362	183	0.51	413	0.6
2-ap06g07	33	0.051	93	451	1.7	0.164	26	0.12	1.13	1.8	0.70	9.1	2.8	35	14	72	17	182	38	6890	0.71	7.7	167	309	45	0.53	400	0.5
2-ap06g08	33.2	0.036	94	397	2.4	0.087	30	0.09	0.74	1.9	0.57	8.2	2.3	31	12	63	15	157	33	7790	0.80	8.2	185	327	84	0.44	356	0.6
2-ap06g09	33	0.038	87	349	1.9	0.081	30	0.06	0.84	1.4	0.64	7.7	2.2	28	11	54	13	131	27	7010	0.80	9.7	211	340	105	0.59	307	0.6
2-oc03b04	33	0.032	96	441	2.0	0.077	28	0.04	0.92	1.6	0.59	7.4	2.6	34	13	68	17	180	38	7500	1.01	7.8	158	278	129	0.53	391	0.6
3-oc03a05	33	0.035	112	514	2.1	0.055	39	0.09	0.88	1.9	0.84	9.9	3.2	41	16	76	19	194	40	8220	1.04	13.5	328	439	138	0.59	441	0.7
3-oc04d05	33	0.043	87	629	1.0	0.502	32	0.22	2.29	3.7	1.09	15.5	4.8	57	20	95	24	230	48	8100	0.73	11.1	244	326	23	0.44	533	0.7
3-oc04d07	33	0.042	86	425	1.9	0.665	38	0.18	1.46	2.0	0.71	9.4	2.9	36	14	67	16	164	33	8800	1.14	11.6	285	432	27	0.51	384	0.7
3-oc04c04	33	0.030	98	425	1.8	-	38	0.06	1.12	2.4	0.65	10.1	2.8	36	13	66	16	164	33	8830	1.13	14.5	323	464	-	0.41	383	0.7
3-oc04c06	33	0.047	88	396	1.2	0.158	23	0.05	0.54	1.7	0.48	7.9	2.4	31	12	62	15	160	33	7660	0.82	6.3	134	247	60	0.40	350	0.5
oc03b06	33	0.044	100	508	2.1	0.465	42	0.13	1.23	2.0	0.79	10.2	3.8	44	16	75	18	180	37	7940	1.05	17.9	405	491	41	0.53	430	0.8

(1), (2) and (3) correspond to analyses from cores (1) toward external rims (3). SiO_2 and P_2O_5 are reported in Wt% and the other elements in ppm. * are analyses reported in figure 4.

Electronic Appendix 5: Back-calculation of melt using Dtitanite/melt and Dapatite/melt

R2 Sample

Titanite	Kd*	Avge Core Titanite	Calc Bulk	Apatite	Kd*	Avge Core Apatite	Calc Bulk
La	46	2838	62	La	21,7	406	19
Ce	87	9882	114	Ce	25,8	1155	45
Pr				Pr			
Nd	152	6874	45	Nd	29	690	24
Sm	204	1314	6,44	Sm	31,4	134	4,27
Eu	181	219	1,21	Eu	25,2	25	0,99
Gd				Gd			
Tb	248	110	0,44	Tb	34	12	0,35
Dy	206	560	2,72	Dy	24	60	2,50
Ho				Ho			
Er				Er			
Tm				Tm			
Yb	104	207	1,99	Yb	12,3	24	1,95
Lu	92	24	0,26	Lu	12	3,97	0,33

RT1 Sample

Titanite	Kd*	Average Core	Calc Bulk	*Apatite*	Kd*	Average Core	Calc Bulk
La	46	2830	62	La	21,7	669	31
Ce	87	10065	116	Ce	25,8	1807	70
Pr							
Nd	152	6873	45	Nd	29	993	34
Sm	204	1306	6,40	Sm	31,4	157	4,99
Eu	181	219	1,21	Eu	25,2	38	1,50
Gd							
Tb	248	108	0,44	Tb	34	13	0,39
Dy	206	554	2,69	Dy	24	64	2,66
Ho							
Er							
Tm							
Yb	104	203	1,95	Yb	12,3	27	2,19
Lu	92	23	0,25	Lu	12	4	0,37

RHG-1 Sample

Titanite	Kd*	Average Core	Calc Bulk	*Apatite*	Kd*	Average Core	Calc Bulk
La	46	2990	65	La	21,7	868	40
Ce	87	10067	116	Ce	25,8	2169	84
Pr							
Nd	152	6430	42	Nd	29	1075	37
Sm	204	1154	5,66	Sm	31,4	166	5,28
Eu	181	198	1,09	Eu	25,2	34	1,35
Gd							
Tb	248	96	0,39	Tb	34	13	0,39
Dy	206	492	2,39	Dy	24	65	2,72
Ho							
Er							
Tm							
Yb	104	183	1,76	Yb	12,3	30	2,45
Lu	92	21	0,23	Lu	12	5	0,39

RA1 Sample

Titanite	Kd[α]	Average Compo	Calc Bulk	*Apatite*	Kd[β]	Average Core	Calc Bulk
La	8,2	1866	**228**	**La**	4,32	885	**205**
Ce	28,4	7019	**247**	**Ce**	5,17	2331	**451**
Pr	77	1173	**15**	**Pr**	5,94	316	**53**
Sm	364	1145	**3,1**	**Sm**	8,25	234	**28,4**
Eu				**Eu**			
Gd	368	671	**1,8**	**Gd**	7,44	144	**19,4**
Tb							
Dy							
Ho							
Er							
Tm							
Yb							
Lu	50	9	**0,2**	**Lu**	1,62	1,96	**1,2**

***Luhr et al. (1984)**
° Fowler et al. (2001)

[α]Protwake and Kemme (2005)

[β]Protwake and Kemme (2006) **[&]Tiepolo et al. (2002)**

Electronic Appendix 5 (Suite): Back-calculation of melt using Dtitanite/melt and Dapatite/melt from e

R2 Sample

Titanite	Kd[&]	Avge Core Titanite	Calc Bulk	Kd[α]	Calc Bulk	Apatite	Kd[β]
La	4,73	2838	**600**	1,88	**1510**	**La**	16,6
Ce	7,57	9882	**1305**	3,61	**2737**	**Ce**	18,1
Pr				7,39		**Pr**	20,6
Nd	12,4	6874	**554**			**Nd**	
Sm	14	1314	**93,86**	20,4	**64,41**	**Sm**	25,7
Eu	13,8	219	**15,87**			**Eu**	
Gd	11,9	819	**68,82**	18,2	**45,00**	**Gd**	21,5
Tb		110				**Tb**	
Dy	8,27	560	**67,71**			**Dy**	
Ho						**Ho**	
Er	5,54	245	**44,22**			**Er**	
Tm						**Tm**	
Yb	3,02	207	**68,54**			**Yb**	
Lu		24		2,38	**10,08**	**Lu**	3,01

RT1 Sample

Titanite	Kd[&]	Average Core	Calc Bulk	Kd[α]	Calc Bulk	*Apatite*	Kd[β]
La	4,73	2830	**598**	2,17	**1304**	**La**	16,6
Ce	7,57	10065	**1330**	4,6	**2188**	**Ce**	18,1
Pr				9,7		**Pr**	20,6
Nd	12,4	6873	**554**			**Nd**	
Sm	14	1306	**93,29**	31,2	**41,86**	**Sm**	25,7
Eu	13,8	219	**15,87**			**Eu**	
Gd	11,9	845	**71,01**	30,5	**27,70**	**Gd**	21,5
Tb		108				**Tb**	
Dy	8,27	554	**66,99**			**Dy**	
Ho							

Er	5,54	240	**43,32**				
Tm							
Yb	3,02	203	**67,22**			**Yb**	
Lu		23		3,65	**6,30**	**Lu**	3,01

RHG-1 Sample

Titanite	**Kd[&]**	**Average Core**	**Calc Bulk**	**Kd[α]**	**Calc Bulk**	*Apatite*	**Kd[β]**
La	4,73	2990	**632**	1,88	**1590**	**La**	16,6
Ce	7,57	10067	**1330**	3,61	**2789**	**Ce**	18,1
Pr				7,39		**Pr**	20,6
Nd	12,4	6430	**519**			**Nd**	
Sm	14	1154	**82,43**	20,4	**56,57**	**Sm**	25,7
Eu	13,8	198	**14,35**			**Eu**	
Gd	11,9	723	**60,76**	18,2	**39,73**	**Gd**	21,5
Tb		96				**Tb**	
Dy	8,27	492	**59,49**			**Dy**	
Ho							
Er	5,54	210	**37,91**				
Tm							
Yb	3,02	183	**60,60**			**Yb**	
Lu		21		2,38	**8,82**	**Lu**	3,01

RA1 Sample

Titanite	**Kdα**	**Average Compo**	**Calc Bulk**
La	4,73	1866	**395**
Ce	7,57	7019	**927**
Pr		1173	
Nd	12,4	5778	**466**
Sm	14	1145	**81,8**
Eu	13,8	284	**20,6**
Gd	11,9	671	**56,4**
Tb			
Dy	8,27	318	**38,5**
Ho			
Er	5,54	106	**19,1**
Tm			
Yb	3,02	79	**26,2**
Lu		9	

XRF°
28
46
19
2,9
0,66
1,61
-
1,01
0,58
0,48
-

XRF°
68,7
117
56,3
9,1
2,22
4,95
-
4,27
1,99
1,6
-

XRF°
48,8
84,8
35,2
5,1
1,43
3,66
-
2,46
1,53
0,96
-

XRF
154
283
-
24,1
6,03
16,6
7
3,13
1,82
-

experimental work only

Average Core	Calc Bulk	XRF°
406	24	28
1155	64	46
155	8	-
		19
134	5,21	2,9
		0,66
99,5	4,63	1,61
		-
60		1,01
		0,58
		0,48
3,97	1,32	-

Average Core	Calc Bulk	XRF°
669	40	68,7
1807	100	117
231	11	-
		56,3
156	6,07	9,1
		2,22
113	5,26	4,95
		-
		4,27

		1,99
		1,6
4	**1,33**	**-**

Average Core	Calc Bulk	XRF°
868	**52**	**48,8**
2169	**120**	**84,8**
264	**12,82**	
		35,2
166	**6,46**	**5,1**
		1,43
118	**5,49**	**3,66**
		-
		2,46
		1,53
		0,96
5	**1,66**	**-**